Biceps Femoris Long Head and Short Head Muscle Modeling and Kinematics during Four Classes of Lower Limb Motion and Gait

By

Alexander Villafranca

A Thesis Submitted to the Faculty of Graduate Studies of The University of Manitoba

In Partial Fulfillment of the Requirements for the Degree of

MASTER OF SCIENCE

School of Medical Rehabilitation

University of Manitoba

Aug 19th 2010

Abstract

Theoretical mechanical benefits of biarticular muscles include reduced displacements and force potentiating shifts in linear velocities during multi-joint coupled motions. A cadaveric model was developed to compute muscle kinematics of biceps femoris (BF_L and BF_S) during four classes of coupled knee and hip joint motion, as well as running and walking gait (Six subjects, Vicon Motion Analysis). The examples of the classes of motion were: KEHE-jump (knee extension and hip extension), KFHF-tuck (knee flexion and hip flexion), KFHE-kick (knee flexion and hip extension), and KEHF-paw (knee extension and hip flexion). BF_L peak and mean velocity shifts relative to BF_S were seen in all four coupling classes ($p<0.05$) and the majority of the gait subclasses ($p<0.05$). Muscle displacements were larger in BF_L for both KFHE-paw and KEHF-kick ($p<0.05$), smaller in KFHF-tuck ($p<0.05$), but not significantly different in KEHE-jump or during most of the running gait subclasses, except for during KFHE-late mid stance and KEHF-mid swing, where they were larger for BF_L ($p<0.05$).

The mechanical benefits associated with BF_L velocity shift relative to BF_s were identified in KFHF, KEHF motions, and certain subclasses of gait. In contrast, there were potential mechanical detriments due to velocity shift relative to BF_s in the KEHE-jump, KFHE-paw, and the majority of KEHE and KFHE subclasses in both gait cycles. The possible mechanical benefits associated with displacement conservation of BF_L relative to BF_s would be realized in KFHF-tuck jump, but not during KEHE-jump and the gait cycle subclasses. The findings of this study reveal both mechanical benefits and detriments of biarticular muscles, and have immediate implications for neural control of biarticular muscle during movement.

Acknowledgements

First I'd like to thank my committee for their guidance and critical assessment of this thesis, as well as their kind words. I'd especially like to thank Dr. Dean Kriellaars, my advisor, who provided a deep insight into both the scientific method, as well as the field of biomechanics. He has undoubtedly helped shape my development as an aspiring academic and scientist. The provision of a Graduate Fellowship by the University of Manitoba is also acknowledged and appreciated.

I'd also like to acknowledge individuals who introduced me concepts which eased the completion of this project: Mrs. Rani Reddy, Mr. Fausto DeLuca, and Mr. Steven Brisson provided insight into calculus, numerical analysis, and vector mathematics which all proved invaluable in the modeling portion of this thesis. Mark Garret was kind enough to teach me the dissection techniques needed to accomplish the cadaveric portion of this thesis. Mr. Colin Bell contributed terrific drawings of my cadaveric setup, which are included in this document. A fond thank you is also extended to Mr. Robert Pryce for being a terrific Matlab instructor and "brother in arms" throughout the course of the medical rehabilitation graduate program.

On a few personal notes, I would like to thank Dr. Eric Jacobsohn for his incredible efforts in permitting me to maintain a flexible work schedule while completing this thesis. Second I owe a big thank you to Natasha Fisher for her (almost) infinite patience during my two years of "multi-tasking" on dates, trips, and other social events not normally associated with thesis writing.

Finally I am profoundly grateful to my parents for their support, guidance, and tolerance during the ebbs and flows of my education. I dedicate this work to them.

Table of Contents

Tables

Figures

Introduction

Biarticular muscles, defined as muscles which span two joints, are found in the vast majority of mammalian species. The main examples of biarticular muscles in Homo sapiens are the short head of biceps brachii, the long head of triceps brachii, the majority of the hamstring muscle group, rectus femoris, and the gastrocnemius. Despite their ubiquity, the exact role that biarticular muscles play in the production of motion remains to be elucidated.

In man, the hamstring muscle group presents an interesting muscle arrangement, since it is made almost exclusively of biarticular muscles, while other muscle groups involving biarticular muscles are composed of an equal or greater number of uniarticular (single joint crossing) muscles, or muscles containing uniarticular heads. The biceps femoris is one of three biarticular muscles which cross the posterior aspects of both the knee joint and the hip joint, forming the hamstring muscle group. The other two are the semitendinosus and semimembranosusnosus muscles. In some ways, the biceps femoris is the most interesting of the three muscles, since it consists of two heads, referred to as the long (BF_L) and short (BF_S) heads, respectively. Both heads have a merging primary insertion site on the head of the fibula. However, BF_S acts as a uniarticular muscle, since its origin is on the linea aspera (Latin for "rough line") of the femur, and therefore only spans the knee joint. In contrast, the BF_L has its origin primarily on the ischial tuberosity of the pelvis, and therefore crosses both the hip joint and the knee joint.

The length of the BF_L can be affected by changes in both the hip and knee joint angles. Hip extension promotes BF_L shortening, while hip flexion promotes BF_L lengthening. In contrast, knee flexion promotes BF_L shortening, while knee extension promotes BF_L lengthening. Rotations of the lower limb segments about the hip and knee are often coupled during human motion. Rotation of multiple limb segments has no additional effect on uniarticular muscles beyond what would be seen with rotation about the joint the given uniarticular muscle crosses. In contrast, a biarticular muscle's length and velocity would be affected by rotations about both joints. Simultaneous rotations about both joints could be promoting the same muscle length change (both joints promoting shortening or both joints promoting lengthening) in some hip and knee couplings. In other couplings they could be promoting opposite effects depending on the coupling of the rotations about both joints. Therefore

predicting the muscle length or velocity of a biarticular muscle is less intuitive than predicting the muscle length or velocity of a uniarticular muscle, which maps to the joint angular kinematics trigonometrically.

The possible benefits of having a biarticular muscle cross two joints have been postulated for over one hundred years, yet no firm conclusions have been reached. Some hypothesized benefits of said muscles include:

1. That a contracting biarticular muscle may be able to transfer power to a joint this contracting muscle does not cross, with the help of another antagonistic biarticular muscle (van Ingen Schenau, 1994).
2. That a single biarticular muscle can act at all the joints it crosses at once, allowing economy in terms of the number of necessary muscles activated during specific couplings (Cleland, 1867; Elftman, 1966).
3. That having a biarticular muscle results in the bulk of a muscle being closer to the whole body center of mass, thus decreasing the amount of torque needed to move the most distal segments by decreasing their moments of inertia (van Ingen Schenau, 1994).
4. That biarticular muscles may be especially suited to increasing limb stiffness and promoting joint stability of the joints it spans (Markee et al, 1955; Loyd and Buchanan, 1996; Raikova, 2000).
5. That biarticular muscles may serve a special role of controlling the direction of the external force of a limb motion through the control of the distribution of net moments at the joints a biarticular muscle spans, based on agonistic and antagonistic activity (van Bolhuis et al., 1998).

Finally, the two most frequently postulated mechanical benefits of biarticular muscle are:

6. Muscle velocity reduction/shift (Elftman, 1966; Fenn, 1938), resulting in an increased muscle force at a given activation level.
   And
7. Force length potentiation (Cleland, 1867; Elftman, 1966; Fenn, 1938), also resulting in an increased muscle force at a given activation level.

These last two possible benefits each require more comprehensive explanations, which are given in the following sections.

Theory 1. F/v shift

To understand the possibility of a mechanical benefit for biarticular muscles based on the force-velocity (f/v) and force length (f/l) relationships, a brief review of these relationships is required. The f/v relationship states that the force a muscle can produce concentrically is negatively related to shortening velocity. The f/v relationship also states that muscle force will be greater during isometric muscle actions than concentric, and will reach upwards of 1.8X isometric values when the muscle is lengthening (eccentric contraction) at the same activation level. Unlike the concentric force reduction with velocity, on the lengthening side of the curve, the relative force enhancement has been shown to increase quickly as lengthening velocity increases. However a peak in muscle force is quickly reached as lengthening velocity increases, and thereafter any further increase in lengthening velocity has little effect on muscle force. It is also commonly believed (but relatively untested) that "bi-articular muscles will have a lower shortening velocity than two mono-articulars would need to have" (van Ingen Schenau, 1994) during specific multi-segmental couplings. In turn, any decrease in muscle shortening velocity arising from a suitably coupled hip and knee motion, would be accompanied by an increase in force production given the same neuromuscular activation. This would be particularly true in a combined knee and hip flexion motion. In this situation, the BF_S would be shortening, while the BF_L could be shifted to a smaller shortening velocity, an isometric condition, or even a lengthening velocity, depending on the ratio of knee motion to hip displacement for given motion. However the underlying mechanical benefit in these situations would not be the tendency towards smaller velocities per se, but rather the left shift on the force velocity curve that would be seen, moving from the velocity associated with low force toward a leftward velocity which would permit greater force generation at the same activation level. Each type of coupling class would have ramifications for biarticular muscle velocity. Despite long time acceptance of the idea of velocity reduction (Elftman, 1966; Fenn, 1938; Raikova, 2000) there is little data supporting or quantifying the idea of a velocity reduction, particularly in the hamstring muscle group.

Theory 2. F/l potentiation

The force production of a whole muscle is also related to muscle length, with the active f/l relationship reaching a peak when a maximum number of cross bridges can be formed between the thick myosin filaments and thin actin filaments, and decreasing as the muscle becomes shortened or lengthened relative to this optimal

muscle length. The passive f/l relationship demonstrates an increase in passive force as muscle length increases beyond the peak overlap due to series elastic components within the muscle.

It has been hypothesized since the time of Cleland (1897) that during what we call incongruent muscle effect circumstances (coupled knee and hip flexion, or coupled knee and hip extension); the net displacements would be less in a biarticular muscle relative to uniarticular muscles crossing the same joints as the biarticular muscle. This reduced displacement is predicted to result in the muscle spending a greater amount of time away from the extreme positions on the f/l relationship. This situation would be associated with a decrease in active force, assuming the muscle length throughout the motion was close to the center of the f/l relationship. This is of particular importance to a biarticular muscle, since this phenomenon could also avoid placing it into a position of passive insufficiency or active insufficiency (Elftman, 1966). Passive insufficiency is a passive tension within a muscle that results in a limitation on the range of motion of the joint(s) it spans (Knudson, 2003).Active insufficiency represents the realization of the shortest length a muscle can achieve, resulting in a limitation on further joint motion (Watkins, 2009), as well as a limitation on the force a muscle can exert, due to its position on the force-length curve (Green and Roberts, 2005).

Biarticular muscles are particularly susceptible to passive and active insufficiency, since both joints the muscle crosses can simultaneously result in lengthening, or shortening, respectively (Knudson, 2003). The former would be true during coupled knee extension and hip flexion motions, while the latter would be true during coupled knee flexion and hip extension motions. Some support exists for this assertion in the biarticular hamstring muscles versus the uniarticular muscle of the cat (Peters and Rick, 1977), and in data published for model validation (Frigo and Pedotti, 1978) on a single subject. These studies report smaller biarticular hamstring displacements than uniarticular displacements, consistent with the f/l potentiation concept. While these results are intriguing, they are by no means compelling or conclusive. The limitations of the Frigo and Pedotti (1978) model of the BF_L are examined in the review of literature. Further research is required during a variety of motions and joint coupling types, using a more realistic model of the BF. It is unclear if BF_L velocity shift and displacement conservation occurs relative to a uniarticular muscle such as the BF_S during common human lower limb couplings. It is also unclear to what magnitude this reduction would reach, if present.

Purpose

To develop and evaluate a model for assessing the kinematics of the long and short heads of the biceps femoris muscle during four classes of lower limb motion and gait.

Experiment 1: Cadaveric Model Development

The first experiment involved generating a model of the BF_L and BF_S muscles using cadaveric data, with inputs being knee and hip joint angle and the output being muscle length.

Experiment 2: Muscle Kinematics during Four Classes of Motion and Gait

The second experiment used the model to derive muscle length and velocity, based upon hip and knee joint kinematics in four classes of hip and knee joint coupling, as well as during walking and running gait. These joint couplings have not been evaluated previously and this nomenclature was developed as part of this thesis (See Selection of Coupled Hip and Knee Motions below).

Selection of Coupled Hip and Knee Motions

Multi-segmental movement classes were divided into four categories, based on a classification system of the specific coupling occurring between the involved knee and hip joints (See TABLE 1). This classification system was chosen since the couplings it represents all the basic sagittal plane couplings that could occur between the knee and hip joints. Of course, within each coupling class the relative magnitudes and sequencing of hip and knee angular kinematics can vary, but the signs would not. Optimization of coupling sequences is not being considered in this thesis, as we require the basic understanding of biarticular muscle function before proceeding to this step.

The four coupling classes of motion used were defined as follows:

- KEHE - where both the knee and hip are extending
- KEHF - where the knee is extending while the hip is flexing
- KFHF - where the knee and hip are flexing
- KFHE - where the knee is flexing while the hip is extended

TABLE 1- Change in BF_L length with knee and hip joint couplings. Legend: ↑= muscle length increase, ↓= muscle length decrease.

BF_L length change			
Coupling class	Knee effect	Hip effect	Classification (new terminology)
KEHE	↑	↓	Incongruent
KEHF	↑	↑	Congruent
KFHF	↓	↑	Incongruent
KFHE	↓	↓	Congruent

One representative example of each motion was chosen for this analysis. Example motions were picked to maximize each coupling's ranges of motion at the knee and hip joints, their frequency of occurrence in active living and sport, and their velocity. These criteria were chosen to minimize the novelty of the movement performance, and thus minimize subject training time and learning effects throughout the trial, while maximizing the possibility of inter-muscular differences in the dependant variables. The chosen examples of each coupling are shown in TABLE 2.

TABLE 2- Coupling representative examples

Coupling Class	Movement	Rationale	Abbreviation
KEHE	Bilateral Squat Jump (Ascent Phase)	Very common and rapid knee extension- hip extension motion	KEHE-jump
KFHF	Bilateral Tuck Jump	Rapid knee flexion- hip flexion motion with full knee and hip range of motion	KFHF-tuck
KEHF	Unilateral Toe Kick	Common and very rapid example of a knee extension-hip flexion motion	KEHF-kick
KFHE	Unilateral Pawing Action of the Foot	Resembles the pre-stance and heel strike action of the walking and running gait cycles. Virtually the only example of knee flexion- hip extension motion in human beings.	KFHE-paw

In another effort to ensure a naturally occurring example of all four couplings, a progressive speed treadmill trial was conducted. This allowed both running and walking gait cycles to be collected and broken down into sub couplings (couplings coded based on their time of occurrence in the gait cycle) thereafter.

This systematic analysis was necessary since prior investigations have focused on either multi-segmental motions containing multiple couplings examined in their entirety (cycling or running), or have focused primarily on KEHE-motions. KEHE motions have been emphasized since they were traditionally thought to result in a smaller velocity and displacement relative to single joint motions and hypothetical uniarticular muscles, as well as represent a motion where the hamstrings and rectus femoris would contribute to a transfer of force/momentum from muscles crossing the knee to the hip joint, and from muscles crossing the hip to the knee joint (Cleland, 1867; Lombard, 1903). Ignoring this possibility of such a paradoxical action, the biarticular hamstring muscles would be acting as promoting the motion about the hip joint, and resisting the motion about the knee joint.

All four classes of motion are necessary components of the systematic analysis, since they will all result in different effects on BF_L muscle kinematics. The effects of the hip and knee joint on the length of the BF_L, during each of the four classes of motion, and the effects of single joint knee motions on the BF_S are identified in TABLE 1.

The effects of KEHE and KFHF motions on BF_L kinematics may vary due to two factors: the size difference between the BF_L moment arms about the hip and knee joint angles, and differences in kinematics that may be seen between the two couplings. The former originates from the fact that the BF_L moment arm about the hip is greater than its moment arm about the knee (Fenn, 1938; Visser, 1990; Hawkings and Hull, 1990). Therefore the muscle kinematics will lean towards that promoted by the hip joint during motions with equal displacements of the hip and knee joints. Since the hip motions in KEHE and KFHF motions are different, the tendency towards a given effect on BF_L (shortening or lengthening) will be different for each. The latter originates from the fact that different motions demonstrate differing proportions of knee movement relative to hip movement (being knee dominant, hip dominant, or both having equal effects on BF_L kinematics). At this point, it is again natural to muse about optimal sequencing of knee and hip motion both within a coupling and between couplings, but this study will be restricted to gauging basic motion patterns that are common.

Selection of a Reference Muscle for Comparison to BF_L

Comparison of results and integration of conclusions between existing investigations examining the mechanical benefits of biarticular muscle is difficult due to the different reference muscles or motions. This is particularly true of the BF_L, where data is scant. Theoretical comparisons have been made between the BF_L during a multi-segmental motion versus BF_L during a single joint motion (Fenn, 1938), BF_L during a multi-segmental motion versus BF_L during another multi-segmental motion (Fenn, 1932), one hypothetical biarticular muscle versus another hypothetical biarticular muscle during multi-segmental motion (Enklaar, 1954), and BF_L versus both a hypothetical knee flexor and a hypothetical hip extensor (Elftman, 1966) during multi-segmental motion.

This investigation will compare the BF_L relative to the BF_S, for a number of reasons. Comparisons of a biarticular muscle's functioning during a multi-segmental motion versus two uniarticular motions, or versus another multi-segmental motion, are not suitable to answer questions about how the biarticular nature of BF_L affects its kinematics. Instead, they provide insight into how the BF_L (who happens to be biarticular) is acting under different circumstances. The actual human coupling examined provides a context for the inter-muscular comparison, and inter-coupling comparisons can be made after to determine the common circumstances when the biarticular nature of the BF_L is mechanically beneficial and when it may be mechanically detrimental. Inter-muscular comparison is in fact what provides insight into the effects of the biarticular nature of a muscle.

Comparisons of the BF_L to an existing uniarticular muscle such as the BF_S are particularly relevant, since they provide insight into how two existing portions of the same muscle may act differently during human motion. Only one investigation compared the kinematics of the BF_S to those of the BF_L during human locomotive motions (Frigo and Pedotti, 1978), and this comparison only occurred in a single subject, using a model who's predictions may be suspect (see review of literature for further details). Comparisons to the BF_S are in some ways even more interesting than comparisons to existing uniarticular hip extensors such as the gluteus maximus, since the BF_L and BF_S are from the same muscle group, and share both a common insertion and a common innervation source (roots L5 to S2 leading to the sciatic nerve, compared to the gluteus maximus, which is innervated by the inferior gluteal nerve, Leis and Trapani, 2000). The BF_L and BF_S would therefore commonly be thought of as having similar neural drive, and circumstance where the inputs they are providing are contradictory could have important implications on motor control theory.

Hypotheses

Velocity Shift Hypotheses during Four Classes of Lower Limb Motion and Gait

1. The biarticular muscle (BF_L) will exhibit a left shift in muscle velocity relative to the uniarticular muscle (BF_S) for the KFHF coupled movement (tuck jump), the walking gait KFHF subclasses, and the running gait KFHF subclasses.

2. The biarticular muscle (BF_L) will exhibit a left shift in muscle velocity relative to the uniarticular muscle (BF_S) for the KEHE coupled movement (jump), the walking gait KEHE subclasses, and the running gait KEHE subclasses.

3. The biarticular muscle (BF_L) will exhibit a left shift in muscle velocity relative to the uniarticular muscle (BF_S) for the KEHF coupled movement (toe kick), the walking gait KEHF subclasses, and the running gait KEHF subclasses.

4. The biarticular muscle (BF_L) will exhibit a right shift in muscle velocity relative to the uniarticular muscle (BF_S) for the KFHE coupled movement (pawing motion), the walking gait KFHE subclasses, and the running gait KFHE subclasses.

5. In these hypotheses, a left shift on the f/v relationship would express as a decrease in shortening muscle velocity or a reversal from a shortening muscle velocity to either an isometric muscle state or a lengthening muscle velocity. A right shift would result in the converse, with a decrease in lengthening velocity, or a reversal from a lengthening velocity to either an isometric muscle state or a shortening muscle velocity. During the KEHE and KFHF couplings, a shift along the f/v relationship in the BF_L relative to the BF_S could be large enough to result in simultaneous lengthening and shortening length changes in a homonymous muscle group.

Displacement Hypotheses during Four Classes of Lower Limb Motion and Gait

1. The biarticular muscle (BF_L) will exhibit a significantly smaller muscle displacement relative to the uniarticular muscle (BF_S) during the KFHF coupled motion (tuck), the walking gait KFHF subclasses, and the running gait KFHF subclasses.

2. The biarticular muscle (BF_L) will exhibit a significantly smaller muscle displacement relative to the uniarticular muscle (BF_S) during the KEHE coupled motion (jump), the walking gait KEHE subclasses, and the running gait KEHE subclasses.

3. The biarticular muscle (BF_L) will exhibit a significantly larger muscle displacement relative to the uniarticular muscle (BF_S) during the KEHF coupled motion (toe kick), the walking gait KEHF subclasses, and the running gait KEHF subclasses.

4. The biarticular muscle (BF_L) will exhibit a significantly larger muscle displacement relative to the uniarticular muscle (BF_S) during the KFHE coupled motion (pawing motion), the walking gait KFHE subclasses, and the running gait KFHE subclasses.

Based on tables presented above and on the stated hypotheses, the KFHF coupling would be the only one where both a mechanically beneficial velocity shift, as well as displacement conservation, could be operating simultaneously. It is also interesting to note that the KFHE coupling could logically be considered the only one where the BF_L is acting as an agonist in both joint motions, and yet it would be predicted to result in both a mechanically beneficial right shift on the f/v relationship, and a shift away from the center of the f/l curve.

It is acknowledged that the initial length of the BF_L would be an important determinant of the effect a given coupling would have on the force production of a muscle based on the f/l relationship. Unlike the f/v relationship, which shows force increasing monotonically up to fast lengthening muscle actions, the active f/l relationship is more parabolic, and the effects of the exponential-like passive f/l relationship must also be considered. Further problems are encountered when inter-muscular comparisons are the intent, since comparisons based on muscle displacements and displacement distances between the BF_L and BF_S can't completely predict differences in force based on the f/l relationship, without first determining the average and/or instantaneous position of both muscles on said curve (what could be termed "length shift" on the f/l relationship of the BF_L compared to BF_S). This determination would require modeling of muscle fibre length normalized to optimum fibre length for a given muscle, which involves a number of additional model assumptions, and is ultimately beyond the scope of this project. However we can still infer that in motions involving muscle lengths close to optimal fibre length, the centripetal shift seen in KEHE and KFHF motions on the f/l relationship relative to their single joint components would likely be mechanically beneficial. Further, since it can be deduced geometrically that the BF_L would be larger than the BF_S in any knee and hip joint configuration, it can also be inferred that any absolute amount of muscle displacement would represent a greater displacement relative to resting length for the BF_S compared to the BF_L. Therefore any absolute displacement conservation seen in the BF_L relative to the BF_S would be of a greater magnitude when expressed relative to a measure of resting muscle length.

A KEHF motion occurring from a position of full hip extension and knee flexion (resulting in an initially shortened BF_L) is unique circumstance, since it is the only situation where congruent circumstances would result in a mechanical benefit in force production based on length shift compared to both its single joint components. This is because a shift towards the center of the f/l relationship from the far left side of the relationship would be mechanically beneficial.

Review of Literature

This section reviews the existing literature with regards to two dimensional BF modeling, as well as existing evidence of velocity shift and displacement conservation of biarticular muscles during human motion.

Models to Predict BF_L Lengths

A few models exist which describe BF_L musculo-tendinous length (defined as the length from the proximal BF_L insertion to the distal BF_L insertion) as a function of hip and knee joint angle (Frigo and Pedotti, 1978; Hawkings and Hull, 1990; Visser et al., 1990). The models share some similarities in their predictions. As expected, all predict the same direction of muscle length change for a given single joint knee or hip motion. However, the magnitude of these length changes varies between models during single joint motion. The muscle length predictions also do not agree during some multi-segmental motions. For example, in combined hip and knee extension motions where the knee displacement is three times the amount of the hip displacement, the model of Visser et al (1990) would predict that the BF_L is shortening, while the model of Hawkings and Hull (1990) would predict that the muscle is lengthening. Beyond the level of disagreement between the models, the existing models estimation of BF_L moment arms about the hip and knee joints is unrealistic.

The following explains exactly why these models lack realism. When a biarticular muscle's length is plotted as a function of one joint, while the other joint's position is held constant, the resulting plot is a line. This line can be described by fitting a polynomial to it. However, the fit of the polynomial is imperfect, meaning the line generating through evaluating the polynomial function will vary slightly in shape from the original line. The degree of the polynomial fit affects the difference between the original line and the polynomial estimation of the line. Since the moment arm of a muscle about a joint affects the rate of length change as a function of joint angle, different polynomial fits will also assume a moment arm of such a shape that the estimated muscle length plot is generated with joint angle changes. In fact, the moment arm- joint angle relationship assumed by a polynomial fit can be estimated by taking the derivative of the polynomial function (a method called the "tendon displacement" method of muscle moment arm determination (Bobbert et al, 1987)). We can evaluate the validity of our polynomial estimations of the line by comparing the shape of the derived moment arm plot to real life estimations of the moment arm joint angle relationship. If the shapes are similar, we can feel confident that we

are making fair assumptions about how the muscle length changes over small portions of the joint range of motion. It has been established that the shapes of BF_L moment arm plots relative to the joints they cross are parabolic (Arnold et al., 2000; Buford et al., 1997; Herzog and Read, 1993- all three studies finding parabolic moment arm relationships relative to the single joints they examined).

It is also important to know that we don't have to take the numerical derivative of the polynomial fit to have an idea of the shape of its derivative. According to the power rule of calculus, taking the derivative of a polynomial function of degree n will result in a derivative of degree n-1. So a 1^{st} degree polynomial fit would result in a derivative that was a constant, indicating a constant moment arm joint angle relationship. A 2^{nd} degree polynomial fit would result in a 1^{st} order derivative, indicating a linear and monotonic moment arm-joint angle relationship. These are obviously not good estimations of the BF_L known parabolic moment arm- joint angle relationships. A 3^{rd} degree polynomial fit would result in a 2^{nd} degree derivative, giving the "proper" parabolic moment arm joint angle plot. Therefore a model with a 3^{rd} degree polynomial estimation of the muscle length- joint angle relationship, and based on more stringent methodology is needed to allow accurate modelling BF_L and BF_S lengths and velocities.

Visser Model (Visser et al., 1990):

This study modeled instantaneous muscle lengths and muscle moment arms of variety of lower body muscles (including the BF_L) as a function of the involved joints. The measures were taken in situ from cadaveric human limbs. It should be noted that the actual origin to insertion muscle lengths were not measured. Instead, two small cuts were made into the BF_L muscle (one 10 cm below the ischial tuberosity and one 13 cm proximal to the head of the fibula, and the distance was measured of the gap between the cut edges of the muscle. Joints were individually moved through their ranges of motion. With knee joint motion, the gap measured was from the distal muscle edge and the edge of tendon extending from the head of the fibula. With hip joint motion, the gap measured was from the proximal edge of the muscle to the edge of tendon extending from the ischial tuberosity. These measures were normalized to thigh length, and were taken to represent the amount muscle length change. This number would then be added to the normalized resting muscle length to generate a normalized muscle length for a given joint position.

The formulae used to determine muscle length were therefore as follows:

Step 1- determining muscle length change due to knee joint angle

$$\Delta lk = \ 0.19826 - 0.04600\ \alpha - 0(\propto)^2$$

Where:

Δlk= change in BF_L length (% thigh) due to knee joint angle

α= knee joint angle (degrees)

Step 2- determining length change due to hip joint angle

$$\Delta lh = \ 0.16644\ + 0.31078\ ß + 0.00061(ß)^2$$

Where:

Δlh= change in BF_L length (% thigh) due to hip joint angle

ß= hip joint angle (degrees)

Step 3- determining the muscle length

$$lBFl = \frac{(100 + \ \Delta lh + \Delta lk\ )}{100} lthigh$$

Where:

lBF_L = BF_L length (cm)

lthigh= thigh length (cm)

The first apparent issue with this methodology is related to the manner the investigators measured muscle length. Although the experimenters attempted to wrap the muscles in gauze to keep them tight to their respective segments, the muscle portions, particularly the section attached to the moving segment are likely to change their angles relative to the moving segment, which could create a systematic error in muscle length

determination. This issue would have been avoided had the straight line distance between the proximal and distal origins been measured instead.

The experimental apparatus used is of some concern, partly due to insufficient detail in its description, and partly due to its design. Each cadaver was placed supine, with the thigh supported by a mounting frame with a superior portion and an inferior portion, which were clamped to the thigh. However, it is unclear whether the apparatus was effective at preventing abduction or internal/external rotation of the thigh, as the device is depicted without a right side, the way the thigh was clamped is not mentioned, and the joints were likely less stable due to reported incisions made into both joint capsules. The investigators mention that a line connecting the anterior superior iliac spine and the patella was kept in the sagittal plane, as was the patella, but by what means this was maintained is unclear. The abduction angle of the hip was not reported for any of the cadavers. Due to differences in hip width between the subjects (especially between the male and female cadavers), even this standardized position would result in a varying hip abduction angle between subjects. This is a particular concern since the length measurements for a given joint were combined across cadavers and a single polynomial was fitted to the single mass of data. A better way to approach this would be to fit the subjects individually with a polynomial, then also take the average of the data for each joint configuration, and fit a polynomial to the averaged muscle length joint angle plot as well.

In the Visser et al model, a square plastic board was secured to the pelvis and was rotated relative to a mounting frame to progressively adjust hip angle. While it is mentioned that the board slid along another board attached to the mounting frame, it is unclear exactly how the hip position was secured, and how the square surface resulted in smooth angle changes, despite its shape. In a depicted drawing within the paper, the square appears to hang beyond the surface the cadaver is lying on and attach posteriorly to the thigh, which would be consistent with measurement of the left leg, but not the right, barring a complete change in the orientation of the cadaver relative to the camera.

The cadaver shank was attached to a pulley, and the cadaver knee angle was adjusted by lowering the shank with gravity under the guidance of the pulley. It is unclear whether any measures were taken to prevent tibial rotation from occurring during this process. It is likely that the line of action of the pulley cable and the force vector exerted on the thigh would change as the orientation of the shank relative to gravity changed.

Joint angle calculations occurred post hoc via direct measurement from photography. Once muscle length-joint angle relationships were determined separately for the hip joint and the knee joint, these relationships were modeled using second order polynomial regression equations. Of great concern is the lack of reporting the position of the camera relative to the experimental setup, particularly in light of the fact that it is a given that both legs were utilized in a single cadaver. Were the camera kept in the same place, that would mean that the distance from the cadaver would change, and the error in angle calculation could be inconsistent across cadavers.

Such details are worthy of note, since the level of cumulative error that these uncertainties may produce is unclear. It is unclear at what level of precision the measurements of muscle displacement (and thus muscle length) were taken. It's also unclear which measuring tool (ruler, two compasses, Vernier calliper) of the four cited was used to measure this distance, why one tool would be used over the other, and if the measures from all tools showed good cross validation.

To determine the moment arms of the lower body muscles, the researchers used the tendon displacement method of moment arm determination (Bobbert et al, 1987). However, since the regression equations for the muscle length-joint angle plots in this investigation were second order, their derivatives with respect to joint angle (i.e. their moment arm functions) were linear, based on the power rule of calculus. As previously explained, this will result in errors in muscle length estimation, and larger errors in any linear velocity calculations derived from the muscle length estimations.

Visser et al (1990) also found large BF_L moment arms at the hip (from approx 20-25% of thigh length i.e. the length from the greater trochanter to the lateral femoral condyle), and increased linearly an increase in hip flexion angle from anatomical position. They also found that the knee moment arm was much smaller (approximately 2% upper segment length), and was constant with changes in knee angle. This is a value much smaller than those existing in the literature. Assuming a 40 cm thigh length, Visser's model would estimate a knee moment arm of 0.8 cm, while prior investigations have found knee BF_L moment arms that varied from 2.5-4.1 cm (Baretta, 1988; Smidt, 1973). Visser et al acknowledge this in their discussion, and suggest the difference is due to the effects of the cadaveric material compared to the in vivo situation. Specifically, they

point out the increased "degrees of freedom of the biceps tendon" observed in the cadaveric situation. This is likely true, and could have been remedied by simply measuring the distances between the bony insertions of the modeled muscles.

The researchers did not take the moment arm interactions of the muscles into account, since they took measures of muscle length through single joint manipulations of each joint associated with a given muscle. It was concluded by the authors that the interaction between moment arms in any lower body muscles was not significant based on a graphical comparison between the effect of knee angle at 0 degrees of hip flexion, and at 45 degrees of hip flexion on the length of rectus femoris. Certain limitations of this methodology should be noted. First, the difference between the two resulting sets of muscle lengths was less than 1% of upper segment lengths throughout a large range of knee flexion angles (0-60); however, these differences did increase to up to 2% at higher knee flexion angles. In fact, at 45 degrees of hip flexion it was observed that compared to zero degrees of hip flexion, muscle lengths were slightly larger until approximately 50 degrees, wherein they reversed to become smaller than the zero hip flexion condition. The second limitation is that the difference between the two RF length hip angle curves was not just a simple constant, as would be expected if changes in a given joint angle did not affect both joints. Were there no interaction, the length of RF would be the sum of the effects of both individual joint. The position of hip flexion would result in an equally decreased RF length at any knee joint angle. Therefore the RF length knee angle plot with the hip flexed would take on the appearance of a line offset from that of the RF length- knee angle plot in with the hip in anatomical position. Third, the graphical representation of the interaction in BF_L was not shown, although it was said to be similar to that of rectus femoris. Due to the two muscle's differing moment arm magnitudes, this conclusion requires greater detail reported in the data supporting it, since the interactions would vary depending on the relative magnitude of both its muscle moment arms. The interaction component would automatically be taken into account as long as the measurements were taken in combinations of different hip and knee orientations, and the data was fitted with a bivariate polynomial. It was not explicitly stated how these effects were determined to be negligible. Most importantly, even if this two position comparison was found to be insignificant, it is unwarranted to extrapolate this finding to all ranges of hip flexion, since the interaction between moment arms may be more pronounced at the extremes of hip range of motion.

Frigo and Pedotti Model (Frigo and Pedotti, 1978):

This geometrical model employed formulas based on the law of cosines and the Pythagorean Theorem. The hip, thigh, and shank were modeled as a three link model based in a coordinate system. The main limitation of this model is the method used to estimate BF_L moment arms. Full details of this geometrical model were not available in English, and were referenced in an Italian thesis which could not be readily accessed via document delivery. Thus the exact moment arm joint angle relationships were not available for examination. However, the researchers modeled the distances between the knee axis and the muscle insertion point as being larger than the distance between the hip axis and the muscle origin (6.7 versus 6.3, units not given). Since these distances are mathematically proportional to their respective BF_L moment arms (Goslow, 1973), by inference we can estimate that unless the moment arms interact to tremendous degrees, the BF_L knee moment arm was modeled as being bigger than at the hip, which is contrary to other literature on the topic (Chelbourn et al., 2001; Fenn, 1938;). Assuming that these distances are constant is another drawback of the model. With motion it can be geometrically deduced that these distances will vary slightly. This is important, since it will affect both moment arm estimation and muscle length estimation (Goslow, 1973).

Delp Model (Delp et al., 1990A, Delp et al., 1990B)

This complex, three dimensional model of the lower extremity was created to study how surgical interventions altering muscle tendon geometry affect muscle force production of a number of lower body muscles (including the BF_L) and joint torques. Existing pelvic and thigh bone surfaces were marked with a combination of polygons and digitized with a three dimensional digitizer, generating either wireframe mesh models or shaded surfaces of the bones which could be displayed in specially made software (Delp et al, 1990B). Such data for the shank and foot data were taken from an unpublished thesis (Stredney, 1982). Muscle paths were modelled using the coordinates of the muscles' origins and insertions. The line of muscle action was normally defined as a single segment. However, if necessary, wrapping points (points where the muscle wraps around a bone) were also used. In these situations the line of muscle action would be defined as series of connected vectors, including the vector wrapping around the bone, and the vector connecting the wrapping point segments. The muscle length was calculated as the sum of the vector lengths, with each vector length calculated using the three dimensional distance formula. Moment arms were then calculated as the partial derivative of the muscle length with respect to the given joint angle.

Muscle force was found by scaling a generic model with 4 parameters: maximum isometric force at optimal fibre length via cross sectional area, optimal fibre length, tendon slack length, and pennation angle. At the time of the initiation of this project, this three dimensional model was only available in proprietary software, and was therefore unable to be recreated. This graphics model requires inputs of hip flexion/extension angle, hip abduction/adduction angle, hip internal/external angle, and knee flexion/extension angle. It assumes a subject height of 1.8 meters tall. Therefore it is the most comprehensive model reviewed herein. However, this model does contain limitations. At the time of the initiation of this project, this three dimensional model was only available in proprietary software, and was therefore unable to be recreated. Also, the fact that this model is not in a simple regression format makes calculation of muscle length impossible without the presence of software containing the coordinate system. Furthermore, it should not be necessary to use a complex three dimensional model to acquire a reasonable estimate of BF lengths and velocities during most human motion. The model also makes use of a number of parameters which are estimated, and assumed to be similar across people (tendon slack length, optimal fibre length, etc…). These parameters were not directly measured, but instead were taken from existing literature.

Hawkings and Hull Model (Hawkings and Hull, 1990):

This model used anatomical measures of the hip and thigh from six cadavers, to allow for a scaled estimate of origin and insertion lengths based on an existing coordinate systems of the lower extremity (Brand et al., 1982). Brand et al (1982) marked the origin and insertion points of muscles on three cadavers with nails, and placed the boney specimens in a "wire cage X-ray surveying device". The three dimensional coordinates of the marked reference points were estimated using "knowledge of the X-ray source and film plane location". These reference points were used to allow scaling of the coordinate system to living subjects, and were defined relative to reference frames at the hip, knee, or ankle.

Hawkings and Hull palpated the scaling factors suggested by Brand on human subjects to scale the model. The most obvious limitation of this methodology (Hawkings and Hull, 1990) is that the actual origins and insertions of the BF_L were never directly assessed for the subjects used. Hawkings and Hull then calculated the straight line muscle origin to insertion distances during a computer simulation of joint configurations for each subject. The motions were all simulated to occur only in the sagittal plane, although it was not reported what the hip abduction angle was simulated to be. The resulting BF_L lengths were normalized to thigh length.

Linear regression equations for muscle length based upon joints angles were determined from mean data. The equation took the following form:

$$L = 1.048 + 0.00209 \propto - 0.00160 ß + 0 ß^2 + 0 \sigma$$

This simplifies to:

$$L = 1.048 + 0.00209 \propto - 0.00160 ß$$

Where:

L= BF_L length (% thigh)

α =hip angle (degrees)

ß= knee angle (degrees)

σ= ankle angle (degrees)

Quadratic regressions were also performed, but were rejected on the basis that they only improved the correlation coefficients marginally. However, it is important to realize that a small change in this correlation would still be associated with an increased accuracy and precision in the measurement.

Summary of Existing Model Limitations

- Models contained insufficient details in their methodology to identify sources of error. Additionally, it was often unclear whether sufficient measures were taken to prevent accessory joint motions such as changes in hip abduction angle, hip external rotation angle, and tibial rotation angle. Our model will make every effort to eliminate accessory joint motions, including hip abduction, hip internal/external rotation, and tibial rotation.

- Models made unrealistic assumptions about BF_L moment arm joint angle relationships. As such there was substantive disagreement between models on this critical parameter. These differences in moment arm calculation would also result in differences in muscle length calculations between models. Our model will make use of a 3rd degree bivariate polynomial with knee and hip angle as inputs. This will result in an assumption of parabolic moment arms, which is a more realistic estimation BF_L moment

arms. Making use of a bivariate polynomial assures that any interaction component between the moment arms on BF_L length will be accounted for.

- Models often only report average regression equations based on a small number of subjects. While this is not without merit, it would also be useful to show both individual equations for each cadaver. This would open the possibility of analyzing the effect of individual anthropometric characteristics on muscle kinematics in future investigations. This would eventually allow compilation of data from multiple investigations to eventually gain a population averaged model based on a greater number of samples. Our model will present both an equation predicting muscle length from the average cadaver muscle length- knee angle- hip angle surface, as well as equations derived from each individual cadaver muscle length- knee angle- hip angle surface.

- Occasionally models would involve extrapolation of sets of muscle length measures to joint configurations not examined, or at least would necessitate this given the model's use with motions of large range of motion. Models should strive to maximize the angular range of motions examined and rely more on interpolation than extrapolation. This will also decrease the need for extrapolation during the application of the model. Our model will include a larger range of motion about the knee joint than previous models, a greater number of measured total multi-segmental configurations, and finally will include a position of full hip extension.

In summary, no existing two dimensional model of the BF_L has estimated muscle lengths derived from realistic moments arms over a full range of hip and knee joint motion, fitted with a bivariate polynomial of the proper degree. A few models cannot be reliably and analyzed recreated due to a lack of existing methodological descriptions in English.

Evidence Supporting the Biarticular Velocity Shift and Displacement Conservation

While the existence of biarticular muscles had been described by Galen in the 2nd century (van Ingen Schenau, 1994), Cleland (1867) appears to have been the first to note a number of peculiarities of biarticular muscles following his study of equine anatomy. Of interest to this investigation, he noted that the muscle

displacements of the human Gastrocnemius were small during coupled ankle and knee flexion and coupled ankle and knee extension, despite large angular displacements at both joints. Due to this fact, he thought those muscles could not be contributing significantly to the production of the joint motion. Instead he postulated that they acted like ligaments, preventing specific joint motions from taking place and pulling on other "ligamentous muscles". These other "ligamentous muscles" would in turn act on the joints they cross; thereby "diffusing" the action of one muscle to a joint it does not cross.

Cleland also made note of the different effects each joint would have on a biarticular muscle crossing them, assuming specific multi-segmental couplings. For instance, flexion-flexion motions of the knee and hip were said to promote biceps femoris and rectus femoris shortening at one joint and lengthening at the other, while such a motion at the shoulder and elbow would result in Triceps Brachii long head lengthening due to both joints. Since the f/v relationship had not been identified at this time, no consideration of this relationship was given by Cleland, although he did mention a possible mechanical benefit of the decreased muscle displacement on muscle force due to the f/l relationship, by avoiding excessive muscle shortening.

Next, Lombard (1903) built on the idea of non-intuitive actions of biarticular muscles through his examination of both frog and human anatomy. He conceptualized that a biarticular muscle could "cause the extension of a joint which it can flex" (later known as one aspect of "Lombard's conjecture" (Kuo, 2001). This action was said to happen as long as the muscle had a biarticular antagonist, had both joints freely moving and not fixed at a specific joint angle, has a larger moment arm at the joint it extends, and has sufficient strength relative to its biarticular antagonist (Lombard, 1903). He was also the first to mention the idea of energy transfer, indicating that if the biarticular pairs at both the hip, knee and ankle joint were to contract simultaneously, the energy would be transmitted by an "endless chain…having the form of a figure eight…. progress(ing) in the direction of better leverage". However, no mention was made of a possible mechanical benefit based on the f/l or f/v relationships.

In 1921 H. Von Bayer (Fenn, 1938) had the foresight to classify motions associated with biarticular muscles as "mitläufige" (coupled flexion or coupled extension at both involved joints) or "gegenläufige" (opposite joint motions occurring at each involved joint). These terms were later roughly translated to "concurrent" and "countercurrent" by Steindler (1935).

This terminology will not be used in this investigation, and instead the four coupling classes defined earlier will be placed in the context of categories based not on joint motions, but instead the combined effects of the two joints affecting the BF_L muscle. "Concurrent motions" will therefore be referred to as "incongruent muscle effects motions" or "incongruent circumstances", and "Countercurrent motions" will be referred to as "congruent muscle effects motions" or "congruent circumstances". See appendix entitled "A Note on Terminology" describing a rationale for a change in terminology.

The first direct mention of a possible mechanical benefit of biarticular muscles based on smaller muscle length changes in an English publication appears to be in the work of Fenn (1931, 1938). Fenn logically deducted based on Euclidean geometry and the concentric portion of the f/v relationship that mechanical benefits due to the biarticular nature of specific muscles would occur during what we would call incongruent muscle effects motions (Fenn, 1938). He stated during such motions the BF_L and rectus femoris would have "their length remain relatively constant, perhaps approaching isometric contraction" Fenn (1938), since net muscle displacements would be relatively smaller than those seen with single joint due to the incongruent effects of both joints.

However, we should be point out that the biarticular muscle may not always see smaller length displacements and velocities relative to <u>both</u> single joint motions, since one of the joints could have an effect on muscle velocity that would be greater than double that of the other joint. A combination of these motions at different joint would result in a displacement and velocity conservation relative to the joint with the larger effect on BF_L, but not the joint with the smaller effect.

Fenn also noted that this smaller displacement would "permit a muscle to exert tension against a rapidly moving limb without a correspondingly rapid shortening" (Fenn, 1938), therefore touching on the possibility of a mechanical benefit to the BF_L based on the f/v relationship during incongruent effects motions.

In terms of potential mechanical detriments of a muscle's biarticular nature, Fenn also acknowledged that during what we call incongruent muscle effects joint motions the biarticular muscle's length would be "changing

in the same direction at both ends simultaneously, either lengthening or shortening therefore with double rapidity" (Fenn, 1938). He also predicted that during such motions in the running gait the force the rectus femoris would only be able to muster "very feeble tension at this point" (Fenn, 1938). Fenn did not offer any kinematic data to quantify these biarticular effects on muscle velocity in his English language publications. However, he did provide some data by Fick, quantifying the BF_L muscle excursions over the knee and hip joint ranges of motion, indirectly demonstrating differences in BF_L moment arms at each joint. The sum of these BF_L excursions due to the knee and hip joints (one lengthening and one shortening) was taken on order to demonstrate that coupled extension of the hip and knee joints would result in smaller BF_L excursions compared to their single joint components (Fenn, 1938).

However, these postulations were not verified or attributed to any specific form of human movement, and a comparison was not made to another existing muscle acting about the hip or knee joints. Such a comparison is also of limited value, since the vast majority of human motions do not occur through the entire movement ranges of the hip and knee joints, and involve different rates of knee motion to hip motion.

In a German article, Fenn (1932) noted smaller maximum shortening velocities of the BF_L during maximum speed cycling (38% resting length/s) compared to sprinting (377% resting length/s) in a single subject. This was likely partially attributable to the vast differences in peak hip extension velocity between the movements (290 degrees/s in the cycling, versus 1025 degrees/s in the running gait). He also found that the BF_L was close to isometric at one point in the pedal cycle.

In a very inventive theoretical paper, Enklaar (1954) described some of the theoretical implications of the existence of biarticular muscles using graphical methods. He described the concept of an isometric line of a muscle (an isoline) -- essentially a line on a cyclogram (joint angle- joint angle plot) where a biarticular muscle would stay at a specific length despite angular displacements at both joints. The slope of the isoline on the cyclogram also effectively indicated the proportion of joint motion (e.g. the ratio of knee to hip motion) needed to result in equal contributions of both joints to a biarticular muscle's displacement. He also pointed out that movements with cyclogram slopes that weren't equal to those resulting in isometric motions would result in either muscle shortening or muscle lengthening, Most interestingly, Enklaar (1954) graphically depicted that two synergistic muscles with equivalent actions at both joints they crossed, but with different moment arms, could theoretically display "antagonism" (one could be lengthening while another shortens) given a minority of

multi-segmental coupling containing specific kinematics. However, he did not determine the kinematics required to generate such a situation, or make any attempt to see if such a situation was seen in human motions. Instead, he simply raised the theoretical possibility.

In 1966, Elftman proposed that during the running gait, a biarticular hamstring muscle would have smaller muscle length changes than a hypothetical uniarticular knee flexor and a hypothetical uniarticular hip extensor, but would be able to perform the actions of both muscles and "eliminate this duplication of effort". He believed this would occur through a stretch-shortening cycle (SSC) of the biarticular hamstrings. It appears that he believed that in a KEHE motion, the hamstrings would act initially as a knee flexor which would "dissipate energy" while lengthening, and then as a hip extensor "doing positive work". This of course assumes that the motion occurring would have the proper ratio of knee displacement to hip displacement at the proper time to facilitate such an SSC. Namely, the motion would initially have to be quite knee dominant, and then switch towards a more hip dominant motion to result in the SSC action he described.

A decade later, Peters and Rick (1977) compared the feline biarticular muscles semitendinosus and semimembranosusnosus posterior to the feline uniarticular muscle semimembranosusnosus anterior during the feline gait cycle. The f/l relationships in these cat muscles were first determined using electrostimulation eliciting maximum tension. This data was combined with the kinematic data of Goslow et al (1973) to determine the maximum possible tetanic tension and calculated torque of the muscles during the cat step cycle. It was found that the mean absolute tension output during the cat step cycle from the biarticular semimembranosusnosus posterior and semitendinosus was larger than that of the uniarticular semimembranosusnosus anterior (n=7), although this difference was not confirmed with inferential statistics. However, the tension-time plots in their results showed that such a benefit was not seen when muscle forces were expressed as a proportion of each muscle's maximum isometric force. Therefore, although the author's concluded that the "biarticular muscles may benefit from the combined action of two joints to maintain near maximal tension", it appears that the differences in absolute mean force between the muscles may be attributable to the inherently larger force producing capabilities of the biarticular muscles, in lieu of an optimization of biarticular muscle force based on decreased muscle displacements. It is also important to note that this study did not take the effects of the f/v relationship into account in the calculation of these tension values, and thus the mechanical benefit seen is related to the f/l relationship, omitting the effects of velocity. It also must be considered that any potential mechanical benefits seen in the feline species are not necessarily applicable to humans for two important reasons: First, the hamstring muscles in the cat differ from those of

humans in a multitude of ways (most importantly- line of action, moment arms, and muscle lengths). Second, the gait cycle characteristics of the feline are substantively different from those of humans, especially as the feline's progress through digit grade locomotion.

The geometrical model of Frigo and Pedotti (1978) predicted that the displacements of the biarticular hamstring muscles were larger during level walking than while ascending and descending stairs. It also predicted smaller muscle displacements of the biarticular hamstring muscles relative to the muscles of the shank, although inferential statistics were not used to evaluate this trend. Furthermore, this trend did not apply to comparisons of the biarticular hamstrings versus the BF_S. Examination of the example muscle length time plots in the paper reveals a displacement (maximum length- min length) of ~6cm in the BF_L versus ~4cm for the BF_S over the course of the level walking condition. A number of limitations of this model are discussed in the previous section entitled "Models to predict BF_L lengths".

Also in 1978, investigators out of Osaka tried to simulate the BF activation of two of the four coupling classes (KFHF, and KFHE) with isometric loads applied to the hip and knee joints simultaneously, as well as individually. At the load representing 100% of the maximum isometric force for each condition, the BF had its highest EMG activity during resisted isometric knee flexion alone, followed by the combined resisted isometric knee flexion and isometric hip extension, and finally the resisted isometric hip extension alone.

A systematic analysis of BF integrated EMG was also done during combined resisted isometric knee flexion and isometric hip flexion, with increasing load about either the hip or the knee joint. A constant load was placed resisting at the knee joint, while the load about the hip was progressively increased in sequential trials. The level of EMG with this action alone was considered 100, and was compared to motions with the addition of a load that would result in and "antagonistic joint action" about the other joint the biarticular muscle crossed. Large inter-subject variability in the changes in BF EMG was seen in response to the increasing load.

The investigators concluded that "the role of two-joint muscles and even of the single joint muscles surrounding the joints in joint movement has no set pattern". While the electrical activity of muscles during multi-segmental motion is undoubtedly complex, it is unlikely we are relegated to such an anarchistic conclusion. This study does in fact show that the BF is active during isometric simulations of KFHF and KFHE

motions. However, it is not entirely clear how these EMG levels would compare during real (dynamic) examples of the four couplings.

Later, smaller contraction velocities for the rectus femoris muscle versus the gluteus maximus muscle, and smaller contraction velocities for the medial Gastrocnemius versus the Soleus muscle were noted during the knee extension phase of jumping (Gregoire et al., 1984) using the a modification of an existing calf model (Grieve et al., 1978). A variety of limitations and an important delimitation of this investigation should be noted before using it to reach conclusions regarding biarticular muscle functioning. First, only a single subject's data was shown in the graphs comparing the muscle velocities, and no further analysis was indicated. Therefore the average magnitude and variation in these inter-muscular velocity differences due to movement kinematics are unknown. Although the data was undoubtedly true for the one subject, the generalisation of it to other subjects is unknown. Second, it should be pointed out that the lengthening velocities of the uniarticular muscles were also greater during the eccentric portion of the jump, which may theoretically result in a mechanical benefit to the uniarticular muscle based on the eccentric portion of the f/v relationship. Third, the contraction velocities calculated were based on moment arm values from prior research, and were taken to be constant functions of joint angle. Finally, inter-muscular differences in velocity of one muscle group are not transferrable to other muscle groups, due to differences in the muscle moment arms (between the two muscle groups, within a given muscle group, within the two joints each biarticular muscle crosses). Each one of these moment arm differences will affect the magnitude of the velocity difference and muscle displacement difference between muscles.

More recently, Visser et al (1990) used their model to predict that the lengthening effects of the knee joint to be larger than the shortening effects of the hip joint during a portion of a jump, initially resulting in a lengthening muscle velocity. Following this brief period, the BF showed a shortening velocity. This is particularly interesting because it conforms to the prediction of Elftman (1966) of an SSC during KEHE motions.

Hawkings and Hull (1990) applied their model to a single gait cycle from one subject. They found that the Gastrocnemius, biceps femoris, and rectus femoris had the largest displacements of all the lower limb muscles examined. This is interesting, since these three biarticular muscles therefore had larger muscle displacements compared to a number of lower limb uniarticular muscles. However, while the muscle length data

was presented for these three biarticular muscles, the other muscle length data was not presented, and thus there was no quantitative support for this conclusion.

A systematic evaluation of these two prevalent theories of the mechanical benefits of biarticular muscles has not been performed to date. Further, an investigation needs to be performed that also evaluates other classes of motion, which may in fact be detrimental to muscle function. Specifically, an investigation is needed which compares the BF_L to the BF_S during all possible types of knee and hip couplings during human motion, as well as gait. Simultaneous evaluation of the possibilities of velocity shift as well as displacement conservation should be included.

Hamstring Strain Injury

Injuries to the hamstring muscle have long been recognized as debilitating, as is evidenced by the word "hamstring", which can be used as a verb. The word's archaic meaning is to "cut the hamstring… and thereby cripple", but evolved to come to mean "to destroy or hinder the efficiency of" (American heritage dictionary). Hamstring strain injuries are a prevalent type of muscle strain (Orchard, 2002; Woodley and Mercer, 2004). Strain injuries are suspected to be due to excessive tensile forces, resulting in partial or complete tearing of the muscle-tendon complex (Speer et al., 1993).

It has been consistently observed and reported by medical practitioners that the BF_L is injured much more frequently than the semitendinosus and semimembranosusnosus muscles (Askling et al., 2007; Koulouris and Connell, 2003; Woodley and Mercer, 2004), making up as many as 124 out of 154 cases observed over a three year period at a given institution (Koulouris and Connell, 2003). These injuries to the BF_L most often occur proximally, either at the muscle-tendon junction (DeSmet and Best, 2000; Garrett et al., 1989), in the proximal tendon (Koulouris and Connell, 2003) or at the bony tendinous junction (the last was observed in water skiers-Sallay et al., 1996). Animal studies of rabbit muscle have heavily supported the idea that most strain injuries occur at the muscle-tendon junction (making up 178 out of 180 of the injury locations), regardless of which muscle was examined and their associated differences in muscle architecture (using one example of a fusiform muscle, a unipennate muscle, a bipennate muscle, and a multipennate muscle) (Garrett et al., 1988). However, in these animal studies the injuries occurred mainly at the distal muscle-tendon junction (Garrett et al., 1988),

which is not in agreement with the human injury reports (Garrett et al., 1989). Strain injuries appear to occur almost exclusively in the long head (DeSmet and Best, 2000; Woodley and Mercer, 2004), although injuries in the biceps femoris that occur at the knee appear to occur much more frequently in the BF_S (Terry and LaPrade, 1996). More extensive strain injuries can involve multiple hamstring muscles (DeSmet and Best, 2000; Garrett, 1996; Garrett et al., 1989). Semimembranosusnosus appears to be the least commonly injured hamstring muscle (Woodley and Mercer, 2004).

BF_L injuries are commonly known to occur in sprinters and track athletes (Askling et al., 2007). They also frequently occur in novice water skiers, who consistently report the injury occurring during resisted hip flexion with an extended or extending knee (Sallay et al., 1996) during the initial acceleration of the boat.

It is unclear where exactly in the step cycle strain injury of hamstring muscles normally occurs, although it is thought to be either the late swing phase, or in the early stance phase. The late swing has been modeled as the point where the largest stretching of the hamstring muscle group occurs (Frigo & Pedotti, 1978, Thelen et al., 2005b). The early stance phase has be found to contain the largest muscular forces due to ground contact (Orchard, 2002). A case study of an unexpected BF_L strain injury during a pilot study involving human inclined running presented a unique opportunity to estimate when during the running step cycle a hamstring muscle could be injured (Heiderscheit et al., 2005).Through analysis of marker trajectory deviations with adjustments for neuromuscular latencies, the investigators suggested the injury was most likely to have occurred in the late swing phase, when coupled hip and knee extension was occurring (a KEHE motion), although it may have also occurred very shortly after foot contact (Heiderscheit et al., 2005).

It has been suggested by some investigators that the biarticular nature of the hamstring could be one of the factors promoting its susceptibility to injury due to increased stretch (Garrett et al., 1984). Although logically we can predict specific circumstances where both the knee and hip joints would promote BF_L lengthening (KFHE motions) it is unclear what reference muscle the BF_L is being compared to for such a conclusion to be reached, and whether greater lengths would be seen in the various coupling types.

This investigation provides a unique opportunity to provide a graphical description of BF_L and BF_S muscle kinematics during the walking and running step cycles. This study may provide insight into possible hip and

knee coupling patterns which could exacerbate the length changes and/or force production in BF_L and predispose it to injury. Further, we hypothesize that a shift along the f/v relationship is possible in the BF_L relative to the BF_S, resulting in simultaneous shortening and lengthening muscle actions in a homonymous muscle group, during hip classes of motion traditionally associated with a mechanical benefit in terms of muscle displacement conservation and velocity shift (KEHE & KFKF). As a result of this phenomenon, it could be possible that injury results from conflicting sensory-motor control during a complex sensory feedback process (spindle and GTO based), or even in feed-forward control, during a repetitive task such as running. It is conceivable that motor control errors arise from alpha-gamma activation problems due to the differences in muscle kinematic within a muscle group for a same motion.

Methodology

This empirical study consisted of two parts. The first part involved the development of a model to compute the muscle lengths, displacements, and velocities of the BF_L and BF_S, using cadaveric derived muscle length equations with hip and knee angle as inputs. The second part of this study involved the use the model to compute muscle kinematics during four classes of coupled hip and knee motion, as well as during treadmill walking (3 mph) and running (7 mph).

Model Generation

Overview of Model Development

Cadavers were acquired in order to develop a mathematical model of the BF_L and BF_S muscles. They were dissected and screws were inserted into anatomical landmarks of interest. These landmarks were photographed and digitized with the cadaver sequentially moved through its hip and knee ranges of motion. These digitized points allowed the calculation of knee and hip joint angles, as well as the two dimensional estimation of origin to insertion lengths of BF_L and BF_S for each position. Compiling these measurements allowed the generation of BF_L and BF_S muscle length surfaces as functions of hip and knee joint angles, for each cadaver. Other anatomical measures were taken to allow normalization of muscle lengths to thigh length. A third degree bivariate polynomial was fitted to each of the individual surfaces individual and an average normalized surface was derived.

Cadaver Acquisition and Screening:

Five cadavers were secured from the Department of Human Anatomy and Cell Science, University of Manitoba. They were chosen based on availability. The specimens were full body and had not been dissected at the time of acquisition.

One female cadaver was not used for the model development. During dissection of this cadaver, it was noted that the right hip was locked in a position of hip external rotation. Resistance to internal hip rotation remained after the usual dissection procedure. Upon further investigation, it was discovered that a hip arthroplasty had been done on this leg, with the head of the femur replaced with a metal prosthetic. Since this was likely to result in unnatural joint kinematics upon manipulation, the protocol was not implemented with this cadaver.

Cadaveric Characteristics

All specimens were elderly, although their exact ages were not known. Four of the cadavers were female, and one cadaver was male. All had deceased in mid to late 2006, approximately one to one and a half years prior to dissection.

Measurement

Each cadaver was placed lying prone on a cadaveric dissection table for anatomical measurement with a carpenter's tape measure. All leg measurements were taken solely from the right leg. These measured were taken after the completion of the cadaveric dissection and screw placement. TABLE 3 reviews the characteristics and initial measurements taken on each cadaver.

The length of the shank was taken to be the distance from the proximal end of the lateral tibial condyle to the distal end of the lateral malleollus. The length of the thigh was taken to be the distance from the superior aspect of the greater trochanter to the distal end of the lateral femoral epicondyle. Trochanteric height was taken to be the straight line distance between the superior aspect of the greater trochanter and the distal end of the lateral malleollus. Finally, the distance between the centroid of the screw inserting into the right ASIS and the center of the marker placed superficial to the left ASIS was also measured. Finally, the cadaver height was taken to be the length of a line extending distally from the posterior aspect of the top of the head, to the bottom of the right heel.

The average height of all the cadavers was slightly less than previously reported averages of height for males (174.8 cm) and both males and females (168.3 cm, Shields et al, 2008).

TABLE 3-Cadaveric characteristics

	Average	**1**	**2**	**3**	**4**
Sex	1/3	M	F	F	F
Height (cm)	165.4 (9.24)	176.5	157.4	169.5	158.2
Shank length (cm)	38.3 (2.17)	40.3	38.6	38.1	35.1
Thigh length (cm)	42.8 (2.16)	43.8	43.3	44.4	39.6
Trochanteric height (cm)	81.1 (4.41)	84.4	81.9	83.5	74.7
ASIS to ASIS distance (cm)	24.2 (1.86)	25.6	21.5	25.2	24.4

Dissection

Details of the cadaveric dissection are provided in Appendix 1- Cadaveric Dissection .

Anatomical Land Marking

I. Overview

Marking screws were inserted into pre-specified boney anatomical structures or landmarks. This allowed increased precision and accuracy in the subsequent photography and digitization of said points of interest due to increased color contrast and visibility. The digitized coordinates were used for subsequent length and joint angle calculations.

All marking screws were placed on the right side of the body, and were secured using an electric drill. These marking screws were completely embedded in the involved bone in order to ensure the screw centroids were as close as possible to the boney sites they were meant to landmark. This close marking screw orientation to the bone also acted to minimize the effects of any inadvertent screw inclination relative to the long axis of the involved bone. All efforts were made to ensure each marking screw was inserted along a path perpendicular to the long axis of the bone being landmarked.

II. Landmarks:

- Right anterior superior iliac spine (right ASIS) - The marking screw was inserted with an anterior to posterior direction.

- Right greater trochanter (right GT) - The centroid of the greater trochanter was determined visually. The marking screw was inserted from lateral to medial.

- BF_L and BF_S proximal and insertions- the procedure for determination of these landmarks is discussed in the section entitled 'Muscle Origin and Insertion Centroid Determination'

- Midpoint of the femur - The midpoint of the femur was determined by dividing the thigh measurement in half, and measuring this length from the super aspect of the greater trochanter. Two marking screws were inserted into the midpoint of the femur. One was inserted into the lateral aspect of the mid femur, while the other was inserted into the anterior aspect.

- Right lateral femoral condyle (right LFC) - The centroid of the lateral femoral condyle was modelled as the centroid of an ellipse, and was determined visually. The marking screw was placed in this centroid.

- Midpoint of the shank- The midpoint of the shank was determined by dividing the shank measurement in half, and measuring this length from the super aspect of the lateral tibial condyle. Two marking screws were inserted into the midpoint of the shank. One was inserted into the lateral aspect of the fibula, while another was inserted into the anterior aspect of the tibia, just medial to the anterior border of the tibia.

- Right lateral malleollus (right LM) - A marking screw was inserted into the center of the lateral malleollus in a lateral to medial direction. The center was visually estimated.

- The center of the right and left patellae. The patella was palpated, outlined, and modeled as a triangle. The centroid of this triangle was taken to be the centroid of the patella. To determine the centroid of the triangle, 3 lines were drawn from each point of the triangle to the approximate (visually determined) midpoint of the opposing side. The intersection of these three lines represented the centroid of the triangle. A marker was used to puncture the anterior aspect of the sesamoid patellae. A screw was not used so as not to interfere with patellar motion.

- Left anterior superior iliac spine (left ASIS) - this boney marking was palpated over the skin and a marker labelled it anteriorly.

- Midpoint of the left femur - this was calculated as the midpoint of the measured thigh length. It was measured laterally, shifted anteriorly and marked on the anterior side of the left femur.

- Midpoint of the left tibia - was calculated as the midpoint of the measured shank length. It was measured and marked laterally, and then shifted anteriorly and tacked on the tibial ridge.

The left side of the cadaver was marked to enable calculation of hip abduction angle.

1. Muscle length: Origin and Insertion

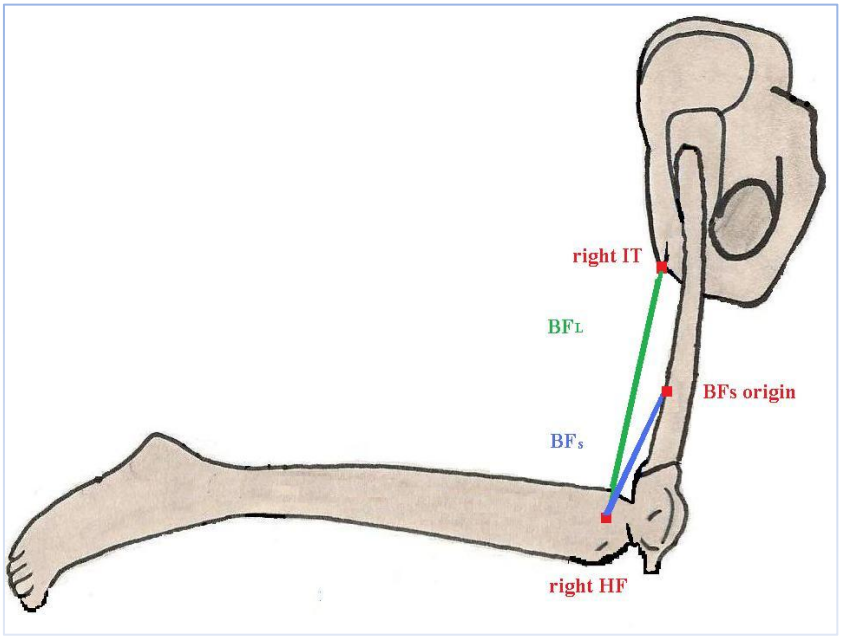

FIGURE 1- BF_L & BF_S muscle lines of action

Since the origin of the BF_S is essentially a segment of the linea aspera of the femur, the origin was estimated to be the midpoint of this segment. The insertion points of both the BF_L and BF_S were taken to be the centroid of the muscle insertion area on the lateral aspect of the head of the fibula (HF), as is commonly described (Moore and Dalley, 1999). The line of muscle action of the BF_S was taken to be a line connecting the bisector of the BF_S origin to the centroid of the insertion area on the HF (FIGURE 1). The origin of BF_L was taken to be the ischial tuberosity (IT) of the ischium. The line of muscle action of the BF_L was taken to be a line connecting the centroid of the origin area on the IT to the centroid of the insertion area on the HF (FIGURE 1).

The origin of the BF_L and the insertion of both the BF_S and BF_L were outlined as quadrilaterals, encompassing the bulk of the muscle attachment but excluding any slips to alternate attachment points. The exact attachment points were modelled as the center of equal masses at the vertices of the quadrilaterals. To calculate this, first the sides of the quadrilateral were measured with a rigid tape measure. The midpoint of each side of the quadrilateral was calculated, marked with a felt pen and carved into the bone with a scalpel. One line connected the superior and inferior side midpoints, and another connected the left and right side midpoints. The point of intersection of these two lines was taken as the attachment site centroid.

It should be noted that while the BF_L was modelled as having single origin and insertion sites, in reality the origin and insertions of the BF_L can be much more complex. The origin can have proximal slips to the sacrotuberous ligament (Gray, 1918), while the insertion can have distal slips to the popliteal tendon, arcuate popliteal ligament, lateral femoral condyle (Tubbs et al., 2006), and lateral tibial condyle (Sneath, 1955).

Cadaver Orientation

A specific cadaveric placement procedure was implemented to reduce the magnitude of undesired joint motions while allowing systematic adjustment of the hip and knee joint angles to cover the range of motion desired for the BF_L and BF_S model development. To ensure confounding accessory movements were reduced, it was necessary to create an apparatus that would secure the cadaver torso on its side, and also an additional apparatus that would allow the thigh to be secured at specific hip angles. The latter device would also be required to limit hip and knee internal and external rotation, and keep hip abduction constant. A pilot trial was done on one of the cadavers to determine the optimal size of the apparatuses components and the level of adjustability the apparatuses needed to ensure an equal amount of positional control for all the cadavers. Pictorial depictions and in depth descriptions of the apparatuses used can be found in "Appendix 2- Additional Cadaveric Setup Details and Figures".

Hip and Knee Angle Determination

The hip angle was defined as the anterior angle between ASIS, GT, and LFC. The knee angle was defined as the posterior angle between the GT, LFC, and the LM (see figure 2). This angle was calculated using the dot and cross product of the known vectors, GT to ASIS and GT to LFC. The measurements gained with this formula were initially cross validated with those of a digital compass (MB ruler, http://www.markus-bader.de/MB-Ruler/) to ensure the vectors were defined to acquire the angle required as opposed to its supplementary angle.

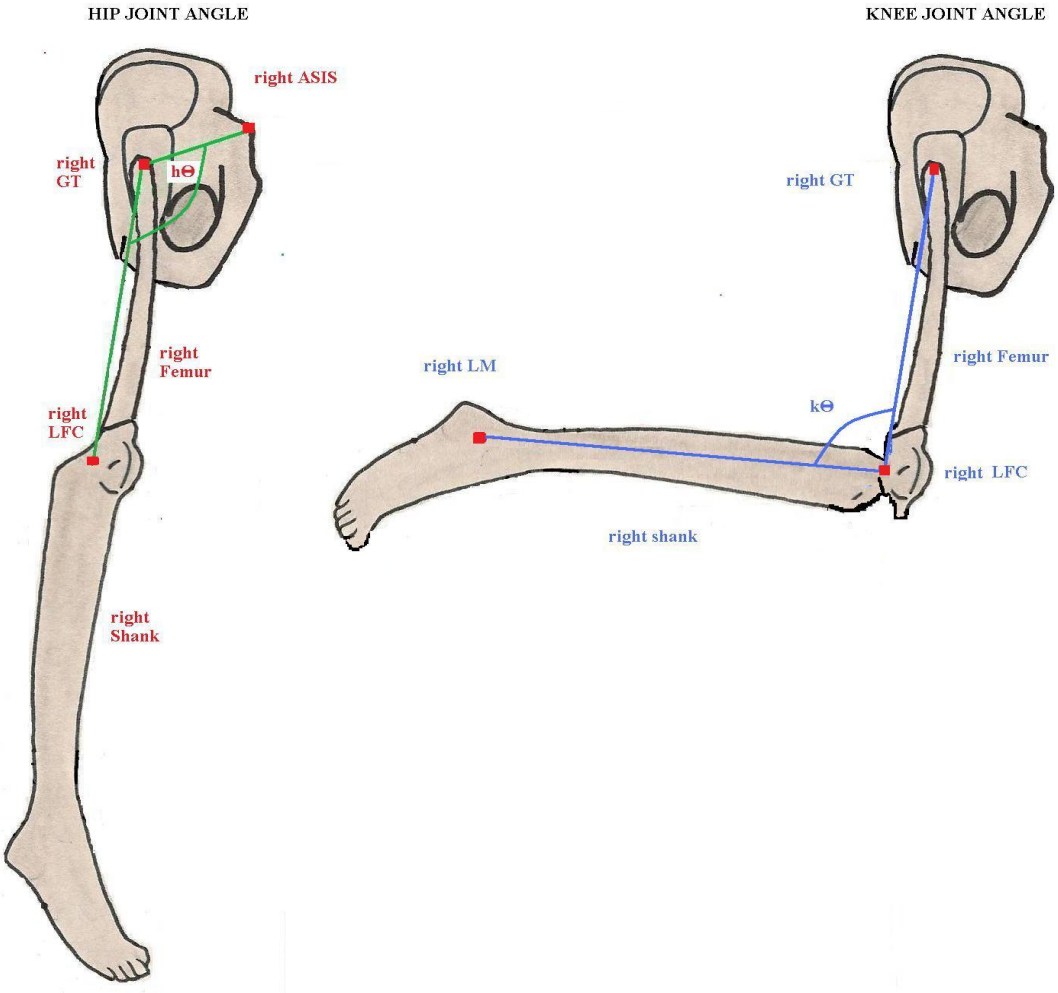

FIGURE 2- Knee and hip joint angle definitions

Hip and Knee Range of Motion

Each cadaver was aligned with the platform in such a way to maximize the range of motion for which the platform could act as a support for the cadaver thigh. Once this position was achieved and the cadaver was secured using the cage apparatus, a marker was placed beside the center of the patella and the thigh was moved through its maximum range of motion. This created a distinct black arc on the platform for each cadaver. This line was measured with a tape measure and was divided into ten equal portions, always including the extremes of the hip range of motion.

The knee range of motion was divided into approximately fourteen portions, which were estimated visually. It was not feasible to use a marking system for the knee joint angle divisions, due to the number of arcs and divisions this would necessitate given the four cadavers. However, these knee joint angles always included positions of full extension and extreme flexion. Thus each cadaver was placed in approximately 140 different hip and knee joint configurations.

As the knee angle was progressively changed through its large range of motion (145 degrees), the hip angle did not remain perfectly constant (mean CV 1.24%). As a result the mean hip angle for each hip position was used for modelling purposes. Further details of this procedure can be found in the Appendix entitled "Hip Angle Position Averaging". Knee and hip ranges of motion throughout the measurements were noted for each cadaver in TABLE 8.

The mean (SD) knee range of motion for all the cadavers was 146 (3.9) degrees, while that of the hip was 106 (5.1) degrees.

Digital Imaging

A digital SLR camera was used (Nikon D40X) to photograph the cadavers. The camera was set to aperture priority mode, with shutter speed automatically adjusted to ensure proper exposure. The aperture was therefore f/3.5; which was the largest aperture available at that specified focal length (18 – 20 mm). Exposure

times varied depending on lighting conditions at the time of the session. A remote control was used to take each picture, to avoid camera movement. The mounting system (FIGURE 3) maximized the possible distance from the camera lens to the cadaveric specimen. A carpenter's level was used to ensure that the camera plane was aligned horizontally from both front to back, and left to right. The distance from the camera lens to the subject's greater trochanter was approximately 118-128 cm (~4 feet), depending on the left to right ASIS distance (hip width) of the cadaver. This distance also enabled the visualization of the entire cadaver movement range with the lens in its least zoomed position. This distance was adequate to prevent fisheye distortion.

FIGURE 3- The camera mount. A) Overall view B) Close up view of mount.

Image Scaling

A scale was established by having two screws set with a known distance (centre to centre) in the femur, at a level equal to that of the origins and insertions of the muscles. The centroids were digitized in the images, and the two dimensional distance (pixels) between the centroids was determined using the distance formula. Thereafter, a scale factor (cm/pixel) was determined using this information. Table 3 illustrates the consistency of the scale factors for each cadaver.

TABLE 4- Scale factor consistency

Photograph to Real Life Distance Scaling					
	D1	**D2**	**D3**	**D4**	**Average**
Mean Scale Factors (mm/pixel) (SD)	0.47 (0.004)	0.47 (0.008)	0.48 (0.008)	0.45 (0.003)	0.47 (0.012)
CV (%)	0.930	1.792	1.578	0.699	

Muscle Length

In order to calculate the length of BF_L and BF_S for each photograph the two dimensional distance formula was used. Once the muscle length in pixels was calculated for each photograph of each cadaver, the length was converted to cm using the scale factor.

A validation of the photographic measure to a real life tape measurement was done. The calculated muscle lengths in 24 knee positions from two hip position setups, from a single cadaver were compared to BF_L origin to insertion distances tape measured in these same positions. The mean error with the calculated lengths was found to be negligible at <0.45mm (TABLE 5). Since hip abduction angle remained constant, the vertical distance from, as well as the orientation to, the camera would remain similar for the thigh throughout the protocol. Therefore it is likely the results of this comparison hold true for the rest of the hip and knee positions of the cadaveric protocol. It is also likely this relationship would hold across all cadavers, since the orientation of the right thigh to the camera was consistently parallel, and its distance from the camera was also similar. Positions of very large knee flexion were omitted, since it was not possible to measure the origin to insertion

distance with a tape measure in these positions. This issue originated from the fact that the calf began pressing into the exposed femur and acted as a mechanical obstruction to the proper placement of the tape measure from a straight line approximation of the muscle length.

TABLE 5- Comparison of photographic estimation of BF_L length versus tape measured length in two hip positions and twenty four knee positions (D4)

Position	Photographic BF_L Length (cm)	Tape Measure BF_L Length (cm)	Difference in Photographic BF_L Estimation (mm)	Mean Error in mm (SD)
H1K1	36.07	36.05	0.2356	0.448 (0.286)
H1K2	35.77	35.7	0.7315	
H1K3	35.26	35.35	0.8684	
H1K4	35.07	35.1	0.2886	
H1K5	34.77	34.8	0.296	
H1K6	34.62	34.7	0.776	
H1K7	34.08	34.15	0.7036	
H1K8	33.52	33.6	0.7758	
H1K9	31.66	31.75	0.8881	
H1K10	31.39	31.4	0.0768	
H1K11	31.23	31.25	0.2	
H2K1	38.03	37.95	0.8417	
H2K2	37.85	37.85	0.0097	
H2K3	37.49	37.5	0.1108	
H2K4	37.46	37.45	0.1319	
H2K5	37.29	37.25	0.3742	
H2K6	36.87	36.8	0.6678	
H2K7	36.54	36.6	0.6131	
H2K8	36.45	36.5	0.5393	
H2K9	36.20	36.25	0.4943	
H2K10	35.67	35.65	0.1851	
H2K11	35.05	35	0.5046	

H2K12	33.70	33.7	0.0783
H2K13	32.94	32.9	0.3747

1) Global moment arms

A global moment arm is a measure of the overall effect of a given joint on the displacement of a muscle (Buford, 2001). Each moment arm is calculated by dividing the maximum joint range of motion and by the amount of muscle displacement measured through that range of motion. Mathematically these calculations are expressed as follows:

i. $$GMAknee = \frac{\mathbf{Lkmax - Lkmin}}{\mathbf{k\theta max - k\theta min}}$$

Where:

GMAknee= global muscle moment arm about the knee joint

Lk_{max}= maximum BF_L length at full knee extension

Lk_{min}= minimum BF_L length at full knee flexion

$k\theta_{max}$= knee angle at full knee extension

$k\theta_{min}$= knee angle at full knee flexion

&

$$GMAhip = \frac{Lhmax - Lhmin}{\mathbf{h\theta max - h\theta min}}$$

Where:

GMAhip= global muscle moment arm about the hip joint

Lk_{max}= maximum BF_L length at full hip flexion

Lk_{min}=minimum BF_L length at full hip extension

$h\theta_{max}$= hip angle at full hip flexion

$h\theta_{min}$=hip angle at full hip extension

Therefore the global moment arm is the partial derivative of muscle length with respect to knee and hip joint angles. Since the moment arms at the knee and hip are geometrically predicted to interact, models which account for this will show a global moment arm at a given joint that will be affected slightly by the configuration of the other joint. In our model it was necessary to repeat the global moment arm calculation with the other joint being progressively moved through its range of motion, since this model accounts for the moment arm interaction at both joints. The mean of all global moment arms at each joint was calculated, resulting in two averaged global moment arm estimations: one for the knee and one for the hip. These average values were taken to allow comparisons with models which did not account for the moment arm interaction.

It is more insightful to compare global moment arms across models in lieu of muscle displacement measures, since the models are often limited to different ranges of motion. Global moment arms provide a measure of displacement normalized per degree range of motion at a given joint, overcoming this issue.

Ratio of Global Moment Arms

The ratio between the average hip global moment arm and the average knee global moment arm was also calculated to give a description of the relationship between the mean hip and knee BF_L moment arms for comparison across models, since differences in this ratio across models are related to differences in muscle length predictions across models. The knee to hip velocity ratio can be compared to the global moment arm ratio of the BF_L in order to determine whether a motion is hip or knee dominant. If the knee to hip velocity ratio is larger than the global moment arm ratio, the motion can be considered knee dominant, and it is likely that both the BF_L and BF_S are undergoing the same length change directions. If the knee to hip velocity ratio is smaller than the global moment arm ratio, the motion can be considered hip dominant, and the BF_L and BF_S are likely undergoing different length change directions. See Figure 4 for how the differing global moment arm ratios of two existing models (Hawkings and Hull, 1990; Visser et al, 1990) affect their predictions of BF_L muscle length change during incongruent effects circumstances with a knee to hip velocity ratio of 4. The model of Hawkings and Hull would predict this movement would see the knee having the larger effect on muscle length, resulting in

similar actions of the BF_L and BF_S. In contrast, the model of Visser would predict the hip joint would be having a larger effect on muscle length, resulting in different BF_L and BF_S actions.

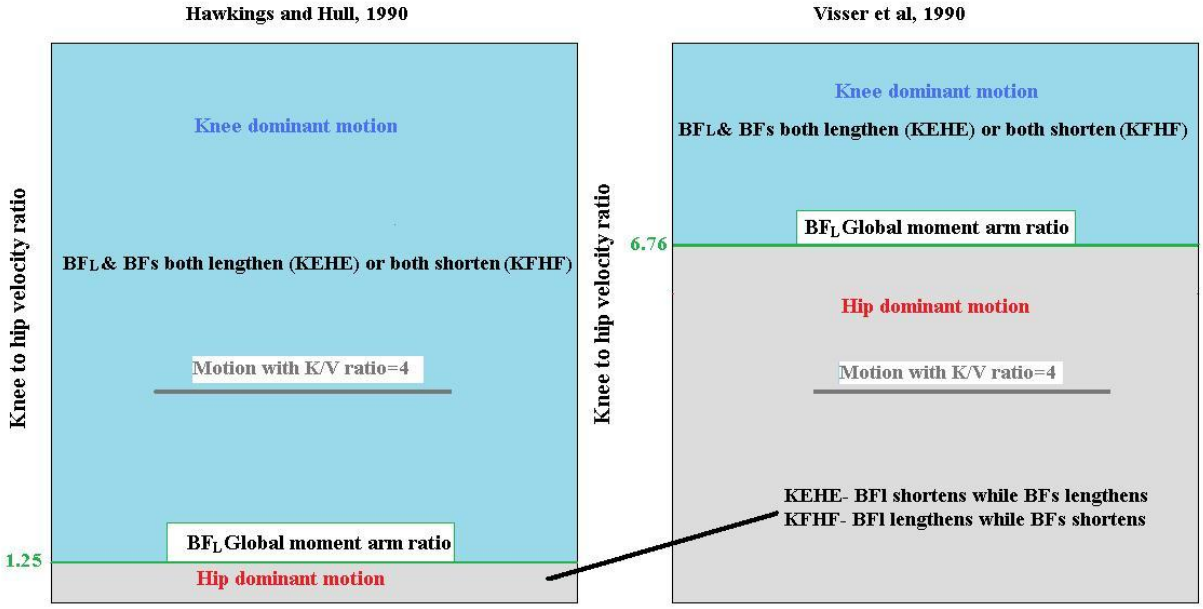

FIGURE 4- Comparison of the predictions of two existing models (Left- Visser, 1990; Right- Hawkings and Hull, 1990). The model on the left (Hawkings and Hull et al, 1990) predicts the same muscle length change direction for BF_L and BF_S for an incongruent effects motion with a knee to hip velocity ratio of 4, while the model to the right (Visser et al, 1990) predicts different muscle actions for BF_L and BF_S.

Muscle Kinematics during Coupled Motions and Gait

Overview of Protocol: First, subjects were recruited and screened. Next, anatomical landmarks were palpated and reflective markers were placed on these landmarks. Then, anatomical measurements were taken with a flexible plastic tape measure. Following this, a movement protocol was performed, with the VICON motion analysis system digitizing and recording the marker coordinates. This protocol included the four coupled motions at maximum velocity, and a progressive speed treadmill trial. The VICON coordinate data was screened and exported. The knee and hip joint angle data was imported into the model to derive BF_L and BF_S muscle kinematics.

Subject Recruitment

- Recruitment and Inclusion criteria

Subjects were recruited from the Bannatyne and Fort Garry campuses, University of Manitoba, via word of mouth. Subjects were acquainted with the investigators, forming a sample of convenience. Subjects were required to be free of hip, knee and ankle pathology, neurological pathology and/or any other medical conditions which would contraindicate their participation in this study. Subjects were also required to have a solid comprehension of the English language and needed to demonstrate that they had the ability to follow directions. Pregnant or lactating females were excluded from participation. Finally, subjects were also required to have not consumed alcohol twelve hours prior, smoked two hours prior, and not performed strenuous lower body exercise forty eight hours prior to the testing session. These criteria were included to reduce the chance that abnormal human movement kinematics would be collected.

- Subject Screening and consenting

Both an REB approved informed consent document and the Physical Activity Readiness Questionnaire (PAR-Q, 2002) were read and signed by all subjects prior to the onset of any physical activity. Subject's who did not meet inclusion criteria or gave a positive answer to the PAR-Q questionnaire were debriefed and dismissed from their participation in the study. All prospective subjects were screened upon their arrival for the testing session.

Subject Population

A total of eight prospective subjects were recruited for the human portion of this investigation. Seven prospective subjects passed the screening process and completed the protocol. The one prospective subject was screened from participation due to a positive answer on the PAR-Q questionnaire. In addition one subject's data was not used due to technical problems with the motion analysis system, resulting in poor digitization of the reflective markers. Therefore six subjects contributed data to this investigation. All subjects were young (20-34 years of age) apparently healthy individuals, who were recreationally active.

This number of subjects exceeded the *n* suggested by a power analysis previously conducted in G-power software (2007, http://www.psycho.uni-duesseldorf.de/abteilungen/aap/gpower3). Due to its importance, mean muscle velocity was chosen for the power analysis. A 25% difference in velocity between the BF_L and the BF_S was assumed, along with an expected variance of 9%. This represents a very modest estimation of the velocity differences that could be seen between the two muscles, since it was anticipated that during incongruent effects circumstance the muscles could have different velocity directions (which would require a difference >100%). These measurements were used to calculate effect size (assuming one group had a mean of 100% thigh length/s while the other had a mean of 80% thigh length/sec, and both groups had standard deviations of 3 and an n of 4). To approximate probabilities of 0.95 for rejecting a false null hypothesis (power) and 0.05 for accepting a false null hypothesis (alpha) based upon the estimated effect size, a sample size of 4 would be required. With the rounding up of the required n, the actual power of the test was in fact slightly higher than the set requirement, at 0.97.

Data Acquisition

A motion analysis system (Vicon Motion Systems) was used. This data was collected as three dimensional coordinates of reflective markers placed on subject anatomical landmarks (see "marker placement" section below). Markers were sampled at 100 Hz.

Marker Placement

The anatomical landmarks identified on the cadavers and used for the model's definitions of hip and knee joint angles were recreated on the live human subjects. Reflective markers were placed on the right side at the following locations: ASIS, the right posterior superior Iliac Spine (right PSIS), GT, LFC, as well as the left ASIS.

In pilot trials, markers were initially placed on the right IT and the right HF, to provide an estimation of the instantaneous origin to insertion length of the BF_L for subsequent cross validation with the cadaveric model.

However, two problems arose. First, the origin to insertion length estimation was found to be inaccurate during due to large shifting of the skin and clothing around the ischial tuberosity, in concert with the upward shifting of the gluteal muscles seen with increasing amount of hip flexion. Second, having the right LFC and right HF markers in such close proximity often resulted in digitizing error due to the markers blurring together, or the disappearance of the right HF marker. Thus use of these two markers (the right IT and right HF) was subsequently eliminated from the protocol. One of the subjects had the marker on the right ASIS obscured during a portion of the running treadmill trial and therefore this subject's data was not used for the treadmill trial (S5). However, this subject's data was good during the four coupling classes, and was therefore used.

Form fitting and non reflective clothing was worn by all subjects. Shoes were also required to be non reflective. If the subject's clothing did not meet these criteria, appropriate clothing was provided by the investigator. The procedure for land marking anatomical measurements is given in the appendix entitled "Human Subject Land marking".

Preliminary Anatomical Measurements

Measurements of subject height, trochanteric height, thigh length, shank length, and inter ASIS distance were taken. These lengths were defined in the same manner as on the cadaveric specimens, namely:

- The length of the thigh was taken to be the distance from the superior aspect of the greater trochanter to the distal end of the lateral femoral epicondyle.

- The length of the shank was taken to be the distance from the proximal end of the lateral tibial condyle to the distal end of the lateral malleollus.

- Trochanteric height was taken to be the straight line distance between the superior aspect of the greater trochanter and the distal end of the lateral malleollus.

- The inter ASIS distance was measured as the distance between the centroid of the marker on the right ASIS and the centroid of the marker on the left ASIS.

- Subject height was taken to be the length of a line extending distally from the top of the head, to the bottom of the right heel.

Subjects were measured in a standing position, with footwear removed. All measurements were taken using a flexible plastic tape measure, with the investigator adjusting his perspective to minimize parallax error in the recorded distance. A summary of these measurements appears below. Measurements were rounded to the nearest 0.1 cm.

TABLE 6- Human subject characteristics

Subject	Mean (SD)	S1	S2	S3	S4	S5	S6
Age	28	26	25	29	34	26	28
Sex	3/3	M	F	F	F	M	M
Height (cm)	175.7 (13.92)	191.5	157.5	172.9	162.6	180.2	189.4
Shank length (cm)	39 (3.86)	43.1	33.5	37.6	36.8	39.6	43.5
Thigh length (cm)	43.4 (3.34)	48.5	41.2	40.6	41.8	41.5	46.7
Trochanteric height (cm)	94.3 (6.84)	102.6	84.3	90.0	94.5	93.1	101.0
ASIS to ASIS distance (cm)	25.6 (0.54)	25.5	26.3	25.6	25.0	24.8	25.1

Testing Protocol

1) Overview

Data collection occurred over 1-2 sessions, totalling 1.5-2 hours of testing per subject. In situations of multiple testing sessions per subject, consistent inter-trial marker placement was achieved by comparing distance measurements between markers across testing sessions, and the use of consistent palpation procedures. Subjects were asked to wear the same clothing, or were provided with consistent clothing. Compared distances (See Above) were allowed to vary by less than 2 mm between testing sessions.

2) Movement Ordering

Each full testing session involved three sections: single joint motions, performance of four types of coupled motion at two different speeds (excluding warm ups), and a treadmill trial with progressive speed increases followed by a walking cool down. Subjects were asked to draw slips of paper out of a bucket to randomly determine the order in which the four couplings would be performed. Due to its fatiguing nature, the treadmill trial was always performed following the performance of the four coupled motions (refer to TABLE 7 for a depiction of the testing session structure). Each performance of a movement was followed by a brief (< 5s) period where the subject would resume the proper starting position. This was done to ensure proper performance of the motion.

3) Subject Positioning

Subjects were centered on a platform below the VICON cameras and aligned to maximize the number of cameras concurrently able to see the markers on the subjects. Subjects faced a direction that allowed the researcher a sagittal view of the subject. This allowed the investigator to visually assess the motion while operating the VICON. The kicking trial required that the subjects face a wall in order to have a solid surface to kick a beach ball against. This requirement originated from a need to decrease the ball's velocity, in order to protect the VICON equipment and to facilitate the quick repositioning of the ball. In response to this new subject position, the investigator adjusted viewing positions to maintain a sagittal perspective.

4) Overall Subject Instruction and Warm-up Trials

Instructions on the performance of each motion were given at the onset of each respective warm-up trial. The instructions contained information about the desired start and end positions of the motions, and the combination of hip and knee joint motion that each motion was meant to represent. In addition, instructions were given on specific arm of trunk positions to be held throughout the motion. The investigator also demonstrated proper execution of each of the required motions prior to the subject's performance of the motion. For the maximal trails, focus was placed on performing the trials at maximum speed, not on exerting maximal effort.

Warm up trials consisted of three consecutive grouping of two trials of the given motion. Each grouping was performed at an increasing perception of maximum velocity (i.e. 2 X 40%, 2 X 60%, and 2 X 80%). The purpose of the warm up trials was threefold. First, it was meant to provide a motion specific warm up with the purpose of increasing muscle blood flow and muscle temperature. Second, it allowed the subject to perform at least six trials of each motion prior to the analyzed trials, thus reducing any novelty associated with the performance of the motion, and providing the opportunity for the subject to acquire a kinaesthetic reference of what a good trial consisted. Finally, the grouping of two trials at the same speed was meant to accustom the subject to performing multiple trials at a consistent speed, with the intent of decreasing trial variability within the maximum speed condition. If desired, subjects were allowed to attempt the required start and end positions on their own prior to performance of the motions in their entirety.

Subjects were provided verbal feedback on their performance of the warm-up trials, and were allowed additional warm-up trials if they lacked self efficacy in the performance of the motion. Breaks were added to the warm-up as needed to prevent fatigue. In turn, subjects were instructed to give feedback to the investigator regarding their perception of the maximum trials in comparison with trials in the warm up that were deemed good.

Five to ten minute breaks occurred between movement couplings to allow the investigator to briefly review the previous couplings trials for quality assurance and provide instruction on the subsequent motion. A longer break (approx 10 minutes) occurred between the final coupling and the treadmill trials, to allow time for equipment set up.

TABLE 7- Testing sequence

Motion	Details	
Coupled Motion 1 Coupled Motion 2 Coupled Motion 3 Coupled Motion 4	Respectively for the four coupled motions: A) Practice trials- 2 reps X 40%, 2 reps X 60%, 2 reps X 80% B) Rest 1 min C) Fast trials- 3 reps, reset between reps, maximum speed	
Treadmill Trial	Progressive Warm Up	
	Time (s)	Speed (MPH)
	0s-30s	2
	30s-1 min	3
	1- 1 min 30s	4
	Progressive Speed Increase	
	1min 30 s- 1 min 40 s	4.2
	1 min 40 s- 1 min 50 s	4.4
	1 min 50 s- 2 min	4.6
	2 min - 2 min 10 s	4.8
	2 min 10 s -2 min 20 s	5
	2 min 20 s -2 min 30 s	5.2
	2 min 30 s -2 min 40 s	5.4
	2 min 40 s -2 min 50 s	5.6
	2 min 50 s -3 min	5.8
	3 min -3 min 10 s	6
	3 min 10 s- 3 min 20 s	6.2
	3 min 20 s- 3 min 30 s	6.4
	3 min 30 s- 3 min 40 s	6.6
	3 min 40 s- 3 min 50 s	6.8
	3 min 50 s- 4 min 20 s	7
	Cool Down	
	4 min 20 s- 6 min- 20 s	3

5) Overall Movement Trial Assessment

Visual assessment of the movement trials occurred in live time. A trial was deemed poor if:

1. The start and end positions deviated significantly from the outlined criteria
2. The subject lost his/her balance
3. It was obvious that the proper coupling had not occurred at any point in the motion
4. The subject indicated that they felt the trial was not at the proper speed

5. The subject showed visual signs of fatigue
6. The performance of the motion was truncated (e.g. subject stubbed toe, stopped the motion, etc…)

When time allowed, VICON playback review occurred after each coupling was complete. The visualization playback function in the VICON Workstation software was used in these cases to briefly review the trial for the above criteria, as well to verify the continuous presence of all the anatomical markers throughout each trial.

If a trial was deemed visually poor, additional repetitions were added. If the number of additional repetitions was to exceed two or the reason the trial was poor was due to subject fatigue, an additional break was inserted prior to the performance of the extra motions. This was done to reduce cumulative fatigue and promote recovery.

If the trial was intended to be maximum speed, but the effort appeared sub maximal, or the motion was visually slow relative to other repetitions, the subject was asked whether they felt the speed was appropriate. If they felt it was an appropriate speed, the trial was kept, otherwise the trial was repeated.

6) Treadmill Trial

A progressive warm up was performed leading to a thirty second running trial. Initially the treadmill speed was increased by one mph every thirty seconds, and then as the velocity reached higher levels, subsequent increases occurred at 0.2 mph every 10 seconds. Following the time at 7 mph, a 3 min cool down walking trial was performed (see TABLE 7 for further details of the protocol).

Subjects were instructed to choose a gait pattern (in terms of stride length and stride frequency) natural for them, and to maintain it until the subsequent speed increase. If a change from the initial gait pattern was needed in the longer 3 mph or the 7 mph portions, this was noted and the initial gait pattern was discounted

from the analysis. Subjects were also instructed to keep an elbow flexion angle of approximately 90 degrees, to avoid having the arm swing interfere with the cameras' views of the markers.

Additionally, only data within the middle twenty seconds of the thirty second 7mph trial was considered for the running analysis. This was to eliminate the analysis of any transition kinematic period as the subject was adjusting to changes in the speed setting of the treadmill. It was also done to allow the subjects some time to try a few gait patterns in the first third of the trial (if needed), and then select the one that felt best. Similarly, only the middle minute of the cool down was considered for the walking analysis, with the additional consideration of allowing the subject some recovery from the thirty seconds of running.

Data Quality Control and Cropping

Trials were cropped based on specific criteria for each coupling. The goal of cropping the four coupling trials was to isolate the part of the motion that was anticipated to contain the desired coupling.

The portion of the jumping trials included for analysis began at the bottom of the squat, following any weight shifting or residual countermovement, and ended once the knee joint was fully extended. Any subsequent hip extension motion (if present) was not included, due to its single joint nature.

The portion of the paw included in the analysis began from the predefined start position, to the point where the hip was fully extended. It was found that subjects had the tendency to flex the hip after peak hip extension, perhaps partly due to elastic resistance of the hip flexors, and perhaps also to facilitate further knee flexion. This part of the motion was not considered for analysis due to it consisting of the wrong coupled motion (KFHF instead of KFHE).

The portion of the kick considered for analysis began with the onset of hip flexion, and ended once the knee was fully extended. Following this, the hip would often keep flexing as the knee re-bent (flexed) to varying degrees. This follow-up motion was not included in the analysis since it was not a KFHE motion.

The onset of the tuck analysis was marked by the point where the subject was in the air, with the knee moving from an extended position to a flexed one. The end of the analysis occurred once the knee reached maximum flexion. Any subsequent hip flexion (if present) was normally accompanied by a re-extension of the knee joint. This part of the motion was not considered for analysis based on the fact that it was comprised of the wrong coupling (KEHF instead of KFHF).

Cropping of the four coupling trials occurred both visually in the VICON workstation software, and a MATLAB script created by the investigators further trimmed that data based on end point triggers (e.g. the occurrence of maximum hip extension, etc...) to allow greater precision (See "Gait Cycle Averaging and Subclass Separation" for further details).

Data Export

The three dimensional coordinates (x, y, z) of all the markers were exported to comma separated value (.csv) format using the VICON Workstation basic export function. A date stamp and an index column associated with the exported coordinates were also included, the latter to enable subsequent calculation of time data. This exporting procedure occurred separately for each movement repetition, with the exception of the treadmill trials.

Calculated Kinematic Parameters

The exported CSV files were batch processed and analyzed with Matlab 2007 software (version 7.5). The following key parameters were calculated among others:

- Time calculation: The sample index data was multiplied by the sampling rate to generate the running time scale for each trial.

- Movement time: This was measured as the difference between the end time and the initial time, and was expressed in seconds.

- Joint flexion/extension angles: Planar versions of the cadaveric joint angle calculations were used to calculate the hip and knee joint angles for the trials. The same steps were used as for the cadaveric angle determination, and the vectors in the knee and hip joint angle calculation were also defined as seen in the cadavers, except calculations involved three dimensional points instead of two dimensional ones.

The possibility of differences between the cadaveric and human marker placement, and therefore angle measurement, should be acknowledged. It was inevitable that some marker movement (both translation and slight rotation) relative to the bony structure it was meant to landmark, would occur during fast motions such as those examined. These shifts originate from movement of skin, as well as clothing (where applicable). Attempts were made to minimize this by placing the markers directly on the skin with the exception of the GT, which was placed on fitted clothing.

There was also less precision in the determination of relevant boney marking locations, as well as in the estimation of thigh length in live subjects compared to cadavers. These issues originate from the necessity of surface palpations. To overcome this issue, multiple palpation techniques were used per landmark when needed, and efforts were made to palpate the top of the GT as well as the tibio-femoral joint in order to better approximate the length of the thigh.

- Muscle length: BF_L and BF_S length (% thigh) were estimated through the application of model equations generated from the cadaveric data (see TABLE 9 for formulae, and section entitled "BF_L and BF_S Model Description" for full details). The equation used hip and knee joint angle as inputs. The normalized muscle length outputs from the model were then multiplied by the respective subject's thigh length to acquire muscle lengths in cm.

- Angular velocities: Angular velocities of the hip and knee joints were taken as the finite difference derivative of the respective joint angle-time plots. They were expressed in degrees/s:

$$\frac{\Delta\theta}{\Delta t} = \omega$$

Where:

= angular muscle velocity in degrees/s

Δl= change in muscle length

Δt= change in time (time step)

Calculated muscle length-time data series were all filtered using a fourth order low pass Butterworth filter with a cut off frequency of 8 for the four coupling classes. This cut off value was chosen based on a systematic examination of the derived BF_L velocity time plots of a single subject during the four classes of motion and the walking and running gaits, using a range of cut off frequencies from 1.5-25. Eight was found to be a cut off frequency that avoided a parabolic over smoothing of the derivative length plots, while still eliminating higher frequency noise from the process of marker digitization during fast motion.

- Linear muscle velocities: Linear velocities of the BF_L and BF_S were calculated as the finite difference derivative of the respective normalized muscle lengths. Thus they were expressed in both units of cm/s and % thigh/s:

$$\frac{\Delta l}{\Delta t} = v$$

Where:

v= linear muscle velocity in % thigh/s

Δl= change in muscle length

Δt= change in time (time step)

Therefore in this investigation a lengthening muscle velocity would be represented by a positive velocity, while a shortening muscle velocity would be represented by a negative velocity, contrary to convention.

- Min and maximum determination: The maximum values of the angular and linear velocities for each of the time series were taken to be the largest sampled measurement for each trial, and the minimum values for each of the time series were taken as the smallest measurement. The maximums and minimums were determined for the hip angle, knee angle, hip and knee angular velocity BF_L and BF_S length, BF_L and BF_S linear velocity.

- Linear muscle displacements & angular joint displacements (ranges of motion): These were taken to be the differences between the measured maximum value and the measured minimum value for the given parameter (muscle length or joint angle, respectively).

- Peak muscle velocity: this was defined as either the maximum or the minimum muscle velocity value, based on the expected muscle length change direction occurring. In the incongruent muscle effects motions, this peak was taken to be the number closest to resulting in a BF_L velocity reversal relative to the BF_S, if such a reversal did not occur.

- Velocity shift: this parameter was calculated to evaluate the magnitude of the shift between the BF_L and BF_S. It was calculated using the following formula:

$$Vshift_{BFl=}\left(\frac{VBFl_{mean}-VBFs_{mean}}{VBFs_{mean}}\right)x\ 100$$

Where:

VshiftBF_L = BF_L velocity shift expressed as a % of BF_S mean velocity

$VBF_{L\ mean}$ = Mean BF_L velocity

VBF_{Smean} =Mean BF_S velocity

Gait Cycle Averaging and Subclass Separation

The gait trials of each subject and speed were broken into step cycles using an algorithm to detect peaks in hip extension. Once separated, the timescale and joint angle data for each step cycle was normalized and interpolated to ensure all step cycles were composed of the same number of data points, regardless of their durations. The normalization and interpolation was necessary since the number of data points for each step cycle varied initially based on differences in the individual step cycle durations. These adjusted step cycles were graphically overlaid for each subject and speed using hip angle-time, knee angle-time, and hip angle-knee angle (cyclogram) plots to help assess the similarity of each step cycle to its peers. Ten step cycles for each subject and speed were then selected from the most densely populated movement trajectory (the attractor) on the respective overlaid cyclogram plots.

The hip and knee data of each group of ten cycles was averaged at each point in the normalized time scale, in order to generate a mean normalized step cycle for each person and speed. This resulted in a total of ten averaged data sets (5 subjects X 2 speeds). The normalized time scale was then multiplied by the mean cycle duration for the respective subject and speed, generating time scales in seconds associated with each averages data set. This conversion back to absolute time units was necessary to enable calculation of angular joint and linear muscle velocities.

Two types of gait analysis followed. First, an analysis of each of the 8 complete averaged gait cycles was performed to enable examination of complete muscle length-time and muscle velocity-time plots for the BF_S and BF_L, and to provide an overall estimation of average muscle kinematics for the entire step cycle. The kinematic outputs were then grouped based on treadmill speed and averaged, resulting in descriptive comparisons of averaged kinematics for the walking and running gaits.

The second more comprehensive analysis involved the separation of the averaged cycles for each subject into their coupling components (the previously defined four classes of motion), and then further division of these components based on the portion of the gait cycle during which each coupling was occurring. This resulted in separation of the gait cycle into what was termed gait coupling subclasses. Occurrence of these subclasses was found to be quite stable between subjects for each gait speed (see Appendix 5- Gait Subclass

Frequency). Only gait subclasses that were present in at least three out of the five subjects were included in the statistical analysis. Appendix 5- Gait Subclass Frequency indicates those gait subclasses excluded (identified in bold font).

Isolation of single joint motions (defined as motion with a joint angle change of less than 5 degrees/s at one joint while the other showed a change greater than this) was also attempted in the gait cycle, but ultimately rejected on the basis that only scattered points on the cyclogram were identified as meeting said criteria. Removal of these points would have resulted in separations of otherwise uninterrupted couplings, which would have further complicated the analysis and interpretation of the data. It is also arguable that no significant single joint motion occurs during the gait cycle on average, since the changes in both joint angles on a cyclogram were visibly monotonic for a given subclass of motion.

Coupling subclasses were named based on both the specific multi-segmental coupling occurring, as well as either the portion of the gait cycle in which the coupling occurred, or a key event that occurs during said coupling (e.g. KEHF-mid swing, KEHF-heel strike). The separation of the gait cycle using said criteria is to our knowledge novel to gait analysis, as current classification schemes either separate the step cycle into portions based on periods (e.g. stance versus swing), key events (e.g. initial contact, mid swing), or the mechanical task being performed (e.g. weight acceptance, limb advancement) (Perry, 1992). The only classification scheme that incorporates either of the joint motions into its classification terminology is one used in the study of knee prosthetics, which combines the gait cycle period and the average knee motion for a particular portion of that period (e.g. stance extension, swing flexion) (Martinez-Villalpando & Herr, 2009). The proposed classification scheme has the advantage of allowing greater insight into changes in multi-segmental coupling throughout the step cycle, and prediction of the direction of velocity shift of a biarticular muscle relative to a chosen reference muscle. Following identification of the subclasses of the gait cycles, these subclasses were color coded and plotted on three types of plots (cyclogram, BF_L length-time, and BF_L velocity-time) to provide a temporal context for the changes in inter-joint coupling and the resulting BF_L muscle kinematics.

A few details regarding the use and interpretation of cyclograms are warranted. Cyclograms are three dimensional plots depicting the position of one joint angle as a function of both time and another joint angle, with the graph perspective angled so that the time axis is ignored. A given combination of joint angles therefore occupies a single point on the two dimensional depiction, and series of positions form a line in this vector space

(Sykes, 1975). Cyclograms are useful tools for the depiction of changes in multi-segmental coupling, as the direction of the vector indicates the type of coupling occurring. Perfectly vertical or horizontal vectors would indicate motions or sections of motions with no multi-segmental coupling (single joint motion). Assuming the joint angle ranges plotted are equivalent, a diagonally oriented line would represent a motion with equal and constant velocities at both joints. Cyclic motions form overlaid closed geometric shapes on these plots (Sykes, 1975). Therefore a single cyclic motion would form a single closed geometric shape. These plots are also useful to identify and compare different inter-class changes within a motion featuring multiple multi-segmental couplings (Winstein & Garfinkel, 1989). When a change in multi-segmental coupling occurs, a turning point is created in the vector plotted on the cyclogram. Turning points with sharp edges demonstrate an inter-segmental coordination of changes in joint displacement direction (termed "turning point synchronization" by Winstein and Garfinkel (1989)). In contrast, those turning points with rounded trajectories demonstrate a "decoupled coordination" and "phase offset". In our terminology this would mean that the ratio of the joint velocities would take on a number of different values through the transition before possibly stabilizing in the next multi-segmental coupling. While this investigation will not explore this idea of decoupled coordination, examination of turning points on cyclograms can identify changes in multi-segmental coupling, which is useful for determining whether the four examples of the classes of motion were performed properly, and will help identify key events in the step cycle. While color coding of these graphs based on multi-segmental coupling is not as essential since the slope of the line gives an indication of this, it can still provide an additional visual cue to facilitate understanding.

The subclasses of each subject's gait cycle were separated and the kinematic outputs for each subclass were calculated. Then the kinematic outputs of each subclass were grouped across subjects and averaged to enable statistical analysis. Running gait data was kept separate from that of the walking gait data, due to fundamental mechanical and temporal differences between the gait cycles (such as the presence of an airborne phase in the running gait cycle). In those subjects who did not have particular subclass of motion present in the analysis of a given gait speed, such trials were deemed missing for statistical purposes.

Any subclasses occurring during the mid swing of the gait cycle were included in the analysis for comparison despite prior observations that hamstring is generally less active during this phase (Thelen et al, 2005a). This was done due to the perceived importance of understanding the passive muscle kinematics occurring during these subclasses in addition to the active muscle kinematics occurring in the other subclasses.

Statistical Analysis

- ANOVAs for four coupling classes:

A within subjects multivariate ANOVA with muscle type as a factor, & mean muscle velocity, peak muscle velocity, absolute muscle displacement, and relative muscle displacement as dependent measures was conducted. This process was repeated on each of the four coupling classes.

To assess inter-coupling differences in specific angular variables not affected by muscle type, a between subjects ANOVA was conducted with coupling class as a factor. The dependent variables included movement duration, absolute mean knee velocity, absolute mean hip velocity, peak hip velocity, peak knee velocity, hip range of motion, and knee range of motion. Tukey's Honestly Significant Difference tests were done in situations where the null hypothesis of no overall effect of coupling type was rejected, with a significance level set at $\alpha=0.05$.

- ANOVAs for gait cycles

A series of between subjects 1 way multivariate ANOVAs with muscle type as a factor, & mean muscle velocity, peak muscle velocity, absolute muscle displacement and relative muscle displacement as dependent measures were conducted. The data was split based on sub coupling and gait type prior, and therefore inter-muscular differences were assessed individually for each subclass.

Results

BF_L and BF_S Model Description

Model Range of Motion

Slight extrapolation was used in two of the subjects to standardize the hip and knee ranges of motion. This extrapolation occurred over a hip range of less than a single degree, except in the male cadaver, which was unable to achieve the same degree of hip extension as the other cadavers. The ranges of motion for each cadaver compared to the cadaver average and the modelled ranges of motion are shown in TABLE 8.

TABLE 8-Cadaveric knee and hip ranges of motion

Knee Range of Motion for Each Hip Position						
Hip Position	**D1**	**D2**	**D3**	**D4**	**Mean (SD)**	**Model**
H1	146.7	151.9	149.5	141.7	147.5 (4.36)	**145**
H2	137.2	150.6	150.9	139.3	144.5 (5.53)	
H3	141.2	146.7	150.7	138.2	144.2 (5.24)	
H4	127.5	141.5	154.5	148.2	142.9 (5.9)	
H5	143.0	144.1	162.2	154.0	150.8 (7.51)	
H6	142.9	151.3	147.2	148.0	147.3 (1.92)	
H7	145.7	146.5	149.9	143.9	146.5 (2.46)	
H8	143.6	148.1	140.3	133.7	141.4 (5.9)	
H9	148.3	149.8	154.8	144.6	149.4 (4.17)	
H10	145.7	150.5	142.3	138.6	144.3 (4.98)	
Mean (SD)	142.2 (6.03)	148.1 (3.44)	150.2 (6.28)	143.0 (5.96)	145.9 (3.08)	
Hip Range of Motion						
Throughout Entire Protocol	110.8	110.7	103.4	100.8	106.4 (4.25)	**104**

Average Cadaver Muscle Length- Knee Angle- Hip Angle Surface Creation

The measures of BF_L length were linearly interpolated across knee angles for each position and then linearly interpolated across hip positions, creating a single BF_L - knee angle- hip angle surface for each cadaver (FIGURE 5). Linear interpolation was chosen above other interpolation methods due to its smoothness and its lack of distortion of muscle length plot surface. Surface endpoint distortion was seen with spline and cubic interpolation, while a nearest neighbour interpolation resulted in a surface characterized by square step-like increases in muscle length with changes in joint angle.

The linearly interpolated surfaces were then divided by their respective subject thigh lengths (FIGURE 6). This transformation resulted in little change in the shapes of the surfaces or their orientation to one another, although it did bring the surfaces that were most separate in the cm plots closer to the other cadavers. Similar surfaces were created for the BF_S.

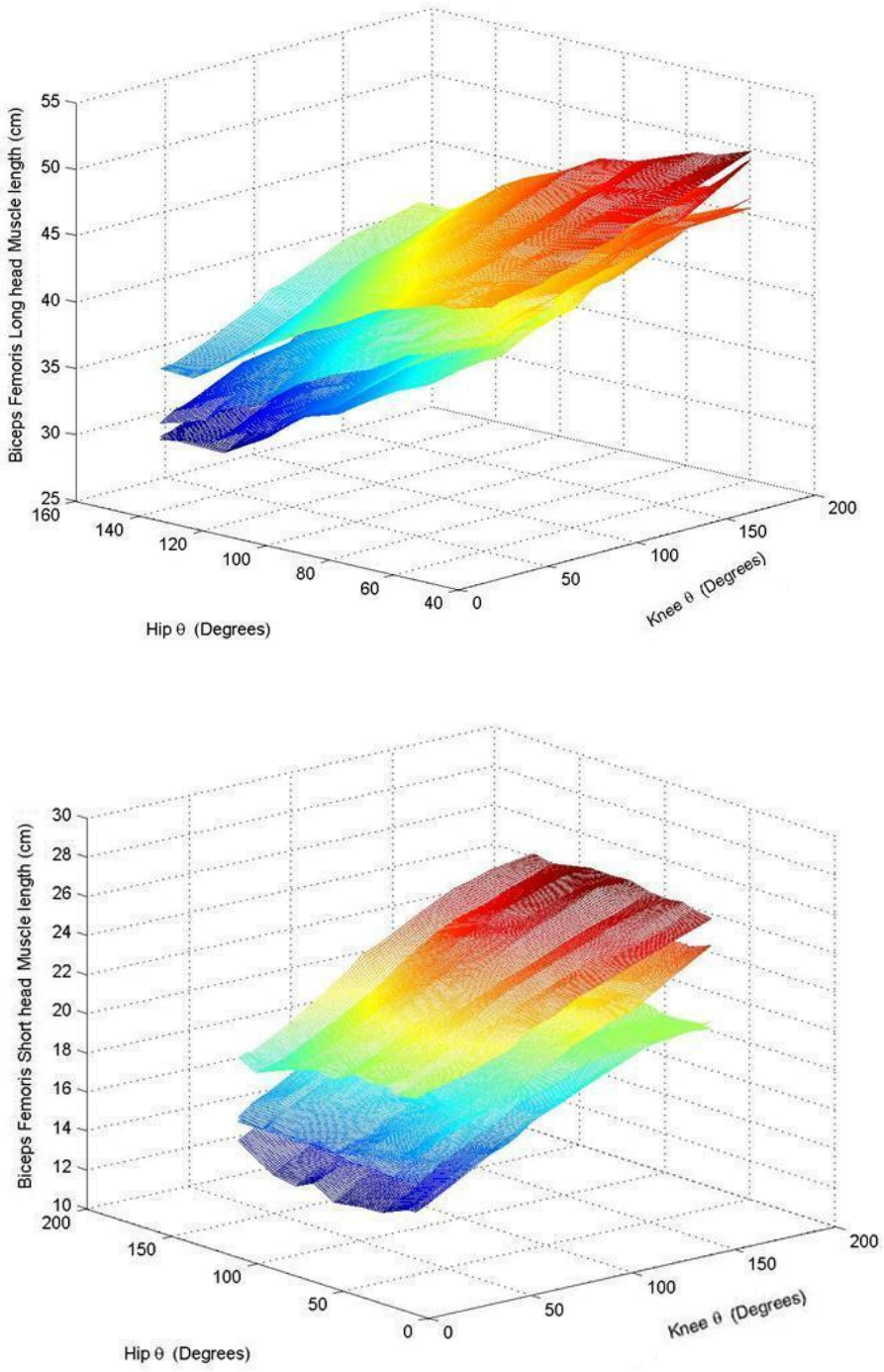

FIGURE 5-Overlaid unsmoothed A) BF_L AND B) BF_S length surfaces as functions of knee angle and hip angle for all four cadavers

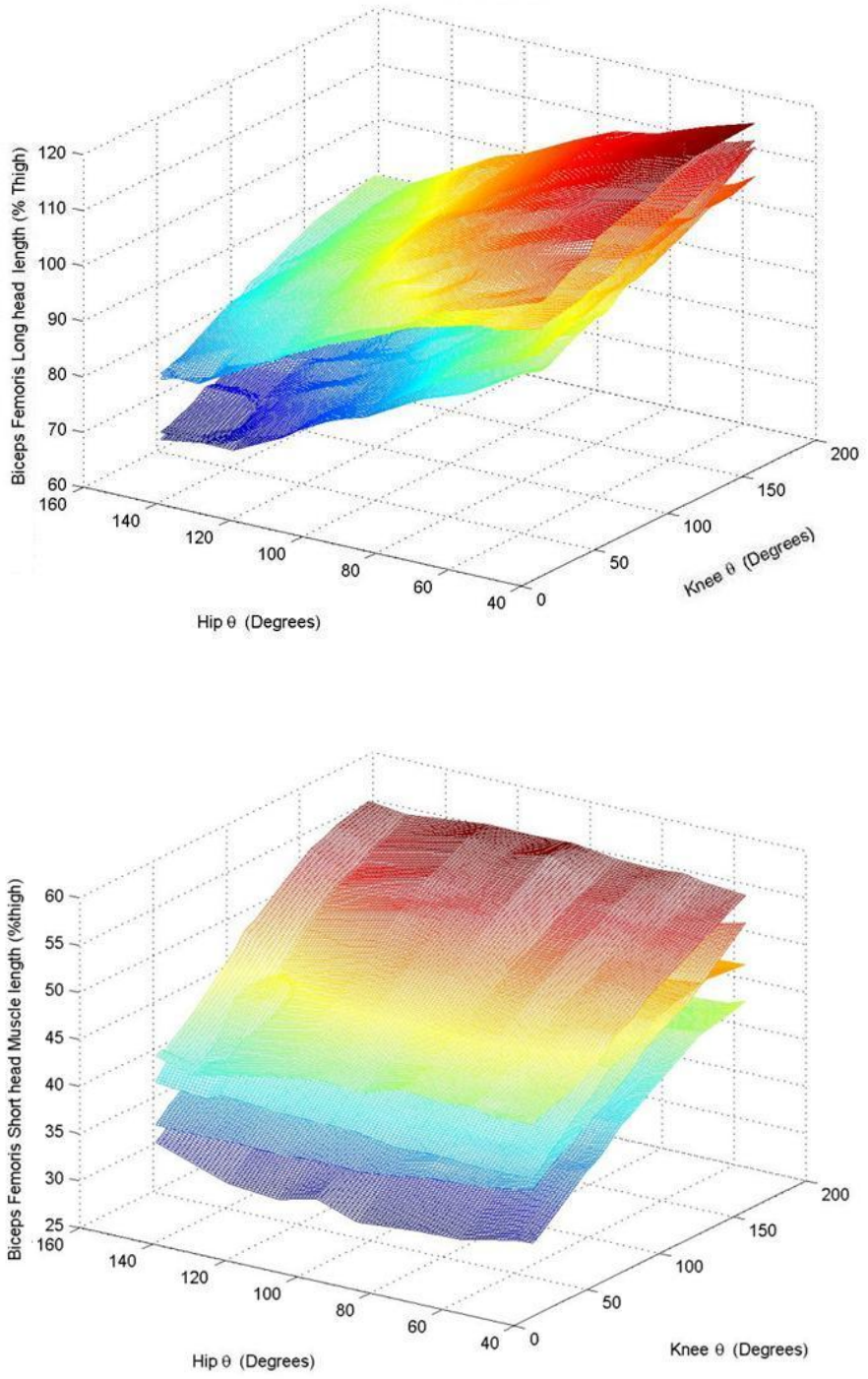

FIGURE 6-Overlaid unsmoothed normalized A) BF_L and B) BF_S length surfaces (%thigh) as functions of knee angle and hip angle

The average of the four individual unfitted surfaces was taken to generate a mean relative BF_L surface (FIGURE 7).

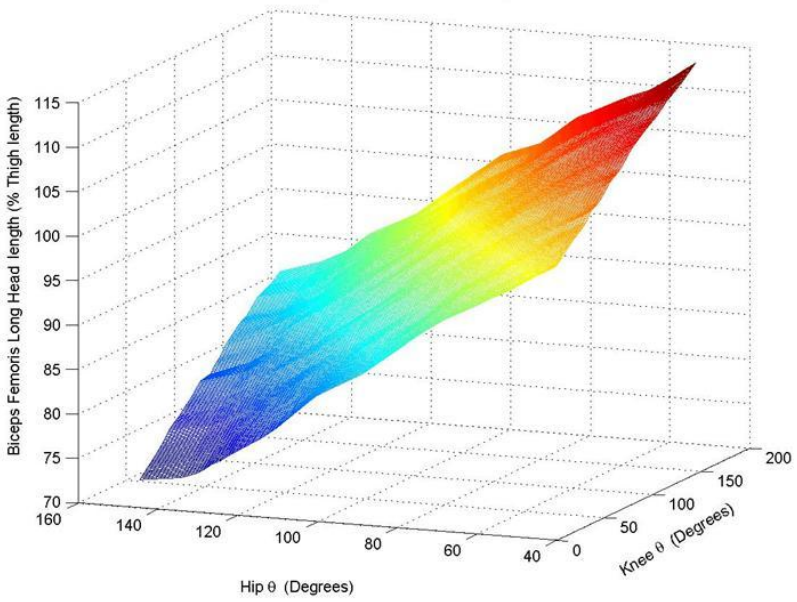

FIGURE 7- Average of the normalized cadaveric BF_L length surfaces

Polynomial Fitting of the Individual and Average Muscle Length- Joint Angle Surfaces

Once normalized, the individual BF_L surfaces were fitted with third degree bivariate polynomials (Appendix 4- TABLE 19, TABLE 18) and descriptive statistics were calculated (

TABLE 10).

Following averaging of the normalized cadaver surfaces, a third degree polynomial was fitted to the mean surface to generate an equation describing this surface as well (FIGURE 8 & TABLE 9).

The polyfitn and polytosympoly functions (http://www.mathworks.com/matlabcentral/fileexchange/10065-polyfitn) were used in MATLAB (v.7) to determine equations for muscle length based upon the knee and hip joint angles. The polyfitn function fits the data to a general polynomial regression model in n dimensions, thereby allowing the generation of a multivariate polynomial predicting muscle length. The polyfitn function also allowed specification of the order of the polynomial, which in all cases was chosen to be three. The equations took the following form:

$$lq = C1\,K\theta^3 + C2\,K\theta^2\,H\theta + C4\,K\theta^2 + C5\,K\theta\,H\theta^2 + C6\,K\theta\,H\theta + C7\,K\theta + C8\,H\theta^3 + C9H\theta^2 + C10\,H\theta + C11$$

Where:

lq= the length of the muscle in question

C1-C11= model constants

Hθ= hip joint angle (degrees)

Kθ=knee joint angle (degrees)

TABLE 9- Model equations generated from the average muscle surfaces & used to estimate muscle length during human kinematic trials (KΘ= knee angle, HΘ= hip angle, both in degrees)

Muscle Equations from Average Muscle Surfaces **KΘ & HΘ in degrees**
BF_L Length (% thigh)= -2.0591e-006 $K\Theta^3$ - 3.5121e-007 $K\Theta^2$ HΘ + 0.00047648 $K\Theta^2$ - 3.5267e-006 KΘ $H\Theta^2$ + 0.00087555 KΘ HΘ + 0.049462 KΘ + 1.7197e-005 HΘ^^{3} - 0.0048745 $H\Theta^2$ + 0.13739 HΘ + 97.744
BF_S Length (% thigh)= -1.2588e-006 $K\Theta^3$ + 4.273e-007 $K\Theta^2$ HΘ + 7.1289e-006 $K\Theta^2$ - 6.053e-007 KΘ $H\Theta^2$ + 8.7081e-005 KΘ HΘ + 0.13731 KΘ - 1.2542e-006 $H\Theta^3$ + 0.00047757 $H\Theta^2$ - 0.0573 HΘ + 33.0001

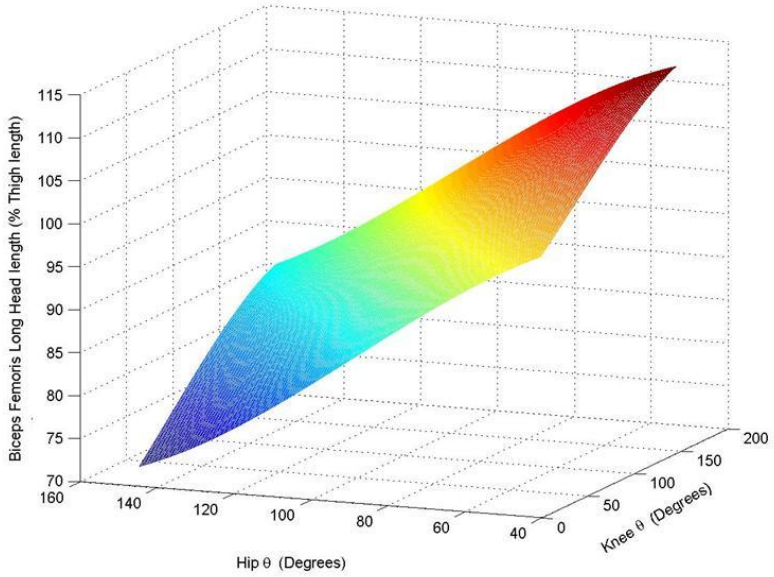

FIGURE 8- Polynomial fitted average BF_L-knee angle-hip angle surface

The mean length difference between the averaged surface and the 3rd degree bivariate polynomial fitting of the surface was 2.7289 X 10^{-13} (SD 0.2391). 1st and 2nd degree estimations of the average surface were also taken, but were ultimately rejected for use in the predictive model due to a poorer fit of the data based on a comparison of their r^2 values. The first degree estimation resulted in insufficient surface curvature, particularly at positions of extreme hip extension. The 3rd degree estimation would make the most reasonable estimation of BF_L moment arms. It also had an r^2 value of 0.9994. Some slight endpoint distortion at combined maximum hip flexion and knee extension was also noted on the 3rd degree bivariate polynomial surface. However, it is worth noting that the maximum difference between the polynomial fit of the averaged surface and the raw averaged surface itself was 1.17% of thigh length (which translates into a 0.47cm difference for a 40cm thigh). It is also important to understand that this maximum error is seen as slight downward distortion occurring in a position unlikely to be reached in most human motions due to passive insufficiency (hip fully flexed with knee extended).

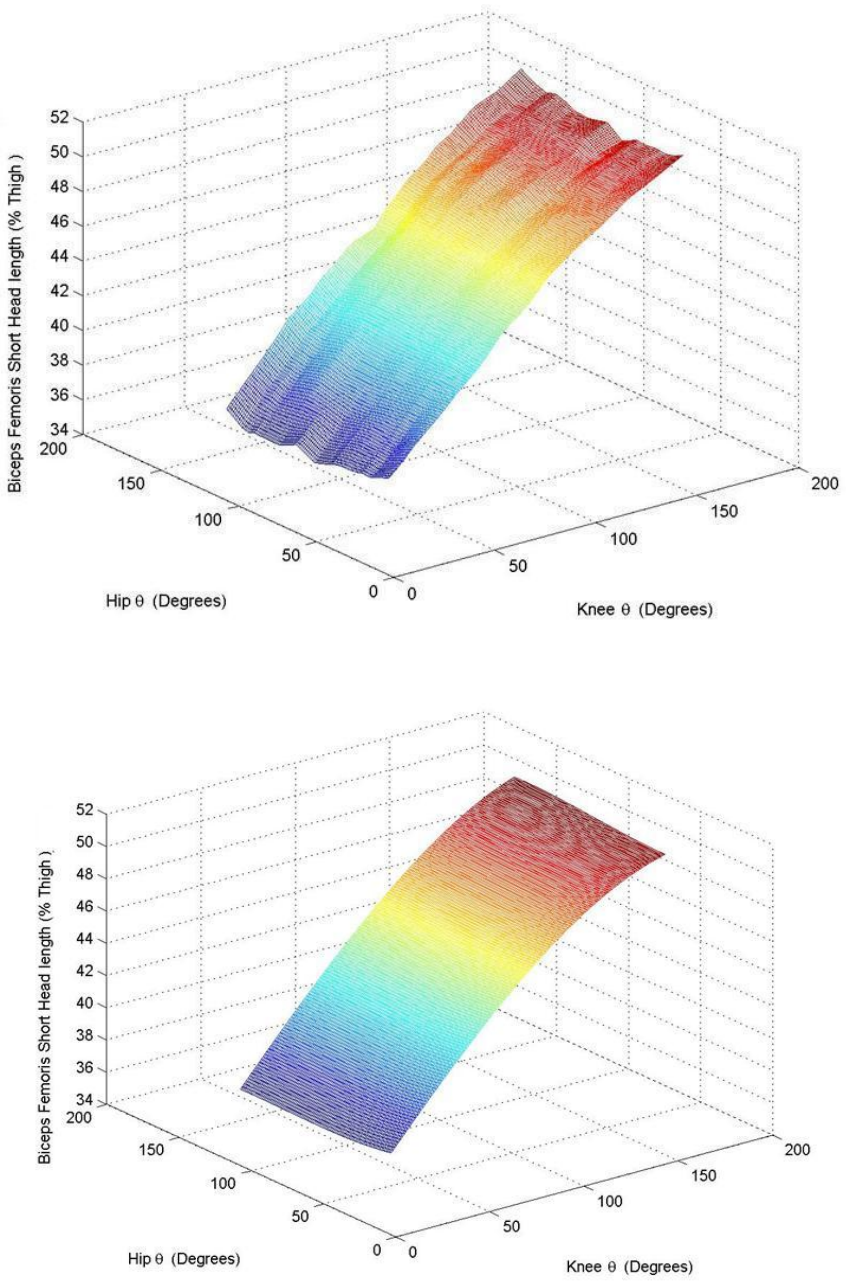

FIGURE 9- A) Average BF_S-knee angle-hip angle surface B) Polynomial fitted average BF_S-knee angle-hip angle surface

TABLE 10- Descriptive statistics of individual polynomial fitted BF_L -knee angle-hip angle surfaces for each cadaver (D1-D4)

	Fitted Average Surface	Fitted D1 Surface	Fitted D2 Surface	Fitted D3 Surface	Fitted D4 Surface
Maximum BF_L Muscle Displacement (% thigh)	42.56	41.85	48.16	38.17	42.18
Maximum BF_L Displacement Over Knee Range of Motion (% thigh)	16.68	17.501	18.38	17.41	15.12
Maximum Possible BF_L Displacement Over Hip Range of Motion (% thigh)	28.00	28.97	31.77	25.82	29.25
Mean Hip Global Moment Arm	0.26	0.27	0.28	0.22	0.28
Mean Knee Global Moment Arm	0.11	0.11	0.12	0.11	0.10
Ratio of Global Moment Arms	2.35	2.41	2.27	2.04	2.70

The smallest and largest knee to hip displacement/velocity ratios that would result in an isometric BF_L muscle associated with angular motions were calculated using the Matlab function countourc.m, which can isolate select lines from a contour plot. The contour plot was defined as the model BF_L muscle length output plotted as a function of both the knee and hip joints, extending the range of motion of both joints. The smallest ratio was determined to be 1.28, while the largest was determined to be 2.71.

BF_L Moment Arm Calculation

The BF_L knee and hip moment arm surfaces were calculated for the average normalized cadaveric surface to enable examination of the BF_L moment arm interaction and comparison of the models moment arms to those of other BF_L models. This was accomplished by taking the partial derivatives of a 3^{rd} degree bivariate polynomial describing the muscle length surface as a function of hip and knee angle in radians, with respect to either the knee or hip angle (the tendon excursion method of muscle moment arm determination). This muscle length equation was therefore separate from the one officially designated as the model equation since its units of measure differed on the input variables (joint angles). However, due to the fact that this would be a linear transformation, the shape of this surface was identical to that of the model equation. Following the calculation of the two moment arm surfaces using hip and knee angle in radians, surfaces were individually plotted as

functions of knee and hip angle in degrees, for consistency of display. See TABLE 11 for the equations of both BF_L moment arms.

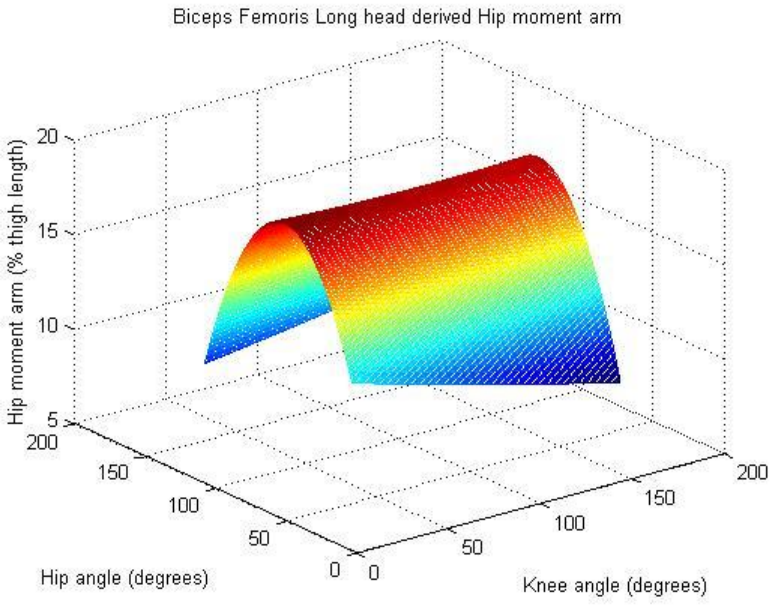

FIGURE 10-BF_L hip moment arms calculated using the tendon excursion method expressed as a function of both joints.

The effect of the knee angle on the hip moment arm is unclear, as the relationship seems to vary depending on the exact hip angle (FIGURE 10). When the hip nears extension, the BF_L moment arm about the hip increases as a function of knee angle (the more extended the knee, the larger the moment arm). Conversely, as the hip begins to flex, the BF_L moment arm about the hip decreases as a function of knee angle (the more extended the knee, the smaller the moment arm).

TABLE 11- BF_L moment arm equations derived using the tendon excursion method

BF_L **moment arm equations from average muscle surfaces (KΘ & HΘ in radians)**
BF_L Knee moment arm (% thigh)= 2.834 + 2.8743*HΘ - 0.66334*HΘ^2+ 3.1284*KΘ - 0.13212*KΘ*HΘ - 1.1619*KΘ^2
BF_L Hip moment arm (% thigh)= 7.8716 - 32.0038*HΘ + 9.7037*HΘ^2+ 2.8743*KΘ - 1.3267*KΘ*HΘ - 0.066059*KΘ^2

The effect of the hip angle on the BF_L knee moment arm was more consistent with geometric expectations. From a position of hip flexion, the BF_L knee moment arm initially increased with hip extension, and then decreased back towards its initial values as the hip reached full extension. The geometric depiction in FIGURE 11 will help explain this geometric expectation. In this figure, the thigh is modelled as a straight line extending from the GT to the LFC, the shank is modelled as a line from the LFC to the LM, and the muscle is modelled as a line from its origin to its insertion. It is apparent that as either the hip joint or the knee joint angle is manipulated, the orientation of the BF_L line of muscle action will change relative to the thigh (FIGURE 11). Not surprisingly, the orientation of the thigh that would bring the BF_L line of action the furthest distance from the respective joint axis of rotation would result in the largest moment arm. When manipulating the knee joint alone, the peak BF_L knee moment arm is achieved when the angle between the GT, LFC and LM reaches 90. If the knee is either flexed or extended beyond 90 degrees, the orientation of the BF_L line of action changes, and brings it closer to the LFC, shortening the moment arm about the knee joint. This explains the parabolic shape seen of the BF_L moment arm plot as a function of knee angle. However, the orientation of the BF_L line of action is also affected by changes in the hip joint angle (in FIGURE 11 this would be defined as the angle between the LFC, GT and IT). Therefore, a change in hip angle not only affects the BF_L moment arm about the hip joint, but also the BF_L moment arm about the knee joint.

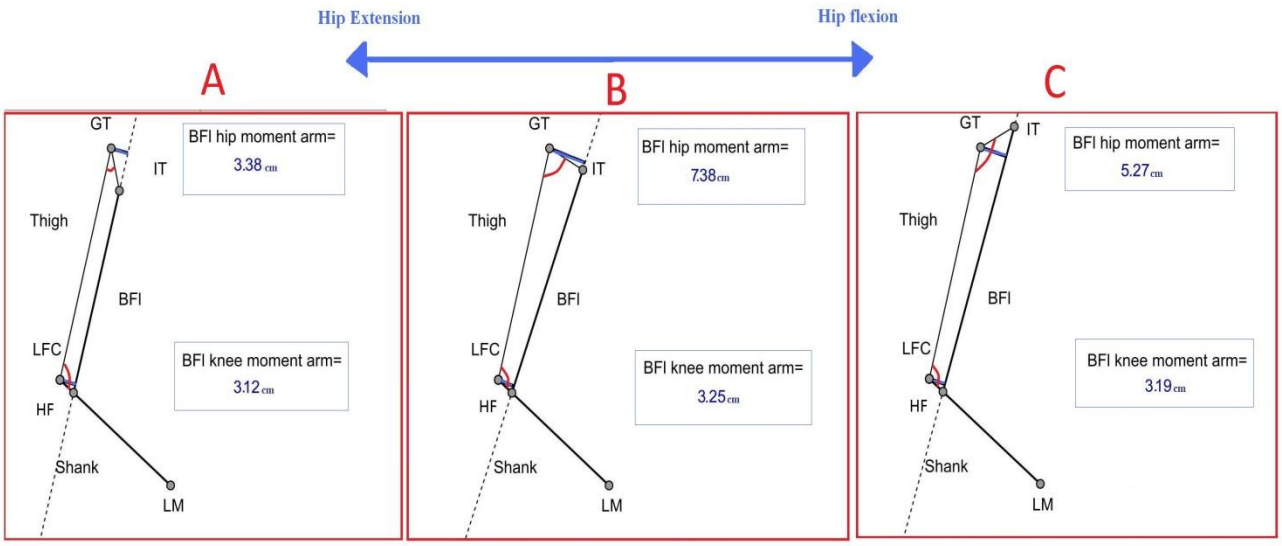

FIGURE 11- Illustration of moment arm interaction using geometrical illustrations employing measurements similar to those of the cadavers. Moment arm values are for illustrative purposes only due to their approximate nature.

Both BF_L moment arms would simultaneously be at their peaks when the hip and knee joint angles were at 90 degrees. As the hip angle (IT, GT & LFC) flexes (FIGURE 11, FIGURE 9) or extends (FIGURE 11

C) beyond 90 degrees while the knee joint is stationary, the BF_L line of muscle action is brought much closer to the GT. Simultaneously, this change in orientation also brings the BF_L line of muscle action slightly closer to the LFC. Therefore, the same parabolic shape should apply to the BF_L knee moment arm as a function of hip angle, albeit a parabola with a much shallower slope than compared to the effect of knee angle. This is exactly what is seen in FIGURE 12. The reason the hip joint is having a more visible effect on the BF_L knee moment arm than the knee joint on the BF_L hip moment arm can be accounted for by the comparatively larger BF_L moment arm about the hip compared to about the knee. This larger moment arm would result in a greater change in the orientation of the BF_L line of action with a change in joint angle, resulting in a comparatively larger effect on the BF_L knee moment arm as well compared to the effect a change in knee angle would have on the BF_L hip moment arm.

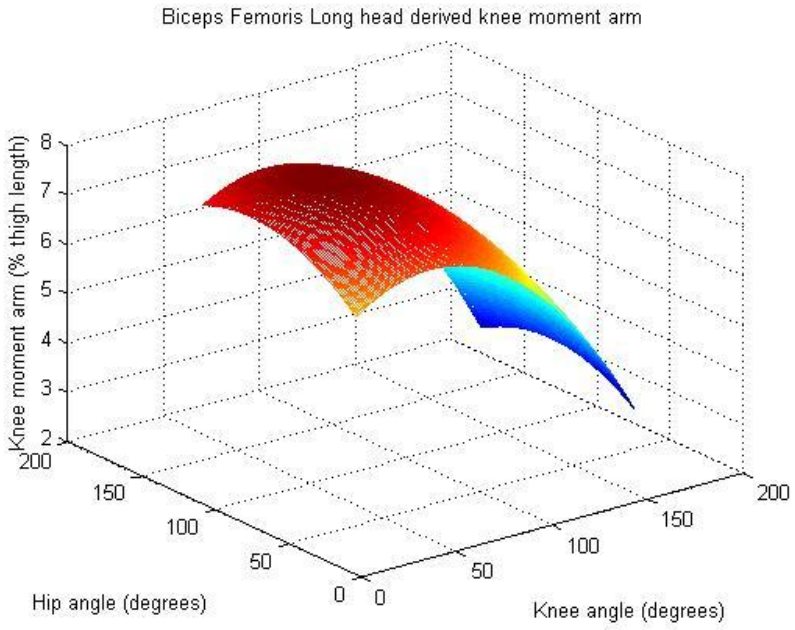

FIGURE 12- BF_L knee moment arms calculated using the tendon excursion method, expressed as function of both joint angles.

In Vivo Model Validation

A calibration trial was performed on a single subject recruited for the human kinematic data collection (S2). This calibration was done to cross validate the model outputs with tape measured muscle length estimates of the distance between the IT and the HF. These measurement occurred in two knee positions (fully flexed and fully extended), with the hip held in full flexion. Similar measurements were attempted in positions of full hip extension. However, identification of the right IT was unreliable in positions of hip extension due to obstruction

of the IT by the gluteal muscles and the gluteal fold. Model estimates of muscle length should be consistent with those estimated by tape measure approximately within a cm.

The subject was selected due to low body fat and musculature, which allowed the right IT to be palpated with greater accuracy. He was also selected due to his standing height (being the tallest of the group at 191.5 cm (~6'3")), his trochanteric height (>100cm), and his sex. These characteristics made him the most anthropometrically dissimilar subject, from the cadavers upon which the model was based. Later, the hip and knee joint angle data was entered into the model to determine the models ability to match manual estimations of BF_L length (see TABLE 12). The model showed good cross validation with the tape measurements, particularly in positions of knee extension.

TABLE 12- In vivo validation of model.

Position	Knee angle (degrees)	Hip angle (degrees)	Thigh length (cm)	Measured BF_L length (cm)	Estimated BF_L length (cm)	Difference Between BF_L Measure and Model Estimation (cm)	Estimated BF_L Length (% thigh)
Knee Extended & Hip Flexed	180	49	48.5	55.5	55.48	0.02	101.76
Knee Flexed & Hip Extended	60	49	48.5	50.2	49.35	0.85	114.41

Description of Coupled Hip and Knee Motions

- KFHF motion – Bilateral Tuck jump

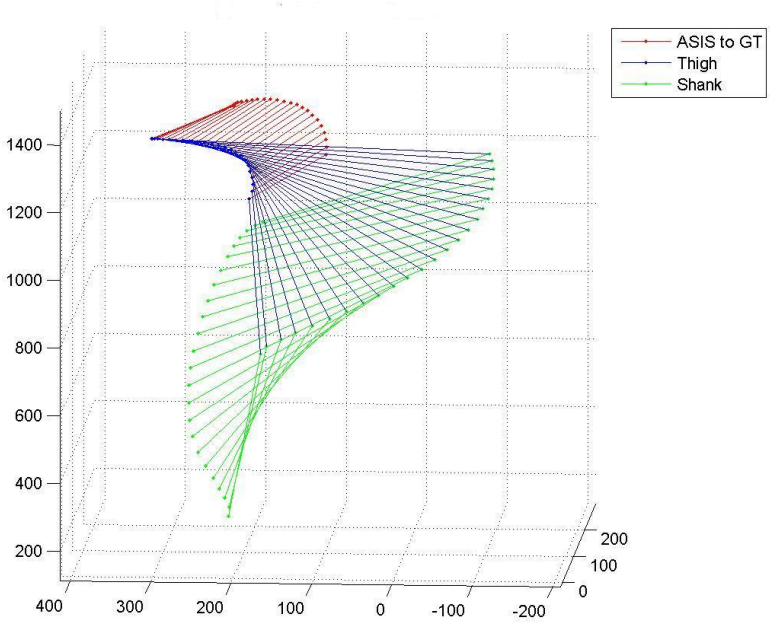

FIGURE 13- Example strobe plot of the KFHF-tuck (Subject S2)

Subjects were instructed to stand with their hands on the sides of their head; feet shoulder width apart, and in line with each other. Bodyweight was evenly distributed between both feet. The motion began from a ¼ squat position, with knees and hip flexed to 45 degrees. This position was held for 1-2 seconds, and was followed by a jump straight upwards. The subjects then quickly pulled their knees as close towards their chest as possible. Following the tuck, the subject re-extended the hip and thigh joints, and landed again in the quarter squat position. Subjects were instructed to focus primarily on the hip flexion aspect of the motion, instead of the knee flexion, to promote a full hip range of motion. However, there was still variance between subjects in terms of the amount of hip flexion that was achieved, due to factors such as jumping height achieved, subject muscular strength, movement speed, etc… It was inevitable that a small countermovement would occur prior to the tuck part of the motion; however this part of the motion was removed from the subsequent analysis (See section entitled "Data Quality Control and Cropping").

- Representative KEHF motion- Unilateral Toe kick

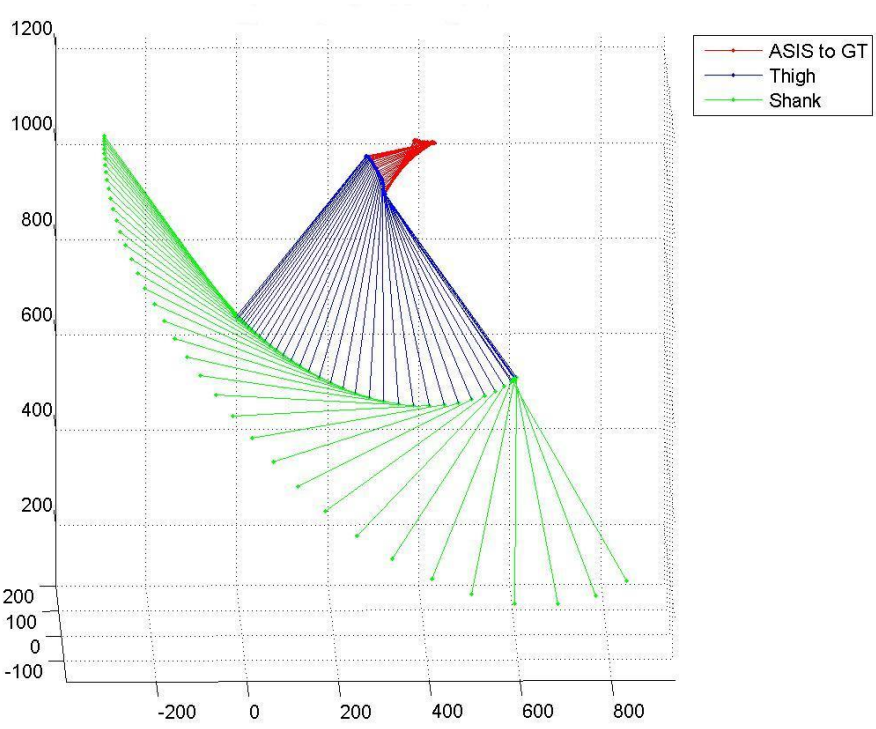

FIGURE 14- Example strobe plot of the KEHF-kick (Subject S5)

Subjects began from a position where the right hip joint was maximally extended, but with the trunk still upright (no spine flexion or compensatory trunk rotation relative to the horizontal to allow additional shifting of the thigh backwards). The right knee was flexed to 90 degrees. The hip was kept in a consistent amount of abduction throughout the motion; with the feet approximately shoulder width apart. Subjects then extended the right hip joint and flexed the right knee joint in order to kick a beach ball against a wall. The subjects made contact with the ball with the tip of the right shoe, resulting in a toe kick. They were instructed to kick the ball for distance, & to try to have the ball travel at a 45 degree angle from the ground. The target end position was a hip flexion angle of 45 degrees from anatomical position, with the knee completely extended. The investigator retrieved and replaced the ball after each trial, to reduce changes in the initial subject position.

- Representative KFHE motion- Unilateral pawing action

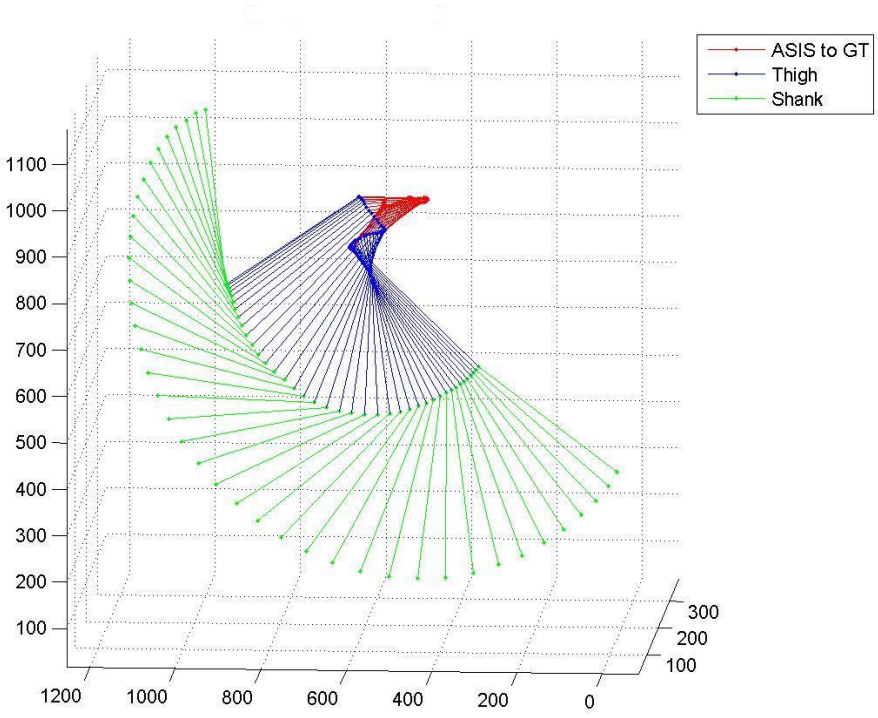

FIGURE 15- Example strobe plot of the KEHF-paw (Subject S1)

Subjects were instructed to begin the motion with their right leg in a position of slight hip flexion (45 degrees from vertical), and their right knee fully extended. Thus the right leg was off the ground, and left leg supported the subject's bodyweight. From this position, the subjects simultaneously extended the right hip and flexed the right knee joint, lightly grazing the ground but continuing the motion until reaching full hip extension and knee flexion of at least 90 degrees.

It was noted that subjects found this task the most difficult to perform of the four couplings. A common error was that subjects would not place enough weight on their supporting leg, which resulted in stomping motion that ended with a forceful contact between the bottom of the foot and the floor. This hard contact decreased the velocity of the limb, most commonly to the point that the motion would stop completely with the hip around anatomical position. It also forced the knee into full extension, resulting in an undesired coupling between the hip and knee joints. In the pilot trials, the inability to balance on one foot during the performance of a maximum speed motion was cited by the subjects as a partial origin of this problem. To address this issue, subjects were allowed to place their left hand on a supporting surface to help them simultaneously stay balanced

and keep their torso upright. The vast majority of subjects (5 out of 6) found it necessary to make use of this supplement to perform the motion within the given parameters.

In two subjects these measures were not able to fully prevent the stomping motion. An additional measure was taken to remedy the situation. These subjects were allowed to perform the motion with a single shoe on their left foot. This reduced the problem for two reasons. First, the socked right foot encountered less friction with the floor than a rubber soled sporting shoe, thus facilitating the grazing motion of the foot in. Second, the modest elevation of the left foot created slightly more room for the left foot to clear the ground. Visual analysis both in live time and through slower replays on the VICON workstation software confirmed this change resulted in a better approximation of the desired coupling and promoted the proper end position with no compromise in stability or trunk position.

- Representative KEHE motion- Bilateral Squat jump

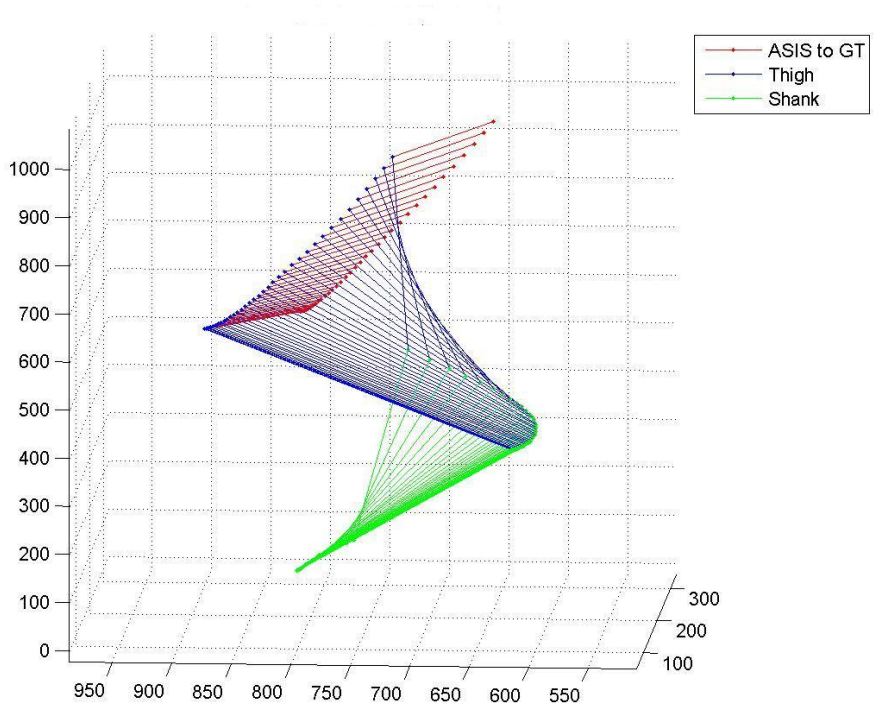

FIGURE 16- Example strobe plot of the KEHE-jump (Subject S1)

Subjects were instructed to take a position of 45 degrees of knee flexion with the hips slightly flexed (1/4 squat position). Subjects held this position for 1-2 seconds, and then jumped straight upwards. Instructions were given to the subjects to try to maximize the height of the jump by performing the motion as fast as possible. The subjects' hands were kept in contact with the sides of their heads to eliminate arm swing variations between subjects, and to prevent obstruction of the anatomical markers. The subject was also instructed to jump in place, and to make every attempt to land on the same point on the platform. Jumps where the subject moved forward, backward, or sideways were taken to be poor trials and were replaced with additional trials.

Hip and Knee Angular Kinematics during Four Coupling Classes of Motion

The results of the angular parameter comparison for the four coupling classes can be found in

TABLE 13. Significant differences between the four classes are noted based on Tukey's HSD post hoc tests.

TABLE 13- Averaged movement characteristics across all subjects for each coupling (Mean (SD)).

Parameter	KEHE-jump	KEHF-kick	KFHE-paw	KFHF-tuck
Movement Duration (ms)	254 (6)	284 (9)	484 (11) *significantly > than all other couplings ($p<0.001$)	214 (35)
Hip ROM (degrees)	50.1 (9.66)	24.7 (9.20) *significance smaller than all other couplings ($p<0.001$)	55.9 (9.06)	64.7 (14.81)
Knee ROM (degrees)	75.7 (4.39) *Significantly smaller than KEHF-kick and KFHF-tuck ($p<0.001$)	101.8 (17.63)	85.7 (18.08)	115.6 (14.16) *Significantly larger than KEHE-jump and KFHE-paw ($p<0.001$)
Absolute Mean Angular Hip Velocity (degrees/s)	193.0 (32.25) *Significantly larger than KEHF-kick and KFHE-paw ($p<0.001$)	87.8 (28.99)	110.3 (25.87)	290.3 (32.410) *significantly larger than all other couplings ($p<0.001$)
Absolute Mean Angular Knee Velocity (degrees/s)	286.5 (45.70)	360.2 (229.86) *significantly larger than KFHE-paw ($p<0.01$)	171.0 (34.79)	522.7 (76.86) *significantly larger than all other couplings ($p<0.01$)
Absolute Peak Hip Velocity (degrees/s)	346.7 (55.37)	178.5 (43.63) *significantly smaller than all other couplings ($p<0.001$)	347.4 (67.13)	470.7 (147.12)
Absolute Peak Knee Velocity (degrees/s)	675.3 (64.68)	1218.1(154.84) *significantly larger than all other couplings ($p<0.01$)	479.9 (132.34) *significantly smaller than all other couplings ($p<0.001$)	707.5 (73.47)
Knee to Hip Velocity Ratio	1.5 (0.30)	4.8 (2.75) *significantly larger than all other couplings ($p<0.01$)	2.1 (1.99)	1.8 (0.38)

Identification of Key Points in the Gait Step Cycle

Since the given couplings were intended to be linked with the key mechanical events and tasks occurring in their proximity, it was necessary to identify the approximate timing of said events relative to the observed couplings. For this purpose, time synched lower limb animations and animated hip- knee cyclograms were examined. The animation consisted of one segment connecting the digitized right ASIS marker to the right GT marker, another connecting the digitized right GT marker to the right LFC marker (representing the thigh), and a third connecting the digitized right LFC marker to the right LM marker (representing the shank). The following events were identified on a few examples of the non averaged cyclograms, as well as the averaged cyclograms:

- Heel strike- this event can be easily identified on a hip- knee cyclogram. The literature consistently reports that this event is marked by a sharp directional change in the cyclogram figure, after reaching a position of hip flexion and knee extension (Sykes, 1975, Goswami, 1998). This position was identified using the time synched animations. Heel strike was also apparent in these animations through a sudden change in angular velocity associated with the stance phase, as seen a change to a higher density of data points per cm of the geometric figure on the cyclogram, and as a slowing of the rotation of the segments on the lower limb animation.

- Toe off: the determination of this event's exact timing remains elusive. Since there was no marker placed on the foot, and no simultaneous high speed cinematography in this investigation, it was necessary to rely on existing characterizations of the running and walking cyclograms to identify this event's location on the hip-knee cyclogram. However, the reported location of toe off on the cyclogram is fairy inconsistent in the literature (Sykes, 1975, Goswami, 1998), spanning the entire top of the cyclogram (a section characterized by slight hip movement combined with knee flexion). It was possible to narrow down the location of toe off based on prior descriptions of the gait cycles. Toe off was assumed to occur prior to the onset of hip flexion in the running gait, and slightly after its initiation in the walking gait. It should also be noted that a change in this slope and a change in the slope of the top portion of the cyclogram in general, could occur between individuals, and varied noticeably between the running and walking gait cycles. Therefore the names of the subclasses, particularly those near the toe off event, reflect their general proximity to said events, and don't ensure that the given event will

always occur at a consistent spot within this subclass. This is particularly true since the exact duration, and also the knee to hip velocity ratio of each coupling would be anticipated to vary slightly between subjects.

- Mid stance- this event was identified as the time when the thigh segment reached a position perpendicular to the horizontal, which corresponded to a hip angle of approximately 120 degrees (anatomical position, approximately 30 degrees from full hip extension). This position was identifiable as a point on the cyclogram where the knee shifts from a flexing motion, to an extending motion, as the center of gravity moves past the longitudinal axis of the thigh.

- Mid swing- this event was taken to be the point where the thigh segment was flexed to the extent that its absolute angle was around 10 degrees past vertical. This thigh position corresponded to a hip angle of ~110 degrees, which represents a position of slight hip flexion relative to anatomical position (~120 degrees). Gait phases between these events were associated with couplings corresponding to their temporal ordering.

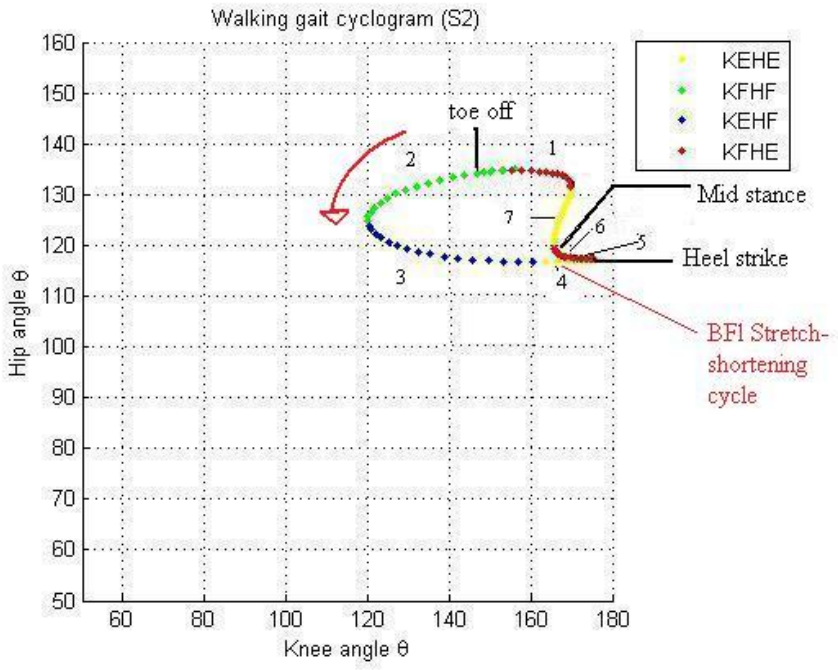

FIGURE 17- Example cyclogram for the walking gait cycle. Key points in the gait cycle are noted. Coupling classes are color coded, and subclasses are numerically coded (Subject S2).

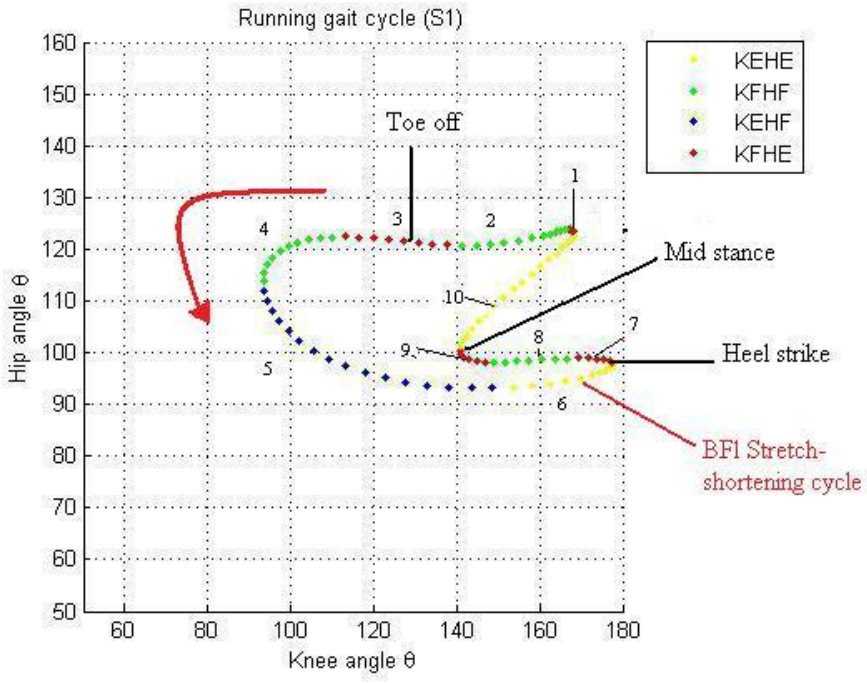

FIGURE 18- Example examples of the running gait cyclograms with the most common temporal sequencing of couplings. Key points in the gait cycle are noted. Coupling classes are color coded, and subclasses are numerically coded (Subject S1).

Hamstring Muscle Kinematics

Velocity Shift Hypotheses

BF_L and BF_S Muscle Velocity during Four Classes of Lower Limb Motion

The results of the inter-muscular velocity comparisons for the four coupling classes can be seen in FIGURE 19. Note that a shortening velocity was indicated by a negative sign, while a lengthening velocity was indicated by a positive sign. It was hypothesized that the BF_L would exhibit a left shift in muscle velocity relative to the BF_S during the KFHF and KEHF coupled movements, and a right shift during the KEHE and KFHE coupled movements.

The hypotheses regarding left shift of the BF_L relative to the BF_S were supported. During the KEHE-jump, the BF_L was found to have both mean and peak lengthening velocities that were significantly left shifted from mean and peak shortening velocities of the BF_S, respectively (mean velocity comparison $p<0.001$,

FIGURE 19A; & peak velocity comparison p<0.001, FIGURE 19B). Similarly, during the KEHF-kick, the BF_L was found to have both mean and peak lengthening velocities that were significantly left shifted from the mean and peak lengthening velocities of the BF_S, respectively; p<0.001 (mean velocity comparison, FIGURE 19A) & p<0.001 (peak velocity comparison, FIGURE 19B)

The hypotheses regarding right shift of the BF_L relative to the BF_S were also supported. During the KFHF-tuck, the BF_L was found to have both mean and peak shortening velocities that were significantly right shifted from the mean and peak lengthening velocities of the BF_S, respectively (mean velocity comparison p<0.001, FIGURE 19A) & (peak velocity comparison p<0.001, FIGURE 19B). Similarly, during the KFHE-paw, the BF_L was found to have mean and peak shortening velocities that were significantly right shifted from the mean and peak shortening velocities of the BF_S, respectively; p<0.001 (mean velocity comparison, FIGURE 19A) & p<0.001 (peak velocity comparison, FIGURE 19B).

Therefore the BF_L was significantly shifted from the velocity of the BF_S in geometrically predictable ways during the examples of the four classes of motion. It is also of note that two of the four couplings (KEHE & KFHF) resulted in simultaneous shortening and lengthening muscle actions in a homonymous muscle group.

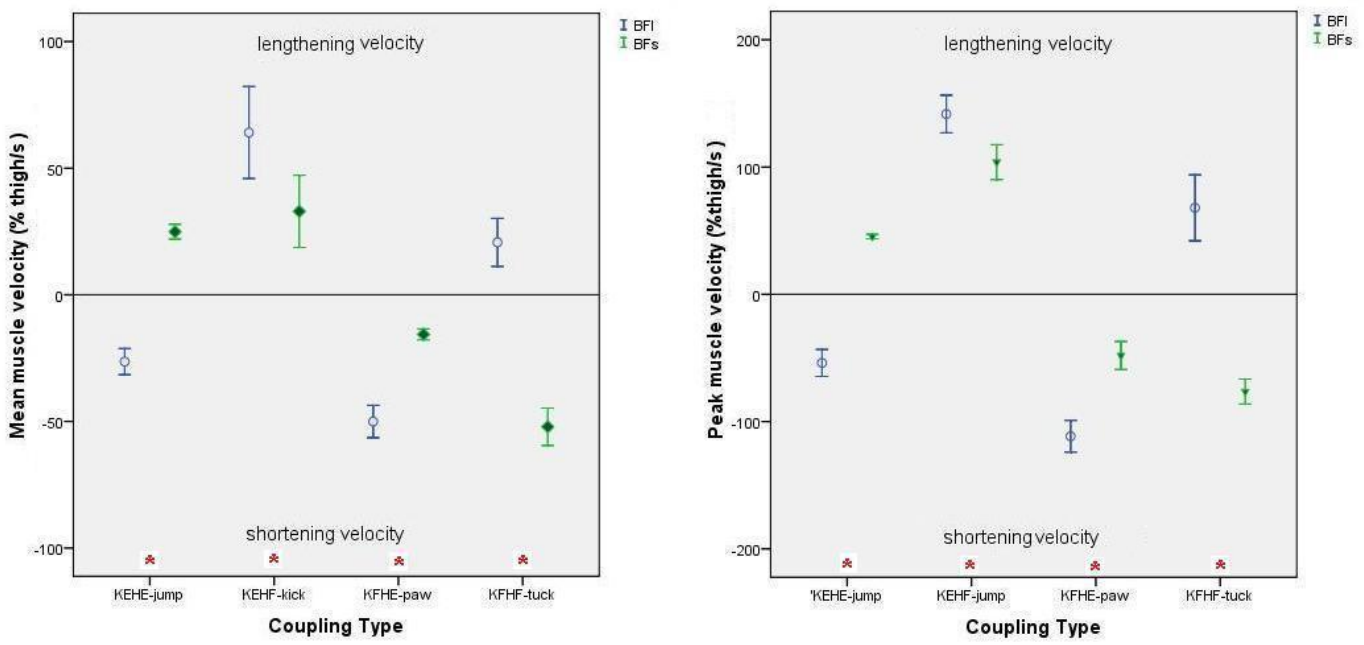

FIGURE 19- A) Mean BF_L and BF_S velocity for each coupled motion. B) Peak BF_L and BF_S velocity for each coupled motion. Error bars indicate 95% confidence interval of the mean for each muscle during each coupled motion. A red asterisk near the category axis (x axis) indicates when a particular coupling showed a significant difference between the BF_L and BF_S.

BF_L and BF_S Muscle Velocity during Subclasses of the Walking and Running Gait Cycles

The results of the inter-muscular velocity comparisons for the running and walking coupling classes can be seen in FIGURE 24 and FIGURE 25. A temporal sequencing of the running gait subclasses is shown in FIGURE 20 and FIGURE 21, while that of the walking gait is shown in FIGURE 22 and FIGURE 23. It was hypothesized that the BF_L would exhibit a left shift in muscle velocity relative to the BF_S during the KFHF and KEHF gait subclasses, and a right shift during the KEHE and KFHE gait subclasses.

The left velocity shift hypothesis for the KFHF subclasses was partially supported in both the walking and running gaits. The BF_L exhibited a significant left shift in both mean and peak muscle velocity relative to the BF_S for KFHF-toe off/initial swing subclass of the walking gait ($p<0.05$, FIGURE 25). The BF_L exhibited a significant left shift in peak muscle velocity relative to the BF_S for two of the three KFHF subclasses of the running gait ($p<0.05$,). However, it only exhibited a significant left shift in mean velocity relative to the BF_S during the KFHF-initial swing ($p<0.001$) of the running gait, and not the KFKF-late terminal stance or the KFHF-foot flat (FIGURE 24).

The left velocity shift hypothesis for the KEHF subclasses was supported in both the walking and running gait. The BF_L mean and peak lengthening velocities were significantly left shifted from those of the BF_S during the KEHF-mid swing phase ($p <0.05$ (FIGURE 25)) of both the walking and gait cycles.

The right velocity shift hypothesis was partially supported for the KFHE subclasses in both the walking gait and in the running gait. The BF_L mean velocity was significantly right shifted for the KFHE-early mid stance ($p<0.05$) and the KFHE-early terminal stance ($p<0.001$) of the walking gait, but not the KFHE-heel strike ($p=0.247$) of the walking gait. However, the peak BF_L velocity was only significantly right shifted in the KFHE-early terminal stance ($p=0.05$, FIGURE 25) ($p=0.314$ (heel strike), $p=0.07$ (early mid stance)). The BF_L mean velocity was significantly right shifted from that of the BF_S for all the KFHE subclasses of the running gait ($p<0.05$). In contrast, only one of the peak velocities (KFHE-toe off, $p<0.05$) was significantly shifted from that of the BF_S (FIGURE 25).

The right velocity shift hypothesis for the KEHE subclasses was partially supported for the walking gait and was supported in the running gait. The BF_L velocities were significantly right shifted from those of the BF_S during the KEHE-late mid stance during the walking gait (both mean and peak are significant, $p<0.001$). However during the KEHE-terminal swing, the BF_L velocities were only significantly right shifted from those of the BF_S FIGURE 25) when examining the muscles' peak velocities; not their mean velocities (peak- $p <0.001$; mean- $p=0.195$). In the running gait, the BF_L velocities were significantly right shifted from those of BF_S FIGURE 25A) during all KEHE subclasses (both mean and peak are significant, $p <0.05$).

Sample plots of an average step cycle for a single individual are depicted in FIGURE 18, FIGURE 20, & FIGURE 21. The first plot depicts the hip-knee angle cyclogram for the running gait, demonstrating the geometrical shape of the cyclical gait pattern. The other plots provide a visual comparison of the BF_L and BF_S kinematics over the course of the entire gait cycle. All graphs are color coded based on coupling and numerically coded based on subclass to allow comparisons within a gait cycle. Estimations of the stance and swing phases of gait are indicated in the blue and purple bars below the latter two graphs. The two phases overlap on the left sides of the plot to express the uncertainty regarding the exact location of the toe off event. BF_L activity is also estimated based on prior literature (Thelen, 2005b; Lyons et al, 1983; Perry, 1992; Simonsen et al, 1985).

Simonsen et al (1985) found that the BF_L was not active in the last $1/3^{rd}$ of the stance phase of the sprinting gait in the two subjects examined. Due to the uncertainty regarding the timing of toe off, this could not be clearly depicted on the running gait length-time and velocity time plots. Lyons et al (1983) found BF_L activity in the walking gait started at mid swing, and was complete by toe off of the opposite foot. This is in contrast to other reports (Perry (1992)) indicating the BF_L is active in the walking gait during the pre-swing and initial swing, followed by a period of dormancy until the terminal swing. Perry also found BF_L activity during the first part of loading response (foot flat), and another lack of activity until the pre-swing, and noted the highest BF_L EMG at the end of the mid swing and entirety of terminal swing. Interestingly, Perry (1992) has also examined the activity of the BFs during the walking gait, and found it to be active only for a period from the terminal stance, through the initial swing & and ending in the mid swing.

Aerial periods of the running gait cycle are not indicated on the graphs due to the uncertainty regarding the exact location of the toe off events. However we would expect one aerial period following toe off of the

right leg, continuing until the end of the KFHF-early stance, and another aerial period occurring briefly during the KEHE-late swing subclass.

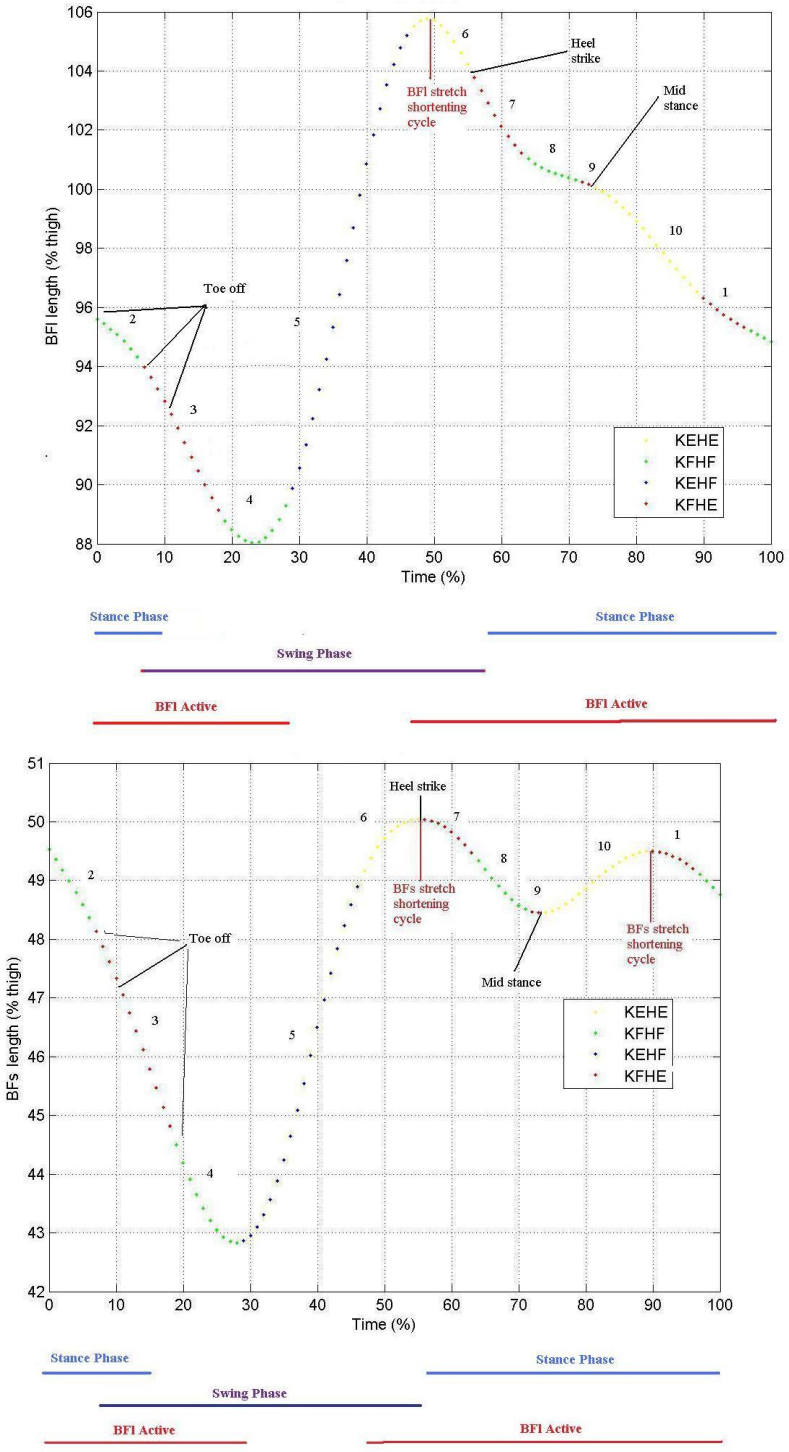

FIGURE 20- Example running gait muscle length-time plot (Top- BF_L, Bottom- BF_S, both from subject S4). Key points in the gait cycle are noted. Coupling classes are color coded, and subclasses are numerically coded.

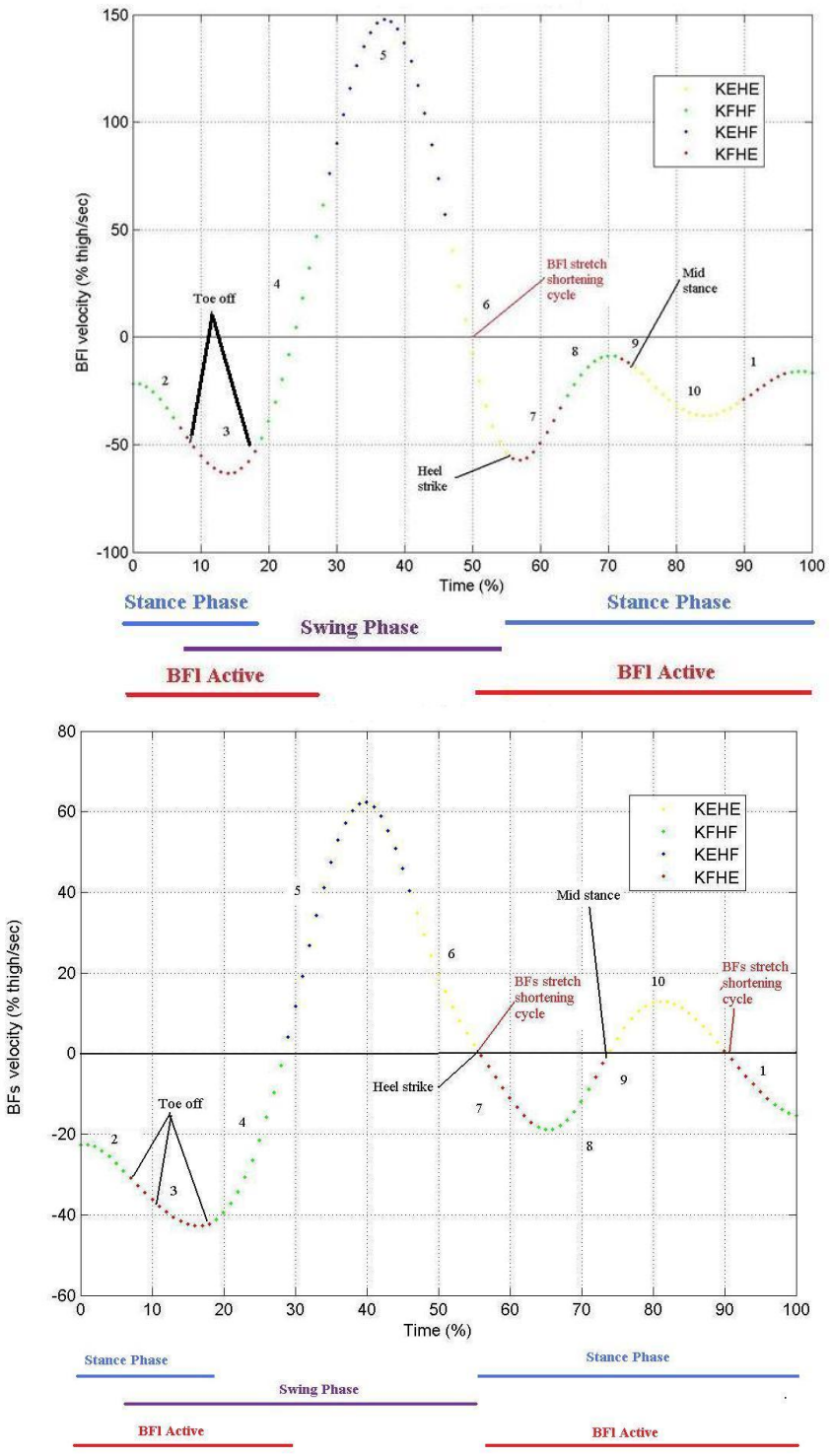

FIGURE 21- Example muscle velocity-time plot for the running gait cycle (Top-BF_L, Bottom- BF_S). Key points in the gait cycle are noted. Coupling classes are color coded, and subclasses are numerically coded.

Similar plots are provided for the walking gait cycle in FIGURE 17, FIGURE 22, FIGURE 23 and Identical color coding is used for the coupling classes, but the numerical codes are based on those outlined prior for the walking gait cycle (numbered 1-7 in lieu of 1-10).

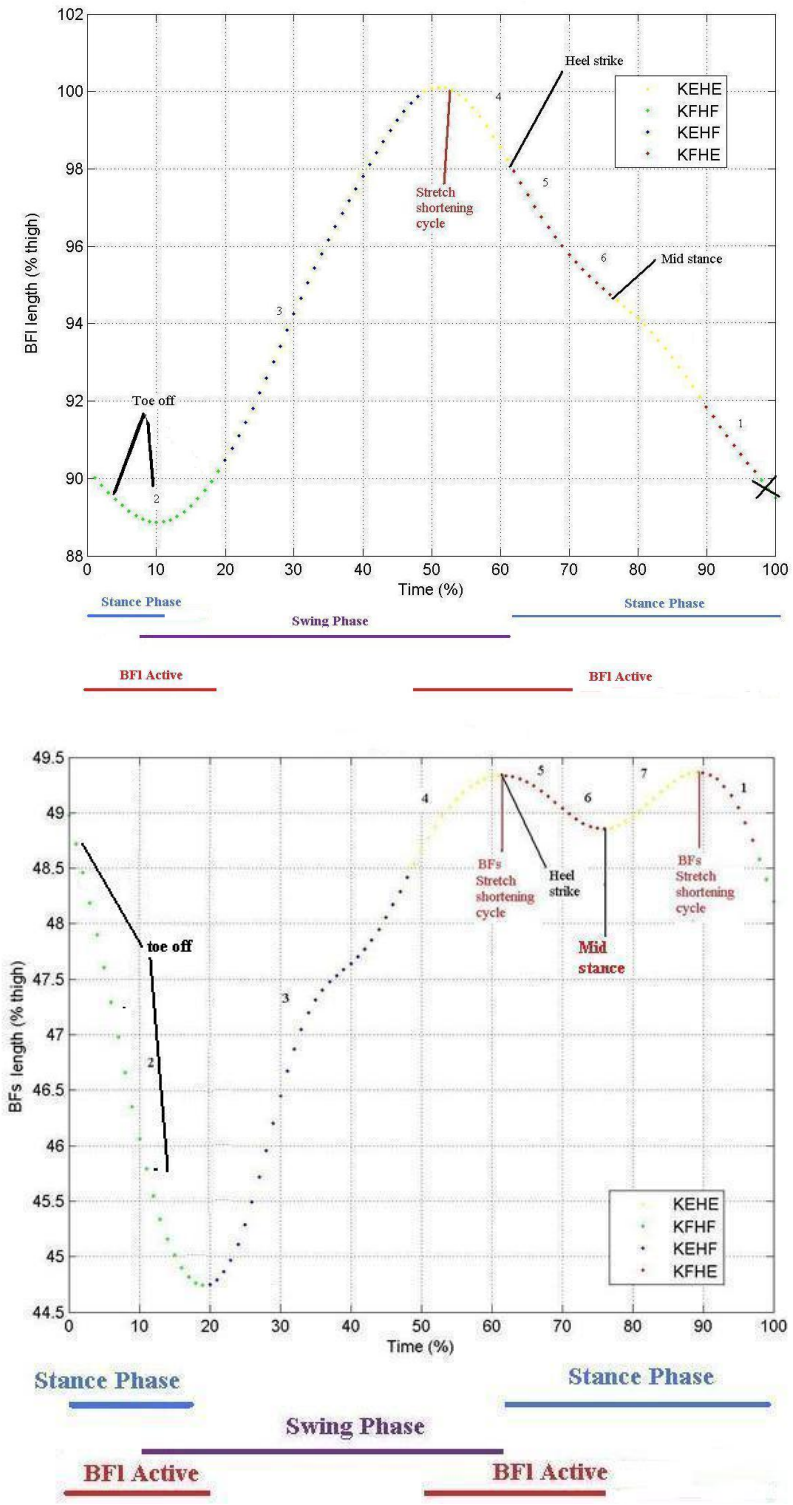

FIGURE 22- Example muscle length-time plot for the walking gait cycle (Top- BF_L, Bottom- BF_S, both from subject S3). Key points in the gait cycle are noted. Coupling classes are color coded, and subclasses are numerically coded.

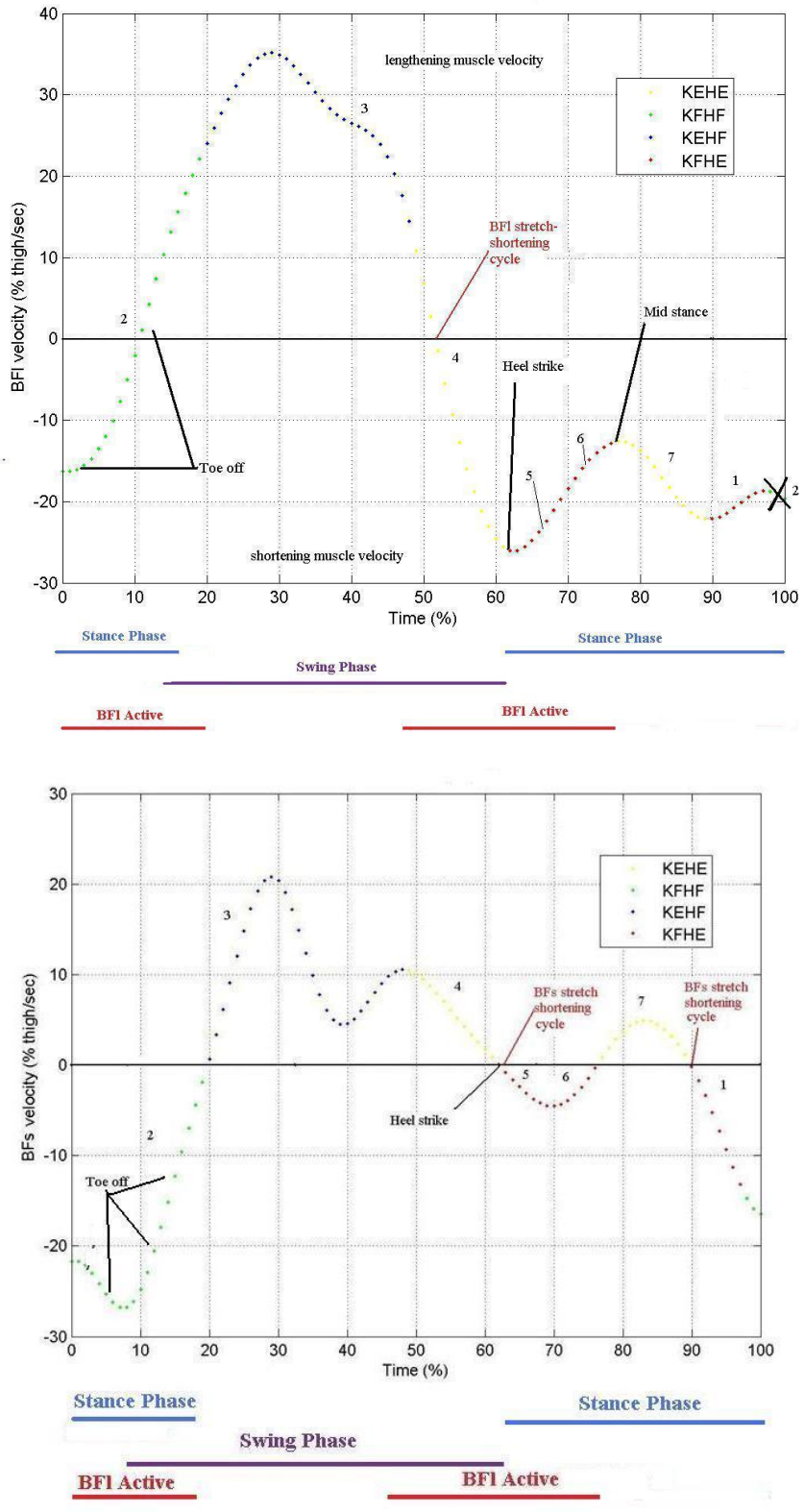

FIGURE 23- Example muscle velocity-time plot for the walking gait cycle (Top-BF_L, Bottom- BF_S, Both from subject S3). Key points in the gait cycle are noted. Coupling classes are color coded, and subclasses are numerically coded.

A few observations are of particular note. The peak BF_L and BF_S muscle lengths are reached in the swing period of both gait cycles, with the BF_L peak shifted to an earlier time relative to the BF_S. The BF_L muscle reaches its peak length in the terminal swing, while the BF_S muscle reaches its peak length around heel strike.

In both gait cycles, there was a single lengthening velocity peak in the BF_L versus two to three in the BF_S. The BF_L lengthening velocity peaks all occurred during the swing phase. In contrast, the BF_L showed an additional lengthening velocity peak during the KEHE-late mid stance in the running gait, and one in the KEHE-terminal swing of the walking gait. It is interesting to note that the large BF_L lengthening seen during the gait cycle is the result of a few gait subclasses occurring in the swing phase, with the majority of the lengthening occurring during the KFHE-mid swing subclass. This peak exceeded 100% of thigh length per second in the running gait. This is in contrast to the BF_L shortening, which occurs more slowly over the course of the stance subclasses of the gait cycles.

The second BF_L shortening peak shifted to earlier time in BF_L relative to the BF_S, with that of the BF_L occurring just after heel strike during the KFHE-heel strike subclass, while that of the BF_S occurring at the beginning of the phase following the KFHE-heel strike.

There are two BF_S stretch shortening cycles (SSCs) and one BF_L SSC during the running gait cycle. The one and only BF_L SSC was seen during the KEHE-terminal swing subclass, which is in agreement with the work of Thelen et al (2005), who modeled BF_L length during the swing phase of the sprinting step cycle using the model of Delp (1990). The first BF_S stretch shortening cycle occurs between the KEHE-terminal swing and KFHE-heel strike and the second occurs over the course of the KEHE-late mid stance and the KFHE-early terminal stance. Interestingly, the amortization point of the first BF_S SSC corresponds roughly to the heel strike event. The SSCs of the BF_S also both naturally coincide with either the absolute maximum BF_S length or with a local BF_S length minimum. The comparative heights of these two peaks varied slightly between subjects, but were larger in the first SSC during the running gait. In the walking gait, the reverse was true for three of the five subjects, although the difference between the heights of the two peaks in this case was slight.

Comparing the first BF_S SSC to the only BF_L SSC, we can see that the latter is shifted to earlier time relative to the former in both gaits cycles. The difference between the numbers of SSC events in both muscles is also notable. A size difference between the two muscles can't account for large inter-muscular changes in muscle velocity direction. Therefore the decrease in the number of SSCs in the BF_L must be due to its hip attachment, which would tend to promote BF_L shortening through the hip extension seen in the KEHE-late mid stance phase.

Near isometric muscle actions were not observed in the BF_L. They were observed in the BF_S in two out of the five subjects. These muscle actions both occurred during the walking gait cycle of the given subject. The most isometric of the two of these motions was during the KFHE-heel strike subclass in S4, where BF_S length-time curve was found to be close to a straight line for the entire subclass. A straight zero line on the BF_S linear velocity-time plot was also found. The BF_S displacement during this specific instance was 0.0006% thigh length with a knee range of motion of 0.38 degrees and a knee velocity to hip velocity ratio of 0.19. This was the only instance of a muscle length being this near to isometric for the majority of a subclass. Additionally, a section of the final gait phase in S5 was found to be isometric. Both occurred as an extension of the amortization phase of a BF_S SSC, however each subject showed this tendency in a different BF_S SSC, therefore no temporal trends in isometric motion were seen between subjects.

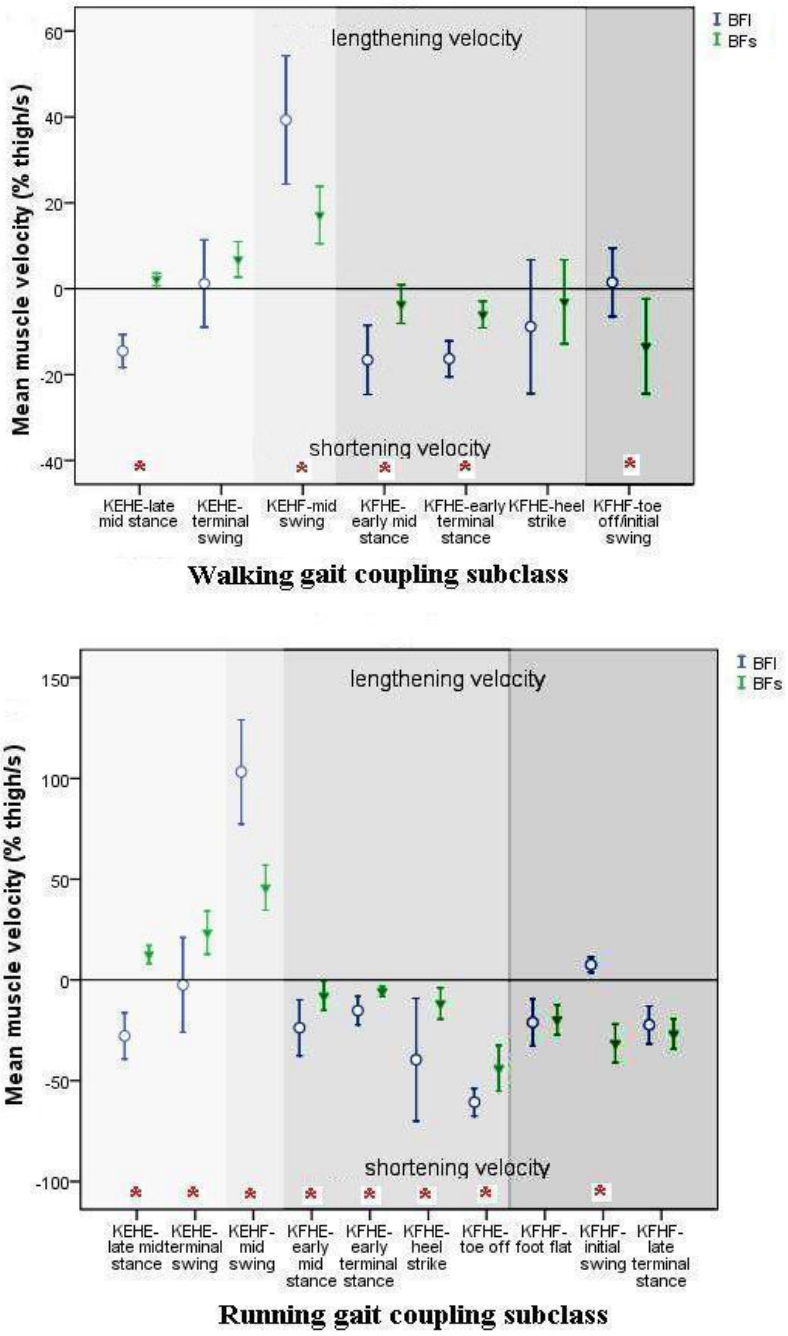

FIGURE 24 -Mean muscle velocity during A) Walking and B) Running gait subclasses. Error bars represent the 95% confidence interval in the mean. A red asterisk near the category axis (x axis) indicates when a particular coupling showed a significant difference between the BF_L and BF_S.

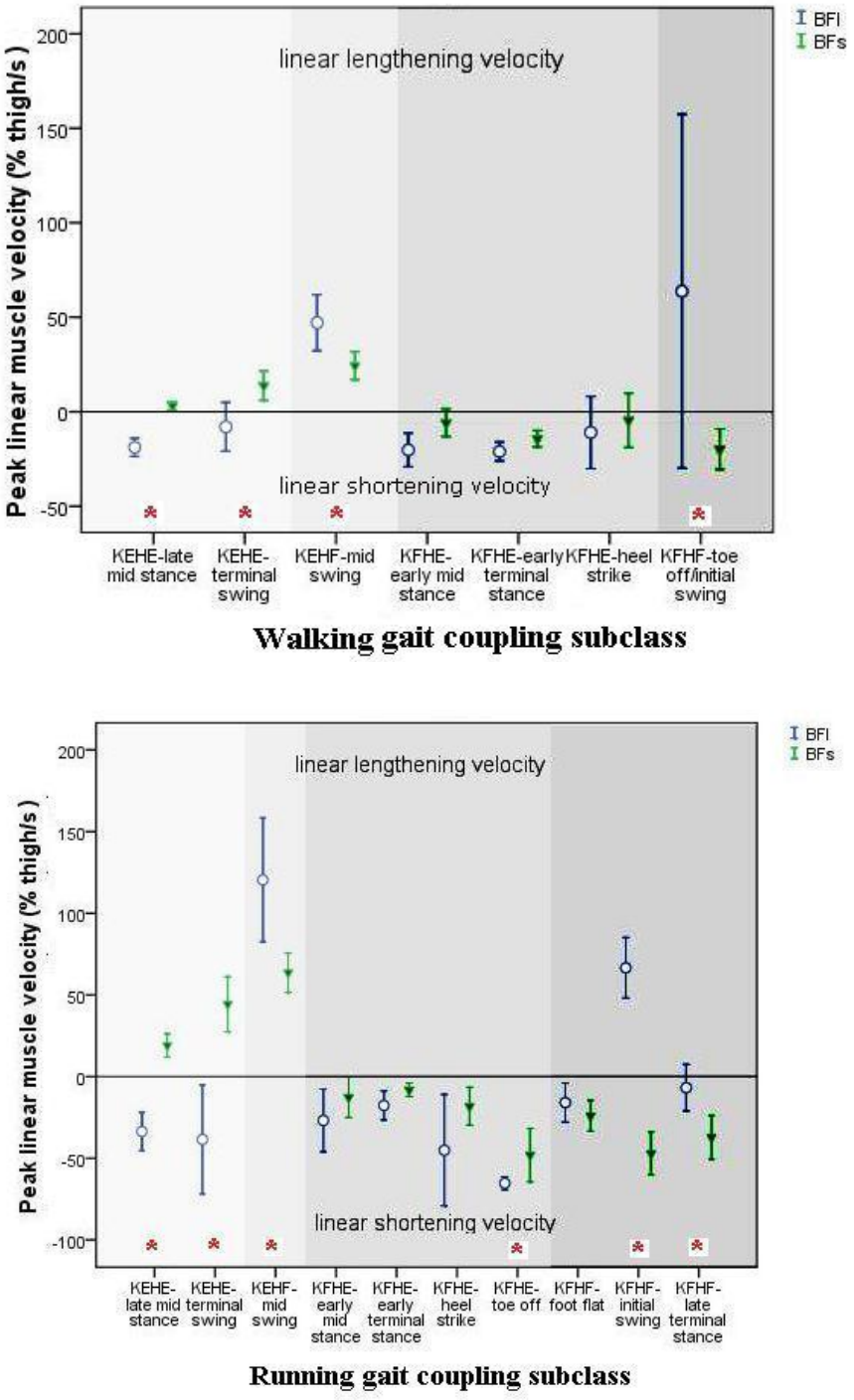

FIGURE 25- Peak muscle velocity A) Walking and b) Running gait subclasses. Error bars represent the 95% confidence interval in the mean. A red asterisk near the category axis (x axis) indicates when a particular coupling showed a significant difference between the BF_L and BF_S.

Muscle Displacement

BF_L and BF_S during Four Classes of Motion

The results of the inter-muscular displacement comparisons for the four coupling classes can be seen in FIGURE 26. It was hypothesized that the BF_L would exhibit a smaller muscle displacement (displacement conservation) relative to the BF_S during the KFHF and KEHE coupled movements, and a larger muscle displacement (displacement exacerbation) during the KEHF and KFHE coupled movements.

The hypotheses regarding displacement conservation of the BF_L relative to the BF_S were supported in the KFHF-tuck, but not the KEHE-jump (FIGURE 26). The BF_L showed a significantly smaller displacement than the BF_S during the KFHF-tuck ($p<0.05$ (relative) & $p<0.01$(absolute)). In contrast, there was no significant difference in muscle displacement between the BF_S and the BF_L during the KEHE-jump ($p=0.625$ (relative) & $p=0.994$ (absolute)).

The hypotheses regarding velocity exacerbation of the BF_L relative to the BF_S were supported (FIGURE 26). The BF_L showed a significantly larger muscle displacement than the BF_S during the KFHE-paw ($p=0.001$ (relative) & $p=0.001$ (absolute)). Similarly, the BF_L showed a significantly larger muscle displacement than the BF_S during the KEHF-kick ($p=0.001$ (relative) & $p=0.001$ (absolute)).

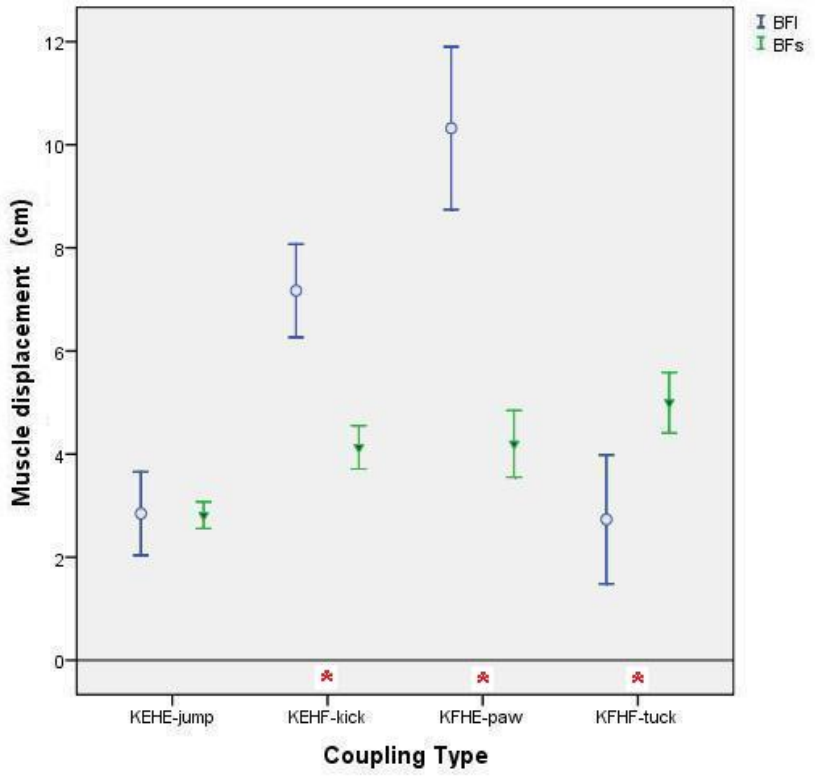

FIGURE 26 A) Muscle displacement (maximum length-min length) b) normalized overall muscle displacement. Error bars represent the 95% confidence interval of the mean. A red asterisk near the category axis (x axis) indicates when a particular coupling showed a significant difference between the BF_L and BF_S.

The hypotheses regarding displacement conservation of the BF_L relative to the BF_S were rejected in the KFHF subclasses of both the walking and running gaits. The BF_L did not have a significantly smaller muscle displacement than the BF_S for KFHF-toe off/initial swing of the walking gait ($p=0.682$). Similarly, the BF_L did not have a significantly smaller muscle displacement than the BF_S for any of the three KFHF (FIGURE 27) subclasses of the running gait.

The hypotheses regarding displacement conservation of the BF_L relative to the BF_S were rejected in the KEHE subclasses of both the walking and running gait (FIGURE 27). The BF_L did not have a significantly different velocity from the BF_S during the KEHE-terminal swing of the walking gait or the running gait ($p=0.713$ & $p=0.582$, respectively). Even more compelling, the BF_L displacement was actually significantly larger (displacement exacerbation) compared to that of the BF_S during the KEHE-late mid stance of both the walking and running gaits (both $p<0.001$).

The hypotheses regarding displacement exacerbation of the BF_L relative to the BF_S were supported in the KEHF subclasses of both the walking and running gait. The BF_L had a significantly larger muscle displacement than the BF_S during the KEHF-mid swing (both $p<0.001$).

The hypotheses regarding displacement exacerbation of the BF_L relative to the BF_S were partially supported in the KFHE subclasses of the walking gait, and rejected in the running gait (FIGURE 27). The BF_L muscle displacement was significantly larger compared to the BF_S in the KFHE-early terminal stance ($p<0.05$) of the walking gait, but not other two KFHE walking gait subclasses ($p=0.190$ (heel strike), $p=0.067$ (early mid stance)). The BF_L muscle displacement was not significantly larger compared to the BF_S in any of the four KFHE running gait subclasses ($p=0.11$ (toe off), $p=0.08$ (heel strike), 0.2 (early mid stance), $p=0.1$ (early terminal stance)).

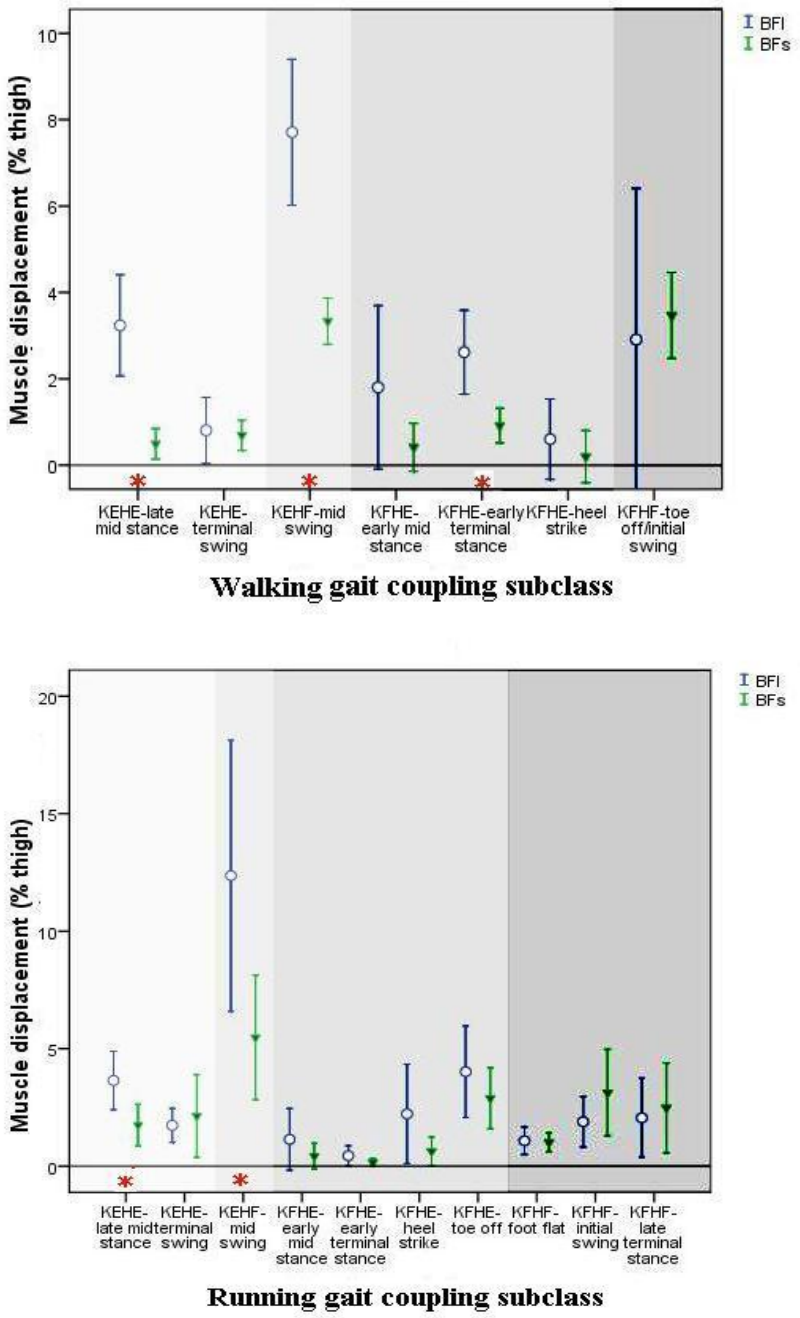

FIGURE 27- Muscle displacements for all subclasses during the walking (A) and running (B) gait cycles. Error bars represent the 95% confidence interval in the mean. A red asterisk near the category axis (x axis) indicates when a particular coupling showed a significant difference between the BF_L and BF_S

Explanatory Variables

Velocity Shift

Descriptions of mean velocity shift during the four coupling classes and the running and walking gait subclasses can be found in TABLE 14.

TABLE 14- Velocity shift during four couplings and gait (Mean (SD)). Bold font indicates where the shift exceeded -200%, representing an incongruent motion where displacement conservation would not be seen.

		Coupling Class/ Subclass	Mean (% shift)	SD
Four Coupling Classes	**KEHE**	**Jump**	**-210.6**	42.11
	KEHF	**Kick**	112.2	46.42
	KFHE	**Paw**	229.2	74.21
	KFHF	**Tuck**	-145.3	33.26
Running Gait		**Late mid stance**	**-336.7**	95.96
	KEHE	**Terminal swing**	-126.4	98.03
	KEHF	**Mid swing**	125.2	21.1
		Toe off	39	9.29
		Heel strike	236.7	168.76
		Early Mid stance	373.4	353.51
	KFHE	**Early terminal stance**	166.4	11.9
		Foot flat	4.7	20.18
		Late terminal stance	-123.6	6.51
	KFHF	**Initial swing**	-17.2	19.84
Walking Gait		**Late mid stance**	**-981.4**	573.9
	KEHE	**Terminal swing**	-99.1	133.47
	KEHF	**Mid swing**	131	23.26
		Heel strike	6547.5	11169.25
		Early Mid stance	525.8	385.24
	KFHE	**Early terminal stance**	205.8	128.9
	KFHF	**Toe off/initial swing**	50	335.75

Inter-Muscular Comparison of Knee to Hip Velocity Ratio

1) Four coupling classes

The knee to hip velocity ratios (95% CI of the mean) for of the four couplings can be seen in FIGURE 28. Of particular note is the high knee to hip velocity ratio of the KEHF-kick, indicating a dominance of knee motion. This was in contrast to the rather low value of the KEHE-jump, which indicates a dominance of hip motion.

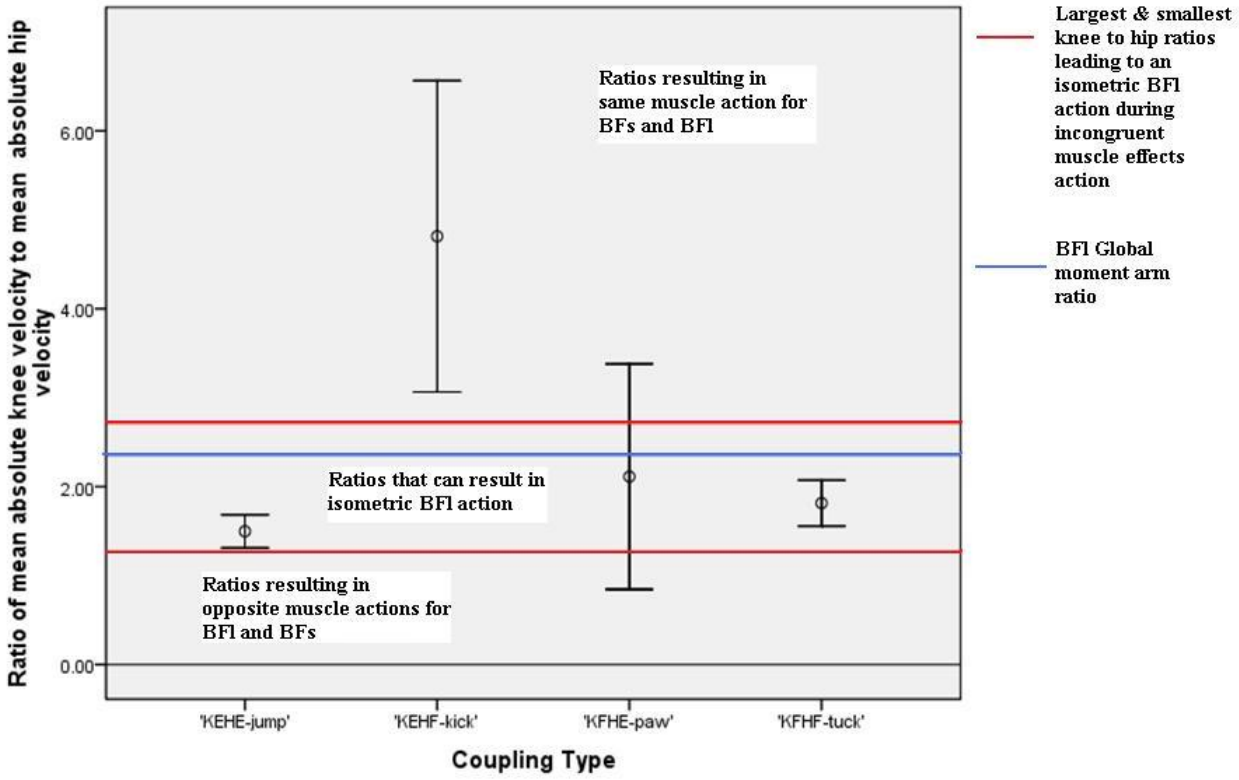

FIGURE 28- Comparison of ratios of absolute knee to hip velocities between couplings. The ratio must be > 0. Error bars represent the 95% confidence interval of the mean.

2) Running and walking gaits

Comparisons of the mean knee to hip velocity ratio for each subclass were calculated to act as an explanatory variable for observed muscle kinematics. The graphical comparison of this measure across couplings in each gait cycle is depicted in FIGURE 29.

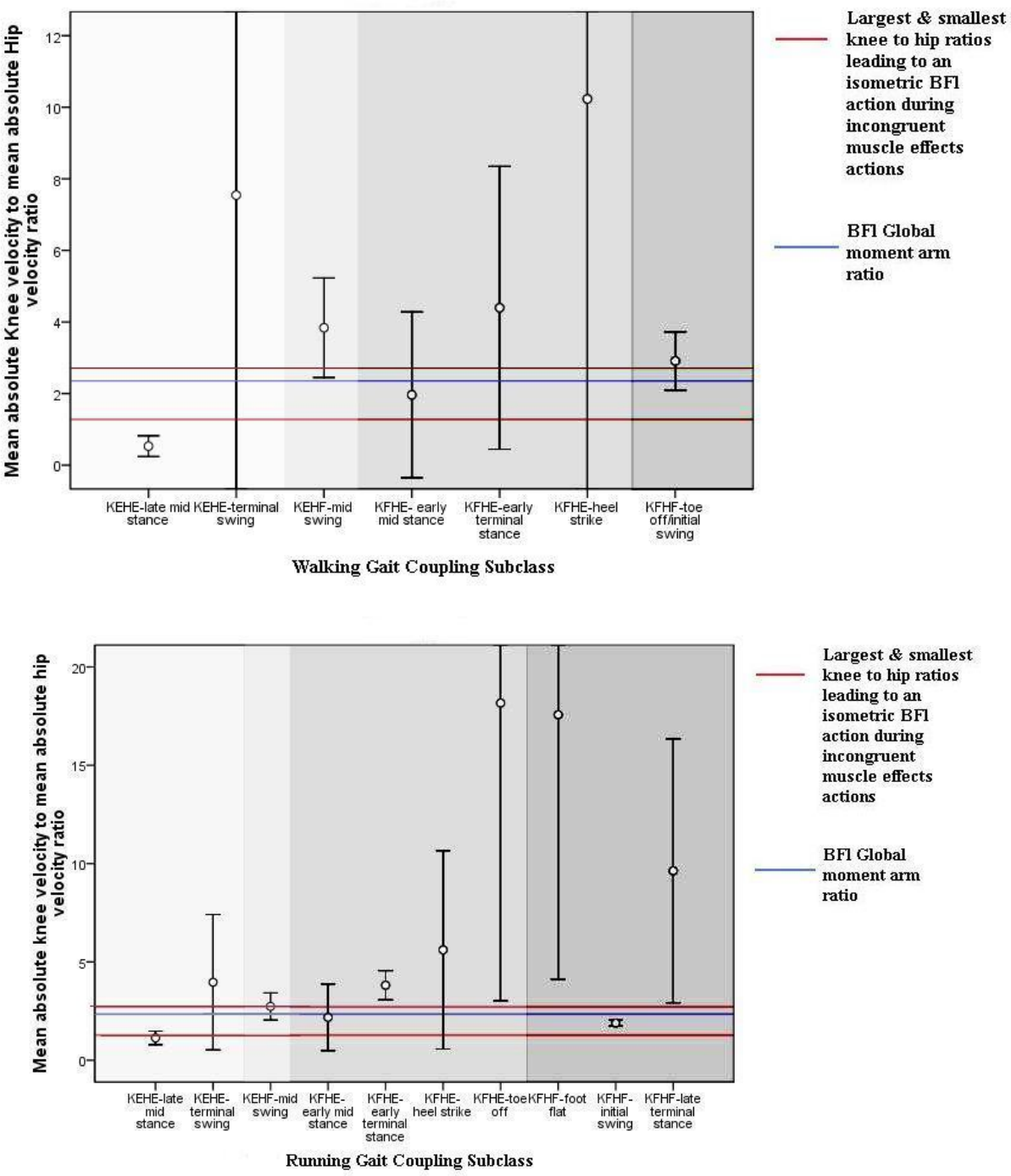

FIGURE 29- Ratio between absolute values of mean knee and hip velocities during the (A) Walking (B) Running Gaits. Error bars represent the 95% confidence interval of the mean.

Comparisons are presented of the overall running and walking step cycles in FIGURE 30 and FIGURE 31, and differences between the BF_L and BF_S were tested with a series of paired t-tests.

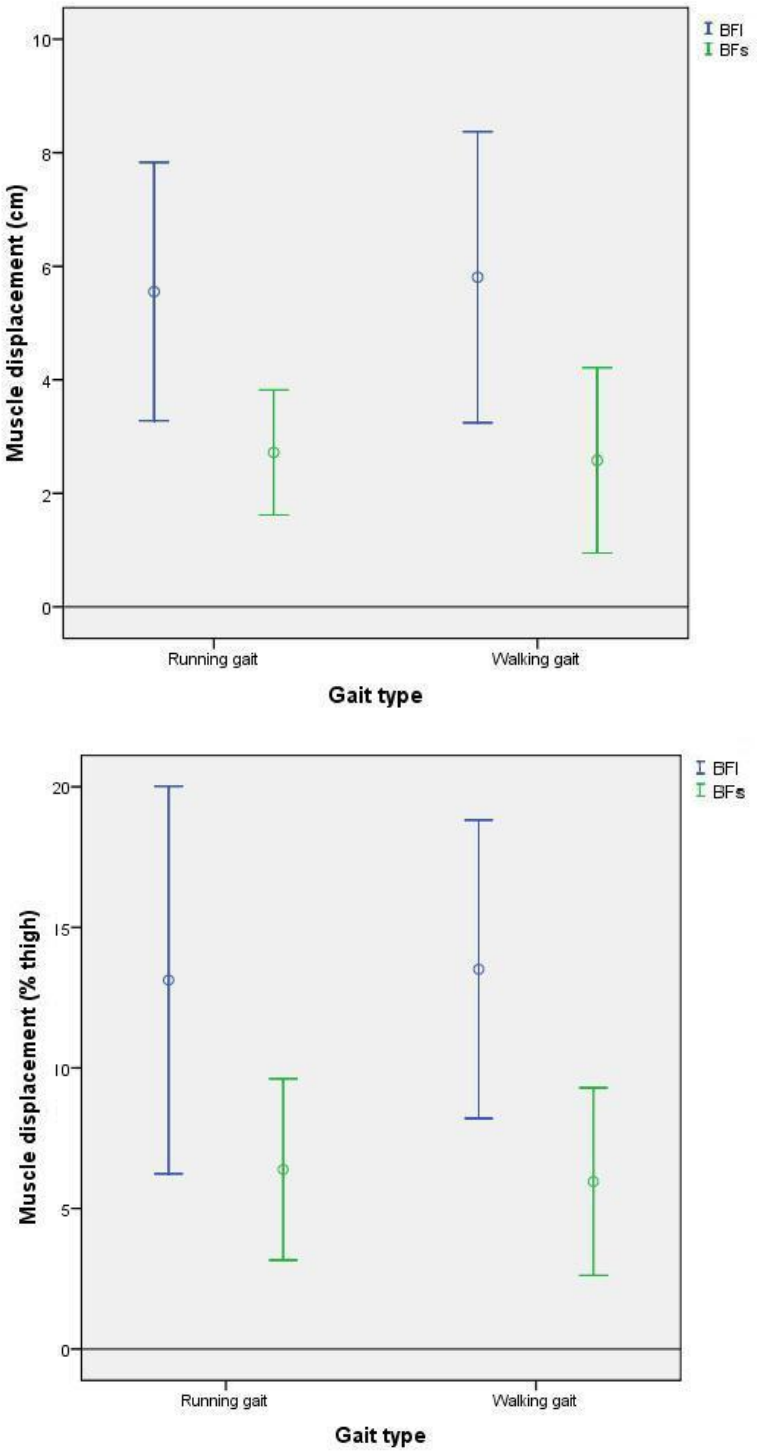

FIGURE 30- Mean muscle displacement over the entire running and walking gait cycles for both BF_L (blue) and BF_S (green). A) Absolute displacement b) relative displacement error bars indicate the 95% confidence interval of the mean (both absolute and relative: $p<0.001$ for walk, $p<0.01$ for run).

Comparing the BF_L and BF_S in terms of muscle displacement over the both gait cycles in their entireties, it is apparent that the BF_L has a greater displacement in both cases (both $p<0.01$).

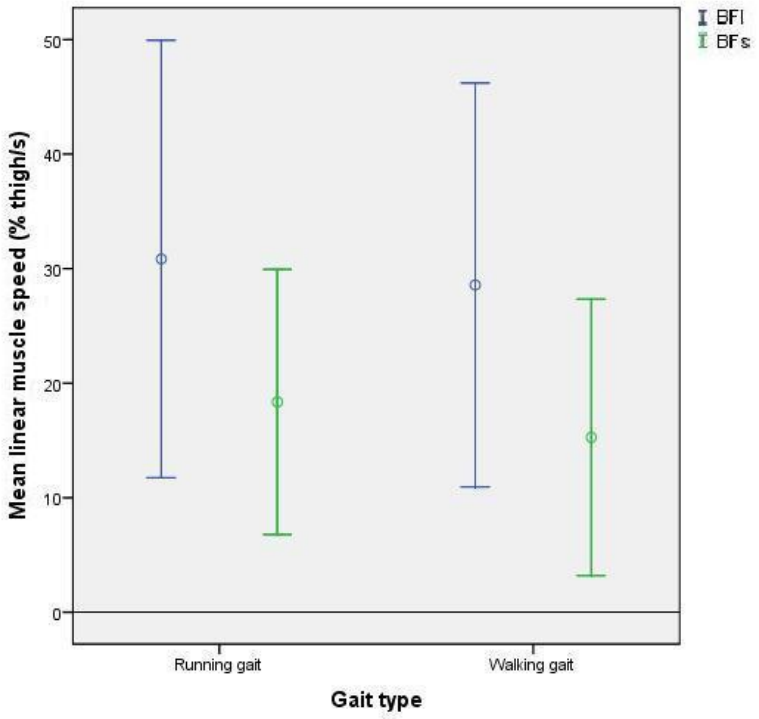

FIGURE 31- Mean muscle speeds over the entire running and walking gait cycles for both BF_L (blue) and BF_S (green). Error bars indicate the 95% confidence interval of the mean.

A similar trend in the inter-muscular speed differences can be seen when examining both the walking and running step cycles (all four comparisons: $p<0.001$).

Note regarding the KFHE-heel strike

In the running step cycle two kinematic approaches to the heel strike were apparent (TABLE 15):

Two subjects showed very large knee dominance during this subclass, while the other three showed much smaller knee to hip ratios. Of these three trials:

- one showed a value beyond the largest BF_L isometric knee to hip velocity ratio, indicating less knee dominance (a knee to hip velocity ratio smaller than the BF_L global moment arm ratio)
- one lay just above the level of the global moment arm ratio indicating the possibility of hip dominance (a knee to hip velocity ratio smaller than the BF_L global moment arm ratio)

- The last one was less than the global moment arm ratio, suggesting a high probability of hip dominance.

A similar division in angular kinematics was seen in the three trials of the walking gait cycle KFHE-heel strike subclass (TABLE 15).

TABLE 15- KFHE-heel strike sub grouped kinematics

KFHE-heel strike Sub Grouped Kinematics								
Running Gait		**Mean BF_L Velocity (% thigh/s)**	**Mean BF_S Velocity (% thigh/s)**	**Knee & Hip Angle Correlation (r)**	**Knee to Hip Ratio**	**Knee ROM (degrees)**	**Hip ROM (degrees)**	**BF_L Velocity Shift (% BF_S Velocity)**
2 knee Dominant trials	**Mean**	-15.56	-6.84	0.88	9.87	4.83	0.48	125.11
	SD	8.910	3.710	0.020	0.346	4.929	0.482	8.171
3 Less Knee Dominant	**Mean**	-55.6	-14.925	0.91	2.78	15.53	6.93	311.10
	SD	14.331	5.679	0.035	1.637	3.371	3.561	190.173
Walking Gait								
2 Knee Dominant	**Mean**	-9.23	-4.53	0.92	15.25	6.39	0.46	98.87
	SD	8.810	4.201	0.048	3.029	5.355	0.443	9.890
Single Hip Dominant Trial		-8.01	-0.04	0.97	0.19	0.38	1.95	19444.67

Discussion

Comparison of Current Model to Pre-Existing Models

Comparisons between parameters of the current BF_L model and two other two dimensional BF_L models (Hawkings and Hull, 1990; Visser et al, 1990) were made (TABLE 16).

TABLE 16- Comparisons of methodologies and BF_L global moment arms (MAs) about the hip and knee joints between existing models.[1]

Parameter	Villafranca & Kriellaars (2010)	Visser et al (1990)	Hawkings & Hull (1990)
Muscle Length Measurement Methodology	Origin to insertion distance measurement	Measurement of tendon displacement	Origin & insertion data from Brand (1982), using scaling parameters
Number of cadaveric specimens (n)	4 total, 3 females, 1 male	5 total, 3 females, 2 males	3 total, 1 female, 2 males
Hip abduction angle	90-95 degrees	Not reported	Not reported
Number of measures of BF_L length/ cadaver	10 hip positions X 14 knee positions= 140 measures	18 hip positions + 15 knee positions = 33 measures	8 hip positions X 8 knee positions= 64 measures
Range of Motion Increments	Approximately 10 degrees	Approximately 5 degrees	Approximately 15 degrees
Knee ROM (degrees)	145	90	120
Hip ROM (degrees)	104	75	120
Global Hip MA (% thigh/degree)	0.26 (mean)	0.31	0.20
Global Knee MA (% thigh/degree)	0.12 (mean)	0.05	0.16
Ratio of Global MAs (Hip MA/Knee MA)	2.34	6.76	1.25

[1] Length estimations and ranges were calculated using the equations provided by the investigators (Hawkings and Hull, 1990; Visser et al, 1990). The BF_L moment arm- joint angle relationships for the two existing models were recreated using the tendon excursion method of moment arm calculation. A thigh length of 40 cm was assumed for all moment arm calculations, to facilitate comparisons to existing direct measures of BF_L moment arms. The global moment arm calculation was simplified for the Visser et al (1990) and Hawkings and Hull (1990) models, since these models did not take the BF_L knee and hip moment arm interaction into account. Thus only a single global moment arm calculation was calculated for each joint in these models.

To gain a more comprehensive understanding of the differences between the model moment arms, the BF_L moment arm-joint angle plots were compared between models and with direct measures of BF_L moment arms (FIGURE 33 & FIGURE 32). FIGURE 32 demonstrates that the BF_L moment arm about the knee seen in our model was more congruent with existing literature (Buford, 1997; Herzog, 1993; Smidt, 1973). It provides a more accurate estimation of knee moment arm compared to the Hawkings and Hull (1990) and Visser et al (1990) models throughout at least the first 90 degrees of the knee range of motion.

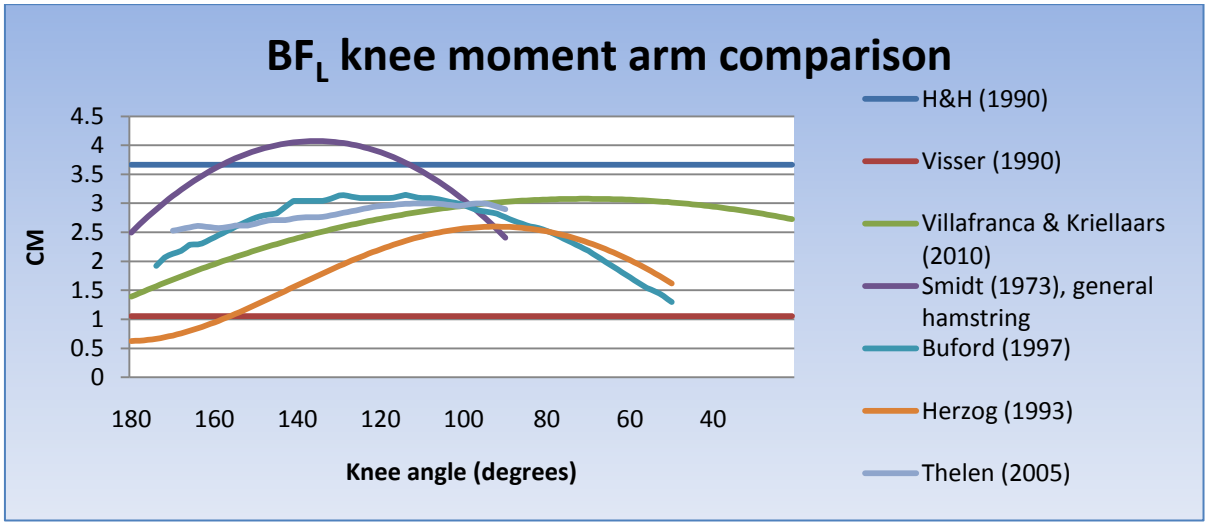

FIGURE 32- Comparison of model predicted BF_L moment arms about the knee with the second joint angle held constant. Direct moment arm measures are depicted for comparison. 180 degrees represents a fully extended knee position.

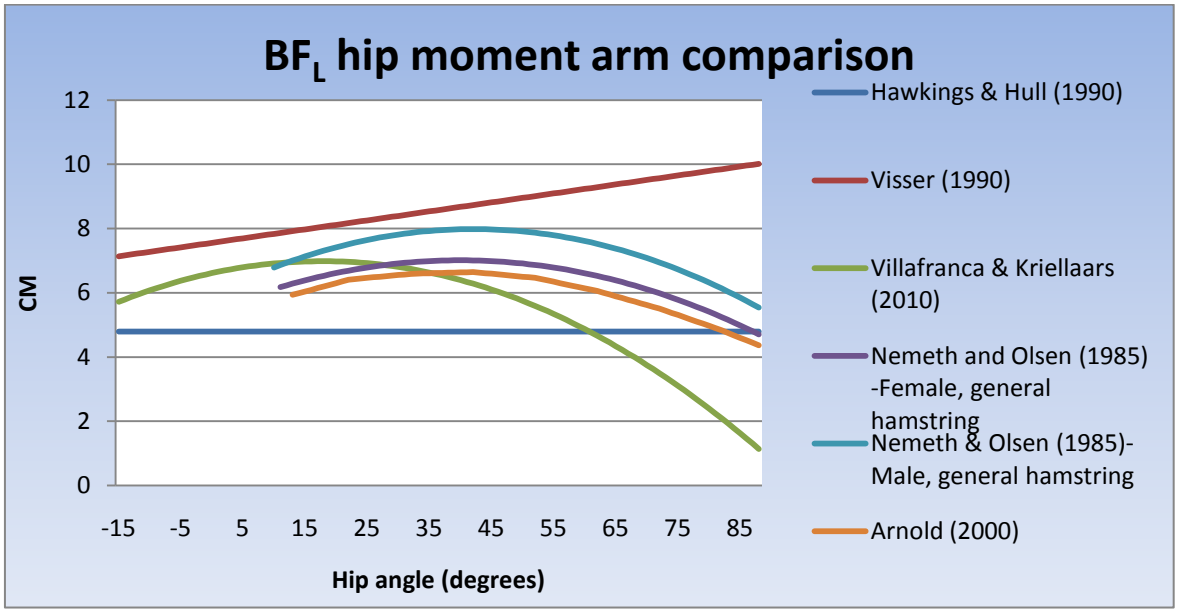

FIGURE 33- Comparison of model predicted BF_L moment arms about the hip with the second joint angle held constant. Direct moment arm measures are depicted for comparison. -15 represent the most extended hip position.

FIGURE 33 demonstrates that the BF_L moment arm about the hip seen in our model was generally more congruent with existing literature (Nemeth & Olsen, 1985; Arnold, 2000). It provides a better estimate of the BF_L hip moment arm for a range of approximately 75 degrees (-15 to 60 degrees). This is noteworthy, since the majority of human motions occur in this range of hip angles.

Data from a greater number of subjects should eventually be compiled with our data to increase mode external validity. However, our model should be given preference over those of Visser et al (1990) and Hawkings and Hull (1990). Reasons for this include our more stringent methodology in BF_L length measurement, our equations' greater geometrical accuracy regarding the interaction of the BF_L moment arms, our more realistic shape of the BF_L moment arm joint angle relationships, and our more reasonable estimate of the BF_L global moment arm ratio.

Evaluation of the Role of Biarticular Muscles

A brief discussion of the key findings will be presented in this section, followed by more elaborate explanations of the individual velocity shift and displacement conservation & exacerbation situations in separate sections.

Motions with significant left velocity shifts of the BF_L relative to the BF_S, and therefore motions that would result in an increased possible force based on the f/v curve, include the KFHF-tuck and KEHF-kick classes, the KFHF-initial swing subclass of the running step cycle, the KFHF-early/mid swing of the walking gait, and the KEHF-mid swing subclass of both gaits. Our hypotheses regarding mechanically beneficial left velocity shifts were supported for the classes of motion predicted, but only in some of the walking and running gait subclasses predicted. Therefore the mechanical benefits associated with left shift are likely a reality in at least some human motions, particularly those with knee to hip velocity ratios indicating hip dominance. However, the exacerbated lengthening velocity seen in the KEHF motions may result in an increased chance of injury.

Motions with significant right velocity shifts of the BF_L relative to the BF_S, and therefore motions that would result in an decreased possible force based on the f/v curve, include the KEHE-jump and KFHE-paw, the KEHE-late mid stance of both gaits, the KEHE-terminal swing of the running gait, the four KFHE subclasses of the running gait, and two of the subclasses of the walking gait. Therefore our hypotheses regarding the mechanically detrimental right velocity shifts were supported for the two classes of motion predicted, and for a number of the gait subclasses, although not all that were anticipated. It is of note that there were a smaller number of gait subclasses predicted to result in left shifted velocities. Also, the percentage of the subclasses predicted to show a significant left shift that actually reached significance was smaller than the percentage of subclasses predicted to show significant right shifts that actually did. It appears as though the detriments associated with right shifted velocities of the BF_L are a legitimate concern during human motion, particularly during gait. Mechanically detrimental shifts on the f/v curve may also be more prevalent in human motion than mechanically beneficial shifts, based on their frequency of occurrence during the gait cycles.

The hypothesized displacement exacerbation would be seen in the KFHF-tuck, but not the KEHE-jump, and not in any of the predicted subclasses of the gait cycles. This is a very important observation, which has its origins partly in the dramatic magnitude (<-200) of the velocity shift of the BF_L relative to the BF_S, which negates the possibility of a displacement conservation. This in turn is a consequence of the knee to hip ratio (the smaller the knee to hip ratio compared to the global moment arm ratio, the more the hip dominance, and therefore the larger the velocity shift between the muscles). The predicted mechanical benefits to BF_L force would only be seen in one of the two coupled motions, and in none of the gait subclasses, and therefore such conservation may not play a significant role in human motion.

Related to this, the KEHE-late mid stance subclasses which were originally predicted to result in a conserved BF_L displacement relative to the BF_S, in fact showed a significantly exacerbated displacement. Such an exacerbation was also seen in the KEHF-mid swing of both gaits, and the walking gait KFHE-early terminal stance. Therefore displacement exacerbation and its possible mechanical detriments is likely a real concern in human motion, even in some examples of a coupling class with incongruent effects (KEHE) - a coupling class which has historically been predicted to result in a mechanical benefit based on the f/l relationship.

Full Discussion of Velocity Results

Coupling classes with <u>Left</u> Shifted Velocities (KFHF & KEHF)

The BF_L velocity was significantly left shifted relative to the BF_S during both the KFHF-tuck and KEHF-kick classes, supporting our velocity hypotheses for these two couplings. It could therefore be said that these examples of the KFHF and KEHF classes are force potentiating based on the f/v relationship. However such a shift could result in a longer muscle length at the end of the motion for a given muscle than for the other couplings. This could result in an increased risk of muscle strain. This is particularly true of the KEHF-kick motion, which is also subject to the highest mean and peak BF_L velocities.

The KFHF-tuck represents a very unique situation, since it is a motion characterized by the largest knee and hip joint ranges of motion as well as the largest mean angular velocities of any of the four couplings (

TABLE 13), combined with small muscle velocities (FIGURE 19). As previously mentioned, it is also an example of the only coupling class which would be predicted to be force potentiated based on both the f/v and f/l relationships, based on its left BF_L velocity shift relative to the BF_S, as well as its predicted displacement conservation relative to the BF_S.

Gait Subclasses with Left Shifted Velocities (KFHF & KEHF)

KFHF

The difference in mean velocity between the BF_S and BF_L was only statistically significant in the KFHF-initial swing subclass of the running step cycle and the KFHF-toe off/initial swing of the walking gait. In addition, the peak velocity of the BF_L was significantly different that of the BF_S during the KFHF-late terminal stance. Therefore notable left shifts on the force velocity curve would be seen during these subclasses, but not in the KFHF-foot flat or the KFHF-late terminal stance of the running gait. The KFHF-initial swing involves a BF_L shortening followed by a BF_L lengthening (FIGURE 21 & FIGURE 23) and would therefore initially be knee dominant and then become hip dominant as the subclass progressed. Therefore the latter part of this subclass would be more mechanically beneficial to BF_L force production based on the force velocity curve than its initial part. This focused mechanical benefit seen during the KFHF-initial swing of the running gait seems reasonable in light of the fact that the main role of the BF_L during the initial swing tasks is likely knee flexion. The hip dominance seen in this subclass (FIGURE 29) would allow the BF_L to lengthen after reaching its minimum length (FIGURE 20) while still promoting the last bit of knee flexion needed to reduce the moment of inertia of the leg. This would therefore increase angular knee velocity for the initiation of the rapid KEHF-mid swing phase that follows.

KEHF

In both gaits the KEHF-mid swing subclass showed significantly larger lengthening velocities than the BF_S. Therefore the BF_L lengthening velocity was left shifted relative to the BF_S in both gait cycles for this subclass. The knee to hip velocity ratio of this motion in the running gait suggests that the hip and the knee would be having comparable effects on muscle velocity. The mean lengthening exacerbation seen during the

KEHF-mid stance was greater than the majority of shortening exacerbations seen during any of the gait KFHE subclasses (FIGURE 24).

The KFHE-early terminal stance subclass of both the walking and running gaits showed significant differences in mean muscle velocities but not peak muscle velocities. This likely occurred since the change in the BF_S velocity throughout this subclass is larger than that of the BF_L (FIGURE 21 & FIGURE 23) in both gait cycles, and therefore although on average the BF_L had an exacerbated velocity relative to the BF_S, their peak shortening velocities were not very different. Therefore the effect of the biarticular nature of the BF_L during the KFHE-early terminal stance was to promote a consistent exacerbation throughout the subclass, as opposed to an increasing shortening velocity following a BF_S SSC.

Coupling classes with <u>Right</u> Shifted Velocities (KEHE & KFHE)

The BF_L velocities seen during the KEHE-jump and KFHE-paw motions were significantly different (right shifted) from those of the BF_S, which is in agreement with the velocity shift hypotheses for these classes of motion. This right shift would place the muscle in a less advantaged position to produce force based on the f/v relationship. This right velocity shifting would mean that either a given force would be unachievable, or that the amount of activation for a biarticular would have to be increased under independent control relative the uniarticular muscle. This would be particularly true in those situations where the velocity shift was so large that it resulted in a reversal of muscle displacement direction (from lengthening to shortening, as seen in the KEHE-jump). However, the right shift may serve another function besides affecting the possible force or activation levels of the specified muscle. One possibility is that the right velocity shift may disable the BF_L to an extent, and therefore enable the improved functioning of other muscles. It may also be simply an unfortunate consequence of enabling the muscle to contribute to hip extension or to indirectly contribute to torque at another joint through its simultaneous activation with the rectus femoris (van Ingen Schenau, 1994).

Nonetheless this right shifting has to be considered in future models of neural control of so called agonists, since having biarticular and uniarticular muscles performing completely different muscle actions would add a layer of complexity and potentially versatility to the neuromuscular system.

The implications of the velocity shifts of the BF_L during KEHE motions are particularly difficult to interpret, since the role of BF_L activation during such motions is equivocal. Two options regarding the function of the BF_L to see during KEHE motions are as follows:

1. *The function of the BF_L in KEHE motions is to produce high forces for hip extension*: In this case we would want the BF_L to be lengthening under tension as the hip extended, in order to produce the greatest hip extension force from the BF_L, since that would place it on the lengthening portion of force velocity curve. The way this would be achieved in KEHE motions would be to have the motion be knee dominant, resulting in a muscle lengthening in both the BF_L and BF_S. Optimization (training or modelling) studies or studies of athletes performing these tasks may shed light on this.
2. *The function of BF_L in KEHE motions is to effectively "transfer force/energy":* If this were the case, we would want the BF_L to be acting isometrically. This would allow it to act as a rigid link, reacting to external forces without deforming (lengthening) or shortening. An isometric BF_L would effectively and quickly exert a reaction force on other structures involved in this "force transfer" since it would minimize the storage of elastic energy that would be seen with a lengthening muscle. In addition, it would still avoid the variation in the muscle's ability to exert force that would be seen if the muscle were shortening (and therefore shifting its position on both the f/l and the torque-length relationships). The way this would be achieved in a KEHE motion would be to have the knee and the hip having equal effects on muscle velocity, resulting in no net change in muscle length. This was not observed in any of the KEHE motions.

However, this discussion of BF_L force optimization during KEHE motions should always be considered in light of the fact that that having the BF_L muscle contribute to hip extension in any capacity is obviously more conducive to that end than having it be a uniarticular knee flexor like the BF_S, whose role in KEHE motions is even more questionable.

Gait Subclasses with Right Shifted Velocities (KEHE & KFHE)

KEHE

In the running gait, the mean velocity difference between the BF_L and BF_S was only significant in one of the two KEHE walking step cycle subclasses (the KEHE-late mid stance), but both reached significance in the running gait. During the other walking gait KEHE subclass (KEHE-terminal swing) the two muscles had similar mean muscle velocities.

KFHE

The four running gait KFHE subclasses did show significantly larger mean shortening BF_L velocities compared to those of the BF_S, but generally not in terms of peak velocities. Two of the four walking gait KFHE subclasses reached significance (early mid stance and early terminal stance). The variability of the KFHE motions, especially those during the first portion of the stance phase, makes interpretation of the results more difficult. However, it's fairly obvious that the greater the shortening velocity exacerbation seen, the greater the associated right shift on the force velocity curve for the BF_L.

Discussion of Muscle Displacement Results

Four Classes of Motion

Our hypotheses regarding inter-muscular differences between muscle displacements were confirmed in three of the four of the examples of the classes of motion. The only exception to this was the KEHE-jump motion.

As hypothesized, the KFHF-tuck resulted in a significant muscle displacement conservation compared to the BF_S. However, since the BF_L velocity shift relative to the BF_S was particularly dramatic in the KEHE-jump

relative to the absolute value of the BF_S velocity (BF_S speed), the KEHE-jump resulted in a larger BF_L shortening displacement than the lengthening displacement of the BF_S. This is a fascinating but unexpected finding, since it is contrary to traditional thinking about KEHE motions and the f/l relationship. It is interesting to note that in light of this finding, the KEHE-jump does not result in a mechanical benefit to BF_L force based on either velocity shift or length conservation.

This novel finding is explained through examination of the magnitude of velocity shift during the KEHE-jump. Velocity shift represents an important explanatory variable, since the idea of displacement conservation of in the BF_L assumes that the velocity shift will bring the BF_L closer to a zero linear velocity. A shift of -100% or would bring the BF_L to a zero velocity condition. Velocity shifts more negative than this would result in the BF_L showing opposite length changes of those occurring in the BF_S. Even more importantly, a velocity shift more negative than -200% would represent a condition where the BF_L is shifted to a faster muscle length change of the opposite type (e.g. being shifted from a lengthening muscle with a mean velocity of 40% thigh length/sec to a shortening muscle with a mean velocity of 50% thigh length/sec). These negative % shifts are only seen in incongruent muscle effects actions. Positive shifts indicate velocity exacerbations, and not surprisingly these shifts would be seen only with congruent muscle effects actions. TABLE 14 demonstrates that the KEHE-jump had a velocity shift just greater than -200%, explaining the lack of significance.

It is true that the BF_L shortening displacement in the KEHE-jump would be smaller than the BF_L lengthening displacement that would been seen the single joint knee motion alone, since the motion is hip dominant based on the knee to hip velocity ratio. Therefore the effect of the knee motion on the BF_L acts to decrease the large shortening displacement caused by the hip motion. The same cannot be said of the effect of the hip motion on the BF_L displacement, since it is not simply decreasing the lengthening displacement caused by the knee motion, but rather decreasing it to zero, and then continuing to increase it in the opposite direction beyond the magnitude seen in with the knee motion. Therefore concurrent motions such as the KEHE-jump should not automatically be associated with displacement conservation. As predicted, a significant displacement exacerbation was seen for the KEHF-kick. This may place the BF_L at a particular risk for injury, since it subjects it to a longer muscle length at its termination. Therefore the KEHF-kick is associated with mechanical benefits to BF_L force based on the f/v relationship, but likely not the f/s relationship and both of these factors may place the BF_L at an increased risk of muscle strain during this motion.

Gait Subclasses

Displacement exacerbation of the BF_L relative to the BF_S is seen in during the walking gait KEHF-mid swing and walking and running gait KEHE-late mid stance subclasses. This is in agreement with the results and the conclusions of these subclass differences in muscle velocity.

The overall cycle description demonstrated that there was no overall BF_L displacement conservation relative to the BF_S in both gait cycles (FIGURE 30, FIGURE 31). This again relates to the larger muscle displacements seen in the swing phase, particularly the KEHF-mid swing phase. The velocity exacerbation was also seen in a single KFHE-early terminal stance. The lack of significance in these exacerbations is likely related to the knee dominance of these couplings (as indicated by the knee to hip velocity ratios), and well as the large variability in displacement in these subclasses.

Implications of this Work on the Understanding of Motor Control

Traditionally the terms "agonist" and "antagonist" are defined in biomechanics as follows:

- Agonist:

"A muscle that is directly responsible for effecting a movement" (Luttgens et al, 1992)

"A role played by a muscle acting to cause a movement" (Hall, 1999)

- Antagonist:

"A muscles that causes the opposite movement from that of the (agonist)" (Luttgens et al, 1992)

"A role played by a muscle acting to slow or stop a motion" (Hall, 1999)

These traditional definitions are generally sufficient when describing the actions of uniarticular muscles. They are even generally sufficient in describing biarticular muscles during congruent effects circumstances. For instance, during KFHE motions, the BF_L is undoubtedly acting as an agonist, since it is promoting the motions

at both the hip and knee joints. Similarly, during KEHF motions the BF_L is undoubtedly acting as an antagonist about both joints, since it is resisting the motions at both the hip and knee joints.

However, the role of the BF_L during the incongruent effects circumstances (KEHE and KFHF) is less clear, and the binary classifications of "agonist" and "antagonist" become insufficient in describing biarticular muscles in these circumstances. In the KFHF-tuck, the BF_L would be lengthening while it is acting as an agonist for knee flexion. This is certainly different from the way it acts as an agonist during joint knee flexion alone, where it would be shortening. Specifying the role of the BF_L about the two different joints would lead to the simultaneous and contradictory classification of the BF_L as both an agonist and an antagonist to the resulting movements.

In addition to challenging the standard nomenclature of muscle roles in joint motion, our discovery of circumstances where the two portions of the same muscle are undergoing opposite length change direction has compelling implications for motor control theory. First, in these circumstances the BF_L and BF_S would not be able to function with common neural drive during hip dominant incongruent circumstances, since they would require different motor unit recruitment strategies based on their different muscle length changes. Second, the gamma motor neurons innervating the muscle spindles would need to be controlled differently during these motions, since they would encounter different muscle lengths and degrees of stretch between the two head of the muscle. Further, special consideration would need to be made to account for this in the spinal cord and higher neuraxis for motor programming. Third, since the BF_L and BF_S are different during all four classes, and the velocity shifts are of different magnitudes for each coupling class, mechanoreceptor feedback to the CNS would be different in all four coupling classes. Therefore the neural circuitry in the spinal cord must be adaptable to account for these different conditions. An overriding theory of biarticular muscle functioning during multi-segmental motion incorporating this new perspective on biarticular muscle functioning is yet to emerge.

It is commonly thought that the time of occurrence of BF_L injury during the running gait cycle is the late swing phase, based on popular clinical opinion (Orchard, 2002) and research on a single incidence of BF_L strain injury (Heiderscheit et al., 2005). The KEHE-terminal swing subclass of the running gait cycle contains many biomechanical factors that may predispose the BF_L to injury during this subclass. The fact that the KEHF-mid swing is the temporal antecedent of the KEHE-terminal swing subclass means that the latter operates under an exacerbated muscle length throughout its duration. It also contains a BF_L stretch shortening cycle, whose occurrence interestingly coincides with the largest BF_L length in the entire step cycle (FIGURE 20). This stretch shortening cycle is predictably associated with a high slope on the muscle velocity time graph (FIGURE 21), indicating a period of large BF_L acceleration.

The late swing is also known to be the point where the BF_L becomes active again following its period of lesser activity during the mid swing (Thelen et al, 2005a). This may be important, as the muscle could therefore be forced to deal with the initiation of BF_L activation during a period of high muscle acceleration and at a very large muscle length.

Additionally, BF_L injury during either the terminal swing may be promoted by motor control error, originating from the combination of a BF_L being required to act alongside both other biarticular muscles, as well as with a uniarticular head sharing a common insertion. To appreciate this possibility, a brief review of muscle mechanoreceptor functioning is in order.

Muscle spindles are mechanoreceptors found spread throughout a skeletal muscle (Sherwood, 2008). Their intrafusal fibres are specialized to detect passive changes in muscle fibre length (flower spray endings & annulospiral endings) and muscle fibre speed (annulospiral endings) (Sherwood, 2008). Muscle spindles can affect muscle kinematics through their associated gamma motor neurons, which are activated under conditions of muscle stretch, in a process called the stretch reflex (Sherwood, 2008). This process causes a muscle contraction in response to this passive muscle stretch, and is also thought to result in inhibitory effects on antagonistic muscles (Sherwood, 2008).

In contrast to muscle spindles, Golgi tendon organs (GTOs) are mechanoreceptors that respond to a muscle's tension, by sending afferent information to the brain. There, it is processed on a conscious level and a subconscious level, the latter normally promoting in a more refined control of a motor task (Sherwood, 2008). Therefore GTO feedback can impact muscle kinematics on both conscious and unconscious levels.

In a muscle system composed of two uniarticular muscles crossing the same joint, we would expect both muscles to have similar mechanoreceptor feedback for a given motion. We would also predict similar length changes and tensions in the muscles.

However, this study has shown that prediction of mechanoreceptor feedback may be less intuitive when you are looking at a system of one biarticular muscle and one uniarticular muscle. We have demonstrated that different muscle actions will occur in a biarticular muscle versus a uniarticular muscle during multi-segmental motions meeting two conditions:

- The multi-segmental coupling must result in incongruent circumstances in the biarticular muscle (KEHE and KFHF couplings, in the case of BF_L)

- The angular kinematics of the motion are organized so that the joint the biarticular muscle is uniquely crossing has a greater effect on the displacement and linear velocity of this biarticular muscle (i.e. the motion must be hip dominant for this situation to arise in the BF_L and BF_S)

Such situation were seen in the KEHE-jump and the KFHF-tuck in the examples of the four classes of motion, as well as the KEHE-late mid stance, the KEHE-terminal swing subclasses of both the running and walking gait cycles, and in the KFHF-initial swing subclass of the running gait cycle. In these motions, one muscle would be shortening while the other would be lengthening. These different muscle actions would likely result in different and simultaneous afferent feedback, even between two heads of the same muscle.

One particular circumstance where there are likely very different mechanoreceptor activations by the BF_L and BF_S would be during incongruent effects motions with knee to hip velocity ratios that change dramatically, such as in the KEHE-late swing phase. This is because motions with a large change in the knee to hip velocity ratio are likely to result in an SSC of the biarticular muscles crossing the hip and knee, as was noted for the BF in the KEHE-terminal swing phase. Therefore during this subclass the BF_L would be undergoing a SSC while the BF_S would simply be lengthening the entire time. It should also be considered that the other biarticular hamstring muscles have slightly different moment arms about the hip and knee joints compared to the BF_L and to each other. Therefore, each muscle would have slightly different global moment arm ratios. While these smaller differences won't result in dramatically different muscle kinematics, it would likely shift the timing of the SSC in each muscle during these incongruent couplings with changing knee to hip velocity ratios. This could result in a different mechanoreceptor activation pattern for each of these muscles.

At this point it is worth noting a possible criticism of this idea and exposing its limitations. It is commonly known that the innervation of the BF_S is different than that of the BF_L (the tibial branch of the sciatic nerve versus the peroneal branch, respectively) (Gross et al, 2009). Some researchers have even asserted that due to its differing distal nerve branching and origin, that the BF_S should not be considered a hamstring muscle. Therefore it might be argued that such a motor control error would not be seen. However, due to the anatomical overlap and connection between the BF_L and BF_S at the distal tendon insertion, it is likely they share at least some mechanoreceptors. Even if they did not, activation of one of the muscles could affect some mechanoreceptors of the other muscle, since the active muscle would exert a force on some of the non active muscles' fibres, resulting in a change in the fibres lengths and tensions. More importantly, the two muscles share the same nerve roots at the spine, leading to the sciatic nerve (Leis and Trapani, 2000); therefore we would not expect dramatically different neural drive based on classical motor control thinking.

It is interesting to speculate on the effects of the differing BF_L and BF_S actions on the risk of hamstring muscle injury. The combination of a KEHE phase in the terminal swing with a KFHE phase in the heel strike seen in the running gait is a very interesting pairing, since it must result in dramatically different afferent inputs from the BF_L relative to the BF_S. The addition of a coupling with knee flexion causes the observed BF_S SSC at the end of the KEHE-terminal swing and the beginning of the KFHE-heel strike. Therefore both circumstances where the BF_L is thought to be susceptible to injury (late swing and heel strike) are likely associated with asymmetrical spindle and GTO activation within a homonymous muscle group.

Now it could be further speculated that human motor control contains some resilience to mechanoreceptor asymmetries, since different muscle actions of the BF_L and BF_S occurred during the majority of KEHE and KFHF motions examined. However, during a repetitive task with mechanoreceptor mediated feedback (such as running), the magnitude and timing of the asymmetry may vary, perhaps eventually exceeding a threshold, and resulting in a motor control error, could in turn result in muscle injury.

In the future it will be important to examine how deviations in the gait cycle which are commonly assumed to increase probability of hamstring injury (e.g. leaning forward to gain extra speed, over striding (Orchard, 2002)) affect the muscle displacements and muscle velocities during the late swing and early stance subclasses, as well as to explore mechanoreceptor functioning during situations where traditionally synergistic muscles, or even different heads of the same muscle, undergo different muscle actions.

Limitations and Delimitations

There are a few important limitations to this work:

This project involved collection of movement kinematics performed by unskilled human subjects. Therefore the possibility exists that a greater mechanical benefit due to the biarticular nature of the BF_L relative to the BF_S could be seen in experienced runners or other athletes (i.e. training may optimize multi-segmental coordination to maximize biarticular muscle force). However, the BF_L velocity directions compared to those of the BF_S are unlikely to change with training for the examples of the four classes of motion, since they involved specified start and end points, and consequently controlled knee and hip ranges of motion. These controlled ranges of motion would in turn put limitations on the variability of the knee to hip velocity ratio both within and between subjects. Therefore the motion where variability between trained and untrained subjects would be highest would likely be the gait cycles, since the ranges of motion for the gait cycles were not implicitly controlled in this investigation.

Another limitation of this investigation was its assumption that changes in the origin to insertion length would be exclusively due to differences in muscle fibre length. This is not true, since the tendon may stretch slightly throughout the motions. However, Thelen (2005), making use of the model of Delp (1990), performed a sensitivity analysis to determine how large an effect on predicted peak BF_L stretch during the sprint cycle would be seen through adjustment of the model tendon compliance parameter. At its most compliant value (0.09), the difference in peak stretch would amount to 10 mm less than when using a much less compliant value (0.03). Therefore any error seen through the omission of such this factor would be minimal, and certainly would not alter the conclusions of this investigation.

Our conclusions regarding mechanical benefits and detriments that would be seen in the BF_L relative to the BF_S based on the f/v curve involve the assumption that the activation levels of both muscles would be comparable. This is less of a concern in situations of large velocity shifts between the muscles, since the difference between the muscle's possible forces would grow larger. Therefore relative changes in activation levels would become harder to overshadow the differences in force (i.e. a fully activated muscle that is shortening very quickly is unlikely to exert more force than a muscle activated at 50% which is lengthening quickly). Systematic analysis of BF_L compared to BF_S muscle activation during the four classes of motion is needed to clarify in what situations this assumption is acceptable.

There were also a few delimitations to our model:

The model was based predominantly on data from female cadavers. Unfortunately the nature of cadaveric research involves severe limitations of availability, which have been apparent in all the models examined. Therefore this delimitation is not unique to our investigation. However, validation of the model in a male subject of much taller stature than any of the cadavers provides confidence that our model still provides good estimations of muscle length in populations less similar to the cadavers examined.

The model also involves a calculation of muscle length based on hip and knee angles in the sagittal plane, and assumes a hip abduction angle of approximately 90 degrees. Therefore the model's predictions will only be valid for motions occurring in the sagittal plane, with a hip abduction angle of close to 90 degrees.

Conclusions

- Significant velocity shifts of BF_L relative to BF_S do occur in examples of the four classes of lower limb motion, and in the majority of gait subclasses characterized by knee dominance, supporting the hypotheses related to velocity shift of BF_L relative to BF_S. Muscle shortening velocity exacerbation during gait is generally seen in terms of mean muscle velocities, but not so in peak muscle velocities. Therefore mechanical benefits and detriments based on the f/v relationship are likely realized during human motion.
- There is no evidence of a BF_L displacement conservation compared to the BF_S in any portion of the walking and running gait cycles, or in the KEHE-jump. Therefore any mechanical benefits associated with displacement conservation based on the f/l relationship are not realized during many important examples of the KEHE and KFHF coupling classes, and may not play an important role in human motion.
- The overall effect of the biarticular nature of the BF_L during the gait cycles on muscle displacement is exacerbation. Displacement exacerbation is also seen during select KEHE and KFHE subclasses of the running gait, as well as the KFHE-kick and the KEHF-paw. The possible detriments associated with displacement exacerbation based on the f/l curve are likely realized during KEHF motions, as well as some KFHE and KEHE motions, and therefore displacement exacerbation is likely a concern in human motion.
- BF_L displacement conservation is not present in the KEHE-jump or the KEHE-late mid stance subclasses of the walking and running gaits due to large velocity shifts caused by hip dominant movement. Incongruent muscle effects motions should not be assumed to result in more moderate muscle displacement for biarticular muscles compared to uniarticular reference muscles.
- The higher frequency of BF_L injury during running gait may be related to its biarticular nature, which results in factors associated with muscle strain: a dramatic length exacerbation in the KEHF-mid swing subclass compared to the BF_S, an SSC during the late swing phase coinciding with a peak in BF_L length, and situations of possible asymmetrical mechanoreceptor activation during both the terminal swing and the heel strike.
- The discrepancies between the functioning of the BF_L compared to that of BF_S during the four classes of motion have large implications for motor control theory.

Further Directions

Future research should focus on the following areas:

- Examine the angular kinematics (specifically the knee to hip velocity ratio) of other important human lower limb motions make predictions of their BF_L muscle kinematics relative to the BF_S. In particular, it would be interesting to see if greater mechanical benefits or detriments in terms of velocity shift and displacements would be seen during the sprinting gait cycle.

- Examine how inter-subject anthropometric and kinematic variations for a given motion affect the knee to hip velocity ratio, and therefore the relationship between BF_L and BF_S linear kinematics. This would give insight into whether multi-segmental kinematics are optimized to maximize biarticular muscle force. For instance, it would be interested to examine how training affects the preferred knee and hip coordination pattern for each class of motion. Simulation of different coordination strategies and their effects on inter-muscular differences in velocity and displacement would also be incredibly insightful.

- Generate similar BF_L models in other species to compare the relationship between BF_L and BF_S kinematics during the quadruped gait cycles, and contrast these results with the findings of this investigation. This could provide insight into the effects of human evolution on biarticular muscle functioning.

Appendices

Appendix 1- Cadaveric Dissection Details

Upon inspection the cadavers had extreme limitations on the possible amount of knee flexion (less than 10 degrees) and hip flexion (less than 45 degrees). To allow a complete range of motion for the development of the mathematical model, cadaveric dissection was needed.

A cadaveric dissection protocol was both planned a priori and empirically adjusted with the help of a trained anatomist. The philosophy employed was to remove and incise the minimum amount of structures necessary to achieve a complete range of motion at both the hip and knee joints for a given cadaver, while maintaining a high level of consistency among the cadaver dissections. Thus all cadavers had a set number of structures removed and incised, based on an initial dissection in the presence of the anatomist. The degree of incisions into connective tissues of the knee and hip varied slightly, but always erred on the side of maintaining joint integrity.

All unrelated tissues (epithelial, adipose, etc…) were dissected and removed from the lower limb. Dissection occurred with the cadaver in multiple orientations, to facilitate precision in the dissection and provide a better perspective for structure identification. Muscles were removed to improve joint ranges of motion and to minimize tissue obstructions to the camera's view of the screws. Connective tissue was generally left intact to preserve joint integrity, although specific incisions where made when joint stiffness was preventing a full range of knee motion. Small portions of the muscles' tendons were kept on the bone to provide landmarks, unless they obstructed structured that needed to be measured for screw placement (e.g. The Ischial tuberosity).

The dissection process in its entirety was photographically documented for a single cadaver.

1. Sequence of dissection:

- Incisions were made in the epithelial tissue of the right leg. These began from 1/3rd of the way down the shank, then medially upwards to and following the inguinal line, following the iliac crest, continued around the majority of the right buttock, and finally connected back to the incision on the medial thigh. The epithelial tissue in that dissection area was then removed.

- All subcutaneous adipose tissue was removed from the right thigh and hip area revealing the different muscular compartments of the leg.

- The muscle sheaths of the different leg muscle compartments were removed, and the muscles within each compartment were separated. Any intramuscular fat, nervous, and vascular tissue was removed, including the sciatic nerve and its branches.

- Systematically the musculature of the right thigh was removed in the following order:

    - The gluteal muscle group (gluteus maximus, gluteus medius, and gluteus minimus)

    - The quadriceps muscle group. All muscles within this group were removed except for the vastus medialis. Rectus femoris was removed to allow greater hip extension. The vastus medialis and vastus Intermedius were removed to increase visibility of the screws inserted in the femur.

    - The entire adductor muscle group. This muscle group was found to limit hip flexion in the majority of subjects.

    - The hamstring muscle group (semitendinosus, semimembranosusnosus, and the biceps femoris long and short heads). This muscle group was found to be the largest delimiter of hip flexion in all the cadavers.

    - The small hip external rotators were all removed, with the exception of the obturator internus and externus. The removed rotators were found to slightly limit hip flexion

Additional incisions were made to specific anatomical structures. An incision was made into the illiopsoas muscle. When intact, this muscle was found to significantly reduce the range of hip extension to no more than slightly beyond anatomical position.

The patellar tendon was also cut perpendicular to its line of action, to promote a larger range of motion for knee flexion. This incision was also made to minimizing the amount of knee joint connective tissue necessarily incised. However, progressive incisions into the connective tissues/ fascia of the knee were still required, to allow for highly flexed knee positions and to minimize excessive tibial rotation at flexed knee positions.

Incisions of varying length were made into the medial collateral ligament (MCL) of the knee joint. These incisions ran perpendicular to the long axis of the thigh. In no case did the incision run through the entire MCL. While incisions into the ventro-lateral aspect of knee were necessary, incisions into the thin lateral collateral ligament were not necessary in any subjects.

Finally, small superior portions of the Peroneus longus and Extensor digitorum longus were excised. This was to allow for screws placement in the superior fibula without visual obstruction to the camera.

Appendix 2- Additional Cadaveric Setup Details and Figures

A. Securing the Cadaver Torso

Cadavers were placed lying on their left sides and secured in this position with an adjustable wooden cage apparatus (FIGURE 34, FIGURE 35)

This cage apparatus was constructed to allow the cadavers to be secured in a side lying position without any change in the vertical or horizontal inclination of the trunk. It consisted of four 8.6 X 3.6 X 60 cm legs, connected superiorly lengthwise by 55 X 2 X 6.1 cm crossbars, and width wise by crossbars measuring 39.2 X 1.9 X 6.1 cm. The top pieces were secured to the legs using screws and wing nuts. Multiple evenly spaced holes were drilled into the crossbars, allowing the adjustment of the cage width and length (FIGURE 35)

To secure the position of the cage relative to the cadaver table, two adjustable fabric straps ran from one side of the cadaver table, over the cage, and finally hooked to the sides of the cadaver table (FIGURE 35). These straps were tightened as needed. In addition blocks of wood of varying sizes were wedged between the four legs of the cage and the table frame to secure the bottom portion of the cage to stabilize the angle of the cage legs relative to the crossbars, and further secure the position of the cadaver relative to the table (FIGURE 35).

The position of the cadaver within the cage was standardized so that the bottom set of legs would not obstruct the view of the ASIS marker, and was thus approximately at the level of the abdomen. The top set of legs was aligned with the head (FIGURE 35). The cadavers were consistently placed in the center of the cadaver table. In order to ensure that the cadavers were completely on their sides, the right and left anterior superior iliac spines (ASIS) of each cadaver were aligned vertically.

B. Securing the Right thigh and shank Segments:

A large platform (maximum length of six feet and maximum width of four feet) was placed under the right thigh of the cadaver (FIGURE 34, FIGURE 35). It was designed to act as a surface on which the right thigh of the cadaver could rest throughout the placement protocol, while simultaneously decreasing the possibility of non sagittal thigh movement. Another important function of the apparatus was to keep hip abduction angle constant at around 90 degrees. The platform shape was also chosen to facilitate its concurrent use alongside the cadaver cage.

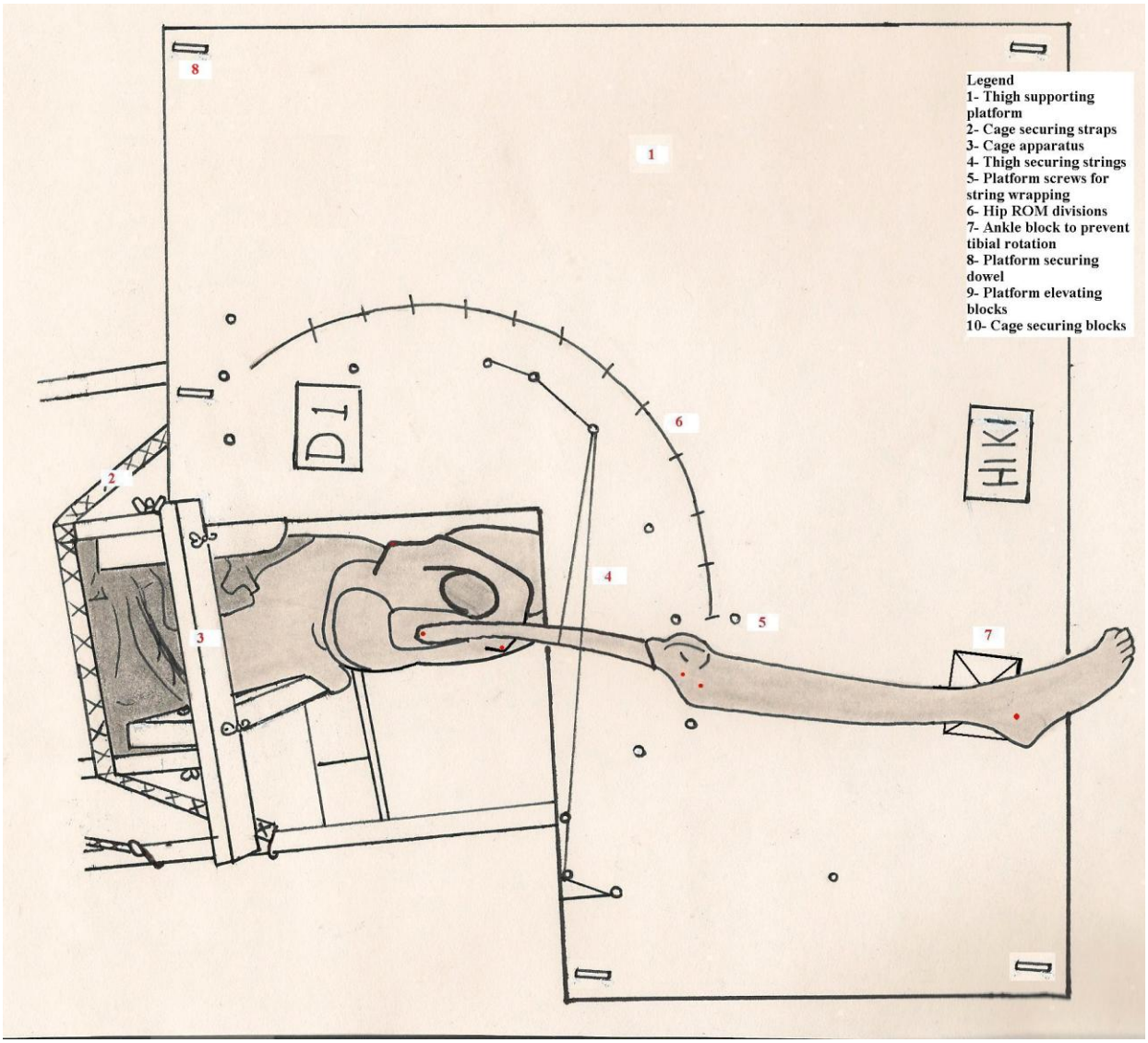

FIGURE 34- Artist's depiction of cage apparatus and leg supporting platform (camera view of setup).

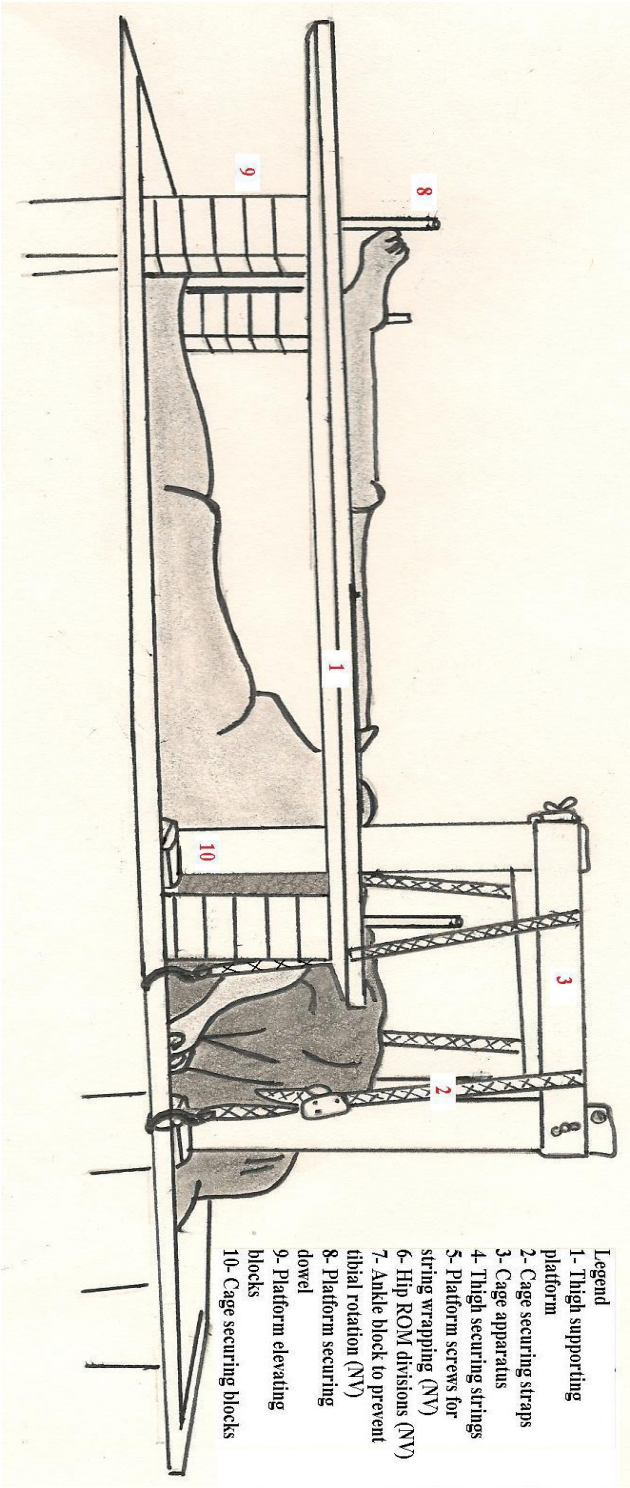

FIGURE 35- Artist's depiction of cage apparatus and leg supporting platform (side view of setup).

A given number of blocks of 1.5 inches in height were distributed equally among various corners of the platform, creating points of contact between the platform and the superior aspect of the cadaver dissection table, proximal to the table frame (FIGURE 35). These blocks also enabled the adjustment of the platform height. In

turn, the height of the platform dictated the amount of hip abduction of the right thigh. The blocks contained holes in their centers, which were aligned with holes on the platform. A 30 cm wooden dowel was placed through each platform hole- block hole set, to ensure there would be no shifting of the platform relative to the blocks. The three bottom blocks were secured to each other at each corner using nails, and had holes that did not extend completely through the bottom block, in order to increase stability of the system (FIGURE 36, FIGURE 37). Blocks of lesser widths were available to allow for smaller gradations of hip abduction angle, but their use was proved to be unnecessary.

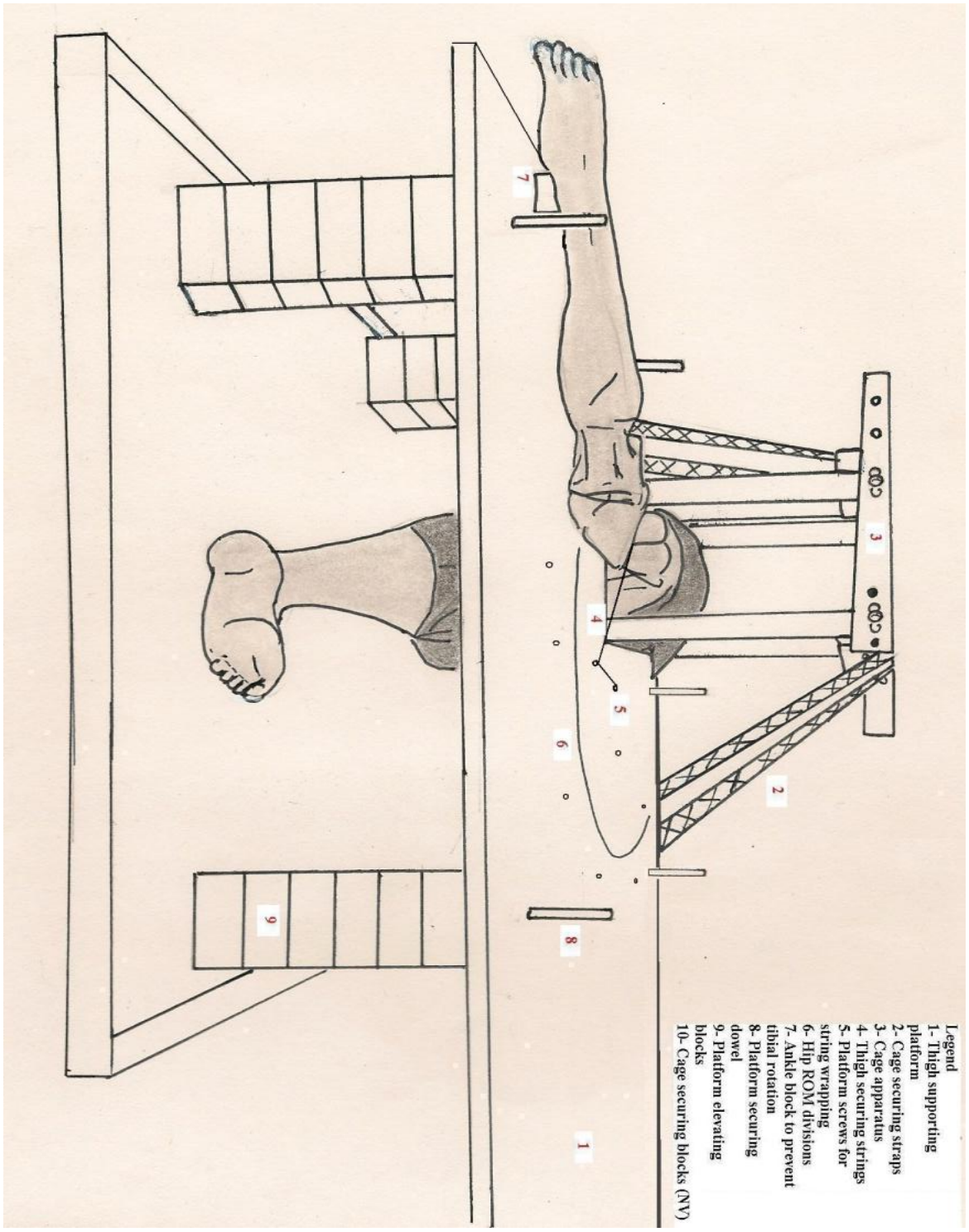

FIGURE 36- Inferior view of setup including block system.

FIGURE 37- Block system separate from the setup, depicting the attached block base and the dowel fitting in the center of the blocks

This desired amount of hip abduction was approximately a 90 degree angle between two segments: one from the marking screw in the center of the right femur to the marking screw in the right ASIS, and one from the right ASIS to the left ASIS. For the determination of this angle, a string was temporarily secured taut between these three markers, and the angle between the sections of the string was measured with a goniometer.

At combinations of extreme hip extension and knee flexion, as well as hip flexion and knee extension, the shank was not able to rest on the platform. In this minority of cases, the shank was manually held at the height of the platform surface, and at the desired knee angle, for that particular picture.

C. Additional Considerations

In order to ensure that each cadaver's right thigh was parallel to the camera, a number of different sized boards were placed underneath the foot end of the cadaver table if needed. This was only necessary for a single cadaver who had particularly narrow hips (D2).

The inclination of the thigh relative to the horizontal was determined using a plastic carpenter's spirit level. The tube centroid of the level was visually aligned to the center of the thigh, and rested posterior to the screw indicating the lateral location of the center of the right thigh.

The thigh was secured to the platform in order to keep the hip flexion/extension angle constant for each hip position. It also acted to reduce internal/external rotation of the hip. This system was comprised of two strings tied to the distal thigh, around the area of the femoral epicondyles. The strings ran approximately parallel to each other, but in opposite directions. Each string was wrapped tight around a wooden screw organized to be perpendicular with the thigh in the given hip position. Screws were systematically placed in the board to maintain a constant hip flexion/extension for each position.

The reference point used to standardize internal/external rotation angle across different hip positions and across cadavers was the screw in the lateral greater trochanter, which was standardize to face vertically.

Due to the angle of the shank relative to the thigh, a wooden block was placed beneath the medial Malleollus of the right leg in order to reduce any tibial rotation. The initial position of orientation was ensuring that the marking screws in the head of the fibula and the lateral malleollus were both aligned vertically. The block was not secured to the medial Malleollus, in order to provide the ability to shift the center of the block slightly from the medial Malleollus. The purpose of allowing this slight instability was to help ensure the block would not to be raised by any unused screws present on the board (which were used for securing of the thigh in other hip positions) which we believed would result in greater shifting of the markers on the shank, especially that of the lateral malleollus. In situations where this square block would inevitably be raised by unused screws on the board, a narrow rectangular block of an equivalent height was used as a substitute. The wider block was always given preference over the narrow block to maximize the contact area between the block and the right ankle and foot, and thus maximize the amount of tibial stability.

Appendix 3- Hip Angle Position Averaging

The hip angle within each hip position was found to vary slightly (standard deviation <3.5 degrees in all situations) as the knee was progressively flexed. To enable interpolation between knee angles for a given hip position, it was necessary to have a single representative hip angle for each hip position. To achieve this, the means of the hip angles for each hip position were calculated, and were taken as representative of the hip angle for their respective hip positions. Descriptive statistics of this calculation in all subjects and positions are depicted in

TABLE 17.

TABLE 17-Descriptive statistics of the mean hip angle calculation. Hip position 1 represents the position of maximum possible hip extension, and position 10 represents a position of the largest hip flexion.

Hip Position Averaging					
Cadaver Number	**Hip Position**	**Mean Hip Angle**	**Standard Deviation of Hip Angle**	**Coefficient of Variation (CV)**	**Mean CV**
	1	142.44	2.71	1.90	
	2	133.11	1.43	1.07	
	3	119.22	0.71	0.59	
	4	108.80	0.38	0.35	
	5	97.40	0.33	0.34	2.20
	6	81.52	0.41	0.51	
	7	68.77	0.39	0.57	
	8	54.03	0.79	1.46	Without Positions 9 & 10
	9	43.73	2.04	4.66	
D1	10	31.69	3.36	10.59	0.85
	1	153.00	1.29	0.84	
	2	136.92	2.65	1.94	
	3	130.40	2.85	2.18	
	4	118.86	1.78	1.50	
	5	107.83	1.16	1.08	
	6	97.65	1.21	1.24	
	7	87.88	0.67	0.76	
	8	78.52	2.39	3.05	
	9	60.68	0.93	1.54	
D2	10	51.51	1.65	3.20	1.73
	1	152.60	2.55	1.67	
	2	142.72	1.50	1.05	
	3	119.95	2.34	1.95	
	4	107.51	0.74	0.69	
	5	96.54	0.99	1.03	
	6	85.00	0.38	0.45	
	7	74.22	0.28	0.38	
	8	65.83	0.36	0.55	
	9	60.44	0.97	1.61	
D3	10	49.20	1.41	2.87	1.22
	1	152.60	2.10	1.38	
	2	138.75	1.69	1.22	
	3	134.97	2.08	1.54	
	4	122.22	1.21	0.99	
	5	110.02	1.32	1.20	
	6	98.25	0.44	0.45	
	7	87.20	0.34	0.39	
	8	75.96	0.36	0.47	
	9	63.16	0.67	1.06	
D4	10	51.77	1.09	2.11	**1.08**
			Overall excluding D1- 9& 10	1.24	

The variability within each hip position was visually determined to be primarily due to shifts in hip internal/external rotation throughout the motion. Internal rotation of hip occurred as the knee reached large flexion angles. The onset of this rotation was noted to occur at more extended knee angles in positions of extreme hip flexion and extreme hip extension. Thus the onset of hip internal/external angle change occurred through a greater number of knee positions in extreme hip positions. This partially explains the greater variability in hip angles in positions of extreme hip extension and flexion.

The male cadaver showed a larger mean coefficient of variation than the females. The coefficients of variation were larger in the position of maximum hip flexion, as well as slightly larger in positions of large knee flexion in all cadavers, but particularly in the male cadaver. Due to the smaller mean angle of the positions of hip flexion, its coefficient of variation was drastically larger than all other hip positions.

The last two positions in the male cadaver were effectively eliminated by restricting the hip angle range upon which the model was based. Thus the lower hip angle degree limit was set at 49 degrees. This was done to eliminate positions containing outliers in terms of range of motion and measures of variability, and avoid the less appealing alternative of matching this cadaver range with extrapolation of up to a 20 hip degree magnitude in the other cadavers.

Appendix 4- Individual Cadaver Equations

TABLE 18- BF_L length equations of individual cadavers (cm)

Cadaver	BF_L length-knee angle-hip angle 2nd order bivariate polynomial fits (cm)
D1	$-1.0663e\text{-}006K\theta^3 + 1.5904e\text{-}006K\theta^2H\theta + 7.5532e\text{-}006K\theta^2 - 1.5335e\text{-}006K\theta\ H\theta^2 - 8.2955e\text{-}005K\theta\ H\theta + 0.07507K\theta - 3.0451e\text{-}007H\theta^3 + 0.00043033H\theta^2 - 0.056133H\theta + 12.2794$
D2	$-6.9614e\text{-}007K\theta^3 - 1.0104e\text{-}006K\theta^2H\theta + 0.00025503K\theta^2 - 4.5469e\text{-}008K\theta\ H\theta^2 + 0.00026355K\theta\ H\theta + 0.021123K\theta - 1.3235e\text{-}006H\theta^3 + 0.00053287H\theta^2 - 0.081487H\theta + 17.383$
D3	$-1.9193e\text{-}006K\theta^3 - 1.1339e\text{-}006K\theta^2H\theta + 0.00064626K\theta^2 - 6.03e\text{-}007K\theta\ H\theta^2 + 0.00051534K\theta\ H\theta - 0.038073K\theta + 1.4817e\text{-}006H\theta^3 - 0.00063735H\theta^2 + 0.051937H\theta + 17.6756$
D4	$1.3043e\text{-}006K\theta^3 + 1.1536e\text{-}006K\theta^2H\theta - 0.00079992K\theta^2 + 1.0062e\text{-}006K\theta\ H\theta^2 - 0.0004823K\theta\ H\theta + 0.16471K\theta - 1.8498e\text{-}006H\theta^3 + 0.00045952H\theta^2 - 0.013493H\theta + 9.8667$

TABLE 19-Normalized BF_L length equations of individual cadavers (% thigh length)

Cadaver	BF_L length-knee angle-hip angle 2nd order bivariate polynomial fits (% thigh)
D1	$-3.4375e\text{-}006K\theta^3 + 2.5883e\text{-}006K\theta^2H\theta + 0.0006302K\theta^2 - 7.7233e\text{-}006K\theta\ H\theta^2 + 0.00089407K\theta\ H\theta + 0.054336K\theta + 1.8304e\text{-}005K\theta^3 - 0.0042044H\theta^2 + 0.003908H\theta + 96.4452$
D2	$-2.4585e\text{-}006K\theta^3 - 4.9374e\text{-}006K\theta^2H\theta + 0.0013066K\theta^2 - 1.7251e\text{-}006K\theta\ H\theta^2 + 0.001538K\theta\ H\theta - 0.088901K\theta + 1.6874e\text{-}005H\theta^3 - 0.0036955H\theta^2 - 0.15655H\theta + 110.6109$
D3	$-4.4583e\text{-}006K\theta^3 - 1.5611e\text{-}006K\theta^2H\theta + 0.0015581K\theta^2 - 2.5807e\text{-}006K\theta\ H\theta^2 + 0.0012009K\theta\ H\theta - 0.10893K\theta + 1.7965e\text{-}005H\theta^3 - 0.0063891H\theta^2 + 0.42204H\theta + 93.1868$

D4	$2.1179e\text{-}006K\theta^3 + 2.5054e\text{-}006K\theta^2H\theta - 0.001589K\theta^2 - 2.0777e\text{-}006K\theta\ H\theta^2 - 0.00013083K\theta\ H\theta + 0.34134K\theta + 1.5645e\text{-}005H\theta^3 - 0.0052089H\theta^2 + 0.28015H\theta + 90.7329$

TABLE 20- BF_S length equations of individual cadavers (cm)

Cadaver	BF_S length-knee angle-hip angle 2nd order bivariate polynomial fits (cm)
D1	$-1.5057e\text{-}006K\theta^3 + 1.1337e\text{-}006K\theta^2H\theta + 0.00027605K\theta^2 - 3.3828e\text{-}006K\theta\ H\theta^2 + 0.0003916K\theta\ H\theta + 0.023797K\theta + 8.0171e\text{-}006H\theta^3 - 0.0018415H\theta^2 + 0.0017089H\theta + 42.2432$
D2	$-1.0891e\text{-}006K\theta^3 - 2.1872e\text{-}006K\theta^2H\theta + 0.00057882K\theta^2 - 7.6403e\text{-}007K\theta\ H\theta^2 + 0.00068126K\theta\ *X2 - 0.039378K\theta + 7.4747e\text{-}006H\theta^3 - 0.001637H\theta^2 - 0.069357H\theta + 49.0006$
D3	$-1.9796e\text{-}006K\theta^3 - 6.9299e\text{-}007K\theta^2H\theta + 0.00069184K\theta^2 - 1.1454e\text{-}006K\theta\ H\theta^2 + 0.0005331K\theta\ H\theta - 0.048361K\theta + 7.9768e\text{-}006H\theta^3 - 0.0028368H\theta^2 + 0.1874H\theta + 41.3744$
D4	$8.3854e\text{-}007K\theta^3 + 9.9206e\text{-}007K\theta^2H\theta - 0.0006292K\theta^2 - 8.2274e\text{-}007K\theta\ H\theta^2 - 5.1801e\text{-}005K\theta\ H\theta + 0.13517K\theta + 6.1955e\text{-}006H\theta^3 - 0.0020628H\theta^2 + 0.11095H\theta + 35.9302$

TABLE 21- Normalized BF_S length equations of individual cadavers (% thigh)

Cadaver	BF_S length-knee angle-hip angle 2nd order bivariate polynomial fits (% thigh)
D1	$-2.4345e\text{-}006K\theta^3 + 3.6311e\text{-}006K\theta^2H\theta + 1.7254e\text{-}005K\theta^2 - 3.5013e\text{-}006K\theta\ H\theta^2 - 0.00018935K\theta$ *X2 $+ 0.17139K\theta - 6.9502e\text{-}007H\theta^3 + 0.00098242H\theta^2 - 0.12815H\theta + 28.0351$
D2	$-1.5714e\text{-}006K\theta^3 - 2.281e\text{-}006K\theta^2H\theta + 0.00057569K\theta^2 - 1.0267e\text{-}007K\theta\ H\theta^2 + 0.00059497K\theta\ H\theta + 0.047678K\theta - 2.9875e\text{-}006H\theta^3 + 0.0012029H\theta^2 - 0.18395H\theta + 39.2396$
D3	$-4.3228e\text{-}006K\theta^3 - 2.554e\text{-}006K\theta^2H\theta + 0.0014555K\theta^2 - 1.3579e\text{-}006K\theta\ H\theta^2 + 0.0011607K\theta\ H\theta - 0.085749K\theta + 3.337e\text{-}006H\theta^3 - 0.0014354H\theta^2 + 0.11697H\theta + 39.8101$
D4	$3.2935e\text{-}006K\theta^3 + 2.9132e\text{-}006K\theta^2H\theta - 0.00202K\theta^2 + 2.5407e\text{-}006K\theta\ H\theta^2 - 0.0012179K\theta\ H\theta + 0.41594K\theta - 4.6712e\text{-}006H\theta^3 + 0.0011604H\theta^2 - 0.034072H\theta + 24.9158$

Appendix 5- Gait Subclass Frequency Table

TABLE 22- Gait Subclass Frequency. Bold font in the frequency columns indicates

Period	Coupling Subclass- Temporal Order Based on Automated Separation	Frequency (Out of 5 Subjects)	
		Running Gait	Walking Gait
Stance Phase	**1) KFHE-early terminal stance**	4	5
	2) KFHF/late terminal stance	5	**0**
	3) KFHE-toe off	3	**0**
Swing Phase	**4A) KFHF- initial swing** **4B) KFHF- toe off/initial swing**	5 **0**	**0** 5
	5) KEHF-mid swing	5	5
	6) KEHE-terminal swing	5	5
Stance Phase	**7) KFHE-heel strike**	5	3
	8) KFHF-foot flat	4	**1**
	9) KFHE- early mid stance	5	4
	10) KEHE- late mid stance	5	5
	Total Subclasses Observed For All Subjects **Total Subclasses Per Person (Excluding Subclasses with Frequency <3)**	46 10	33 7

Appendix 6- A Note on Terminology

The uses of the words "Countercurrent" and "Concurrent" in the context of human movement is inconsistent from their defined meanings, and is therefore ultimately confusing. "Countercurrent" is defined as (American Heritage Dictionary of the English Language, 2009):

1. A current running in an opposite direction to another current.

2. A movement, opinion, mood, etc., contrary to the prevailing one.

This has little to do with human motion. "Concurrent" is a more related, but still inappropriate term for the description of coupled flexion or coupled extension motions. It is defined as (American Heritage Dictionary of the English Language, 2009):

1. Occurring or existing simultaneously or side by side.

2. acting in conjunction, cooperating

The problem arises that all of the two joint couplings include joint motions that are occurring simultaneously and are conjoined. Further, it is unclear how coupled knee and hip flexion, or coupled knee and hip extension would more cooperative than couplings with one joint flexing while the other is extending. In fact, they are promoting different BF_L length changes in the lower limb during "concurrent motion".

The disconnect between the type of coupling and the effect the joints are having on biarticular muscle kinematics is also important to note. Concurrent motions between the hip and knee joints are associated with incongruent muscle effects, meaning the motion at each joint promotes different muscle length changes. Thus the effects of both joints are not congruent with the promotion of a particular muscle length change, and instead sum to a net muscle length change. Countercurrent motions between the hip and knee joints are associated with congruent muscle effects, where both joints are promoting the same direction of muscle length change, additively exacerbating the muscle length change occurring due to either joint. However, if we were examining the long head of the Triceps Brachii, concurrent motions would result in congruent muscle effect, while countercurrent motions would result in incongruent muscle effects. To make this terminology applicable to all biarticular muscles, the higher level terminology must be based on the muscle effects, rather than the joint

coupling occurring, with the subclasses relating these effects with particular joint couplings. Therefore, any further references to these categories will now use this new terminology.

Appendix 7- Within Subjects ANOVA- Four Coupling Classes Linear Variables

TABLE 23-Within subjects ANOVA multivariate tests- Four coupling classes

Multivariate							
Coupling Type	Within Subjects Effect		Value	F	Hypothesis df	Error df	Sig.
'KEHE-jump'	Muscle Type	Pillai's Trace	.997	401.659[a]	5.000	7.000	.000
		Wilks' Lambda	.003	401.659[a]	5.000	7.000	.000
		Hotelling's Trace	286.899	401.659[a]	5.000	7.000	.000
		Roy's Largest Root	286.899	401.659[a]	5.000	7.000	.000
'KEHF-kick'	Muscle Type	Pillai's Trace	.948	25.699[a]	5.000	7.000	.000
		Wilks' Lambda	.052	25.699[a]	5.000	7.000	.000
		Hotelling's Trace	18.357	25.699[a]	5.000	7.000	.000
		Roy's Largest Root	18.357	25.699[a]	5.000	7.000	.000
'KFHE-paw'	Muscle Type	Pillai's Trace	.961	34.677[a]	5.000	7.000	.000
		Wilks' Lambda	.039	34.677[a]	5.000	7.000	.000
		Hotelling's Trace	24.769	34.677[a]	5.000	7.000	.000
		Roy's Largest Root	24.769	34.677[a]	5.000	7.000	.000
'KFHF-tuck'	Muscle Type	Pillai's Trace	.991	125.354[a]	5.000	6.000	.000
		Wilks' Lambda	.009	125.354[a]	5.000	6.000	.000
		Hotelling's Trace	104.462	125.354[a]	5.000	6.000	.000
		Roy's Largest Root	104.462	125.354[a]	5.000	6.000	.000
a. Exact statistic							
b. Design: Intercept Within Subjects Design: Muscle Type							
c. Tests are based on averaged variables.							

TABLE 24-Within subjects ANOVA Univariate tests- Four coupling classes

Univariate Tests								
Coupling Type	Source	Measure		Type III Sum of Squares	Df	Mean Square	F	Sig.
'KEHE-jump'	Muscle type	Mean velocity	Sphericity Assumed	15775.107	1	15775.107	426.556	.000
			Greenhouse-Geisser	15775.107	1.000	15775.107	426.556	.000
			Huynh-Feldt	15775.107	1.000	15775.107	426.556	.000
			Lower-bound	15775.107	1.000	15775.107	426.556	.000
		Peak Velocity	Sphericity Assumed	59184.511	1	59184.511	425.815	.000
			Greenhouse-Geisser	59184.511	1.000	59184.511	425.815	.000
			Huynh-Feldt	59184.511	1.000	59184.511	425.815	.000
			Lower-bound	59184.511	1.000	59184.511	425.815	.000
		Absolute Displacement	Sphericity Assumed	.006	1	.006	.010	.924
			Greenhouse-Geisser	.006	1.000	.006	.010	.924
			Huynh-Feldt	.006	1.000	.006	.010	.924
			Lower-bound	.006	1.000	.006	.010	.924
		Relative Displacement	Sphericity Assumed	.894	1	.894	.252	.625
			Greenhouse-Geisser	.894	1.000	.894	.252	.625
			Huynh-Feldt	.894	1.000	.894	.252	.625
			Lower-bound	.894	1.000	.894	.252	.625

	Error(Muscle Type)	Mean Velocity	Sphericity Assumed	406.807	11	36.982		
			Greenhouse-Geisser	406.807	11.000	36.982		
			Huynh-Feldt	406.807	11.000	36.982		
			Lower-bound	406.807	11.000	36.982		
		Peak Velocity	Sphericity Assumed	1528.903	11	138.991		
			Greenhouse-Geisser	1528.903	11.000	138.991		
			Huynh-Feldt	1528.903	11.000	138.991		
			Lower-bound	1528.903	11.000	138.991		
		Absolute Displacement	Sphericity Assumed	7.382	11	.671		
			Greenhouse-Geisser	7.382	11.000	.671		
			Huynh-Feldt	7.382	11.000	.671		
			Lower-bound	7.382	11.000	.671		
		Relative Displacement	Sphericity Assumed	38.990	11	3.545		
			Greenhouse-Geisser	38.990	11.000	3.545		
			Huynh-Feldt	38.990	11.000	3.545		
			Lower-bound	38.990	11.000	3.545		
'KEHF-kick'	Muscle Type	Mean Velocity	Sphericity Assumed	5807.924	1	5807.924	115.818	.000
			Greenhouse-Geisser	5807.924	1.000	5807.924	115.818	.000
			Huynh-Feldt	5807.924	1.000	5807.924	115.818	.000
			Lower-bound	5807.924	1.000	5807.924	115.818	.000
		Peak Velocity	Sphericity Assumed	8574.266	1	8574.266	128.660	.000
			Greenhouse-Geisser	8574.266	1.000	8574.266	128.660	.000
			Huynh-Feldt	8574.266	1.000	8574.266	128.660	.000
			Lower-bound	8574.266	1.000	8574.266	128.660	.000
		Absolute Displacement	Sphericity Assumed	55.421	1	55.421	51.792	.000
			Greenhouse-Geisser	55.421	1.000	55.421	51.792	.000
			Huynh-Feldt	55.421	1.000	55.421	51.792	.000
			Lower-bound	55.421	1.000	55.421	51.792	.000
		Relative Displacement	Sphericity Assumed	340.077	1	340.077	84.149	.000
			Greenhouse-Geisser	340.077	1.000	340.077	84.149	.000
			Huynh-Feldt	340.077	1.000	340.077	84.149	.000
			Lower-bound	340.077	1.000	340.077	84.149	.000
	Error(Muscle Type)	Mean velocity	Sphericity Assumed	551.619	11	50.147		
			Greenhouse-Geisser	551.619	11.000	50.147		
			Huynh-Feldt	551.619	11.000	50.147		
			Lower-bound	551.619	11.000	50.147		
		Peak Velocity	Sphericity Assumed	733.070	11	66.643		
			Greenhouse-Geisser	733.070	11.000	66.643		
			Huynh-Feldt	733.070	11.000	66.643		
			Lower-bound	733.070	11.000	66.643		
		Absolute Displacement	Sphericity Assumed	11.771	11	1.070		
			Greenhouse-Geisser	11.771	11.000	1.070		

			Huynh-Feldt	11.771	11.000	1.070		
			Lower-bound	11.771	11.000	1.070		
		Relative Displacement	Sphericity Assumed	44.455	11	4.041		
			Greenhouse-Geisser	44.455	11.000	4.041		
			Huynh-Feldt	44.455	11.000	4.041		
			Lower-bound	44.455	11.000	4.041		
'KFHE-paw'	Muscle Type	Mean Velocity	Sphericity Assumed	7111.421	1	7111.421	160.454	.000
			Greenhouse-Geisser	7111.421	1.000	7111.421	160.454	.000
			Huynh-Feldt	7111.421	1.000	7111.421	160.454	.000
			Lower-bound	7111.421	1.000	7111.421	160.454	.000
		Peak Velocity	Sphericity Assumed	24154.487	1	24154.487	70.858	.000
			Greenhouse-Geisser	24154.487	1.000	24154.487	70.858	.000
			Huynh-Feldt	24154.487	1.000	24154.487	70.858	.000
			Lower-bound	24154.487	1.000	24154.487	70.858	.000
		Absolute Displacement	Sphericity Assumed	224.946	1	224.946	83.943	.000
			Greenhouse-Geisser	224.946	1.000	224.946	83.943	.000
			Huynh-Feldt	224.946	1.000	224.946	83.943	.000
			Lower-bound	224.946	1.000	224.946	83.943	.000
		Relative Displacement	Sphericity Assumed	1657.657	1	1657.657	182.323	.000
			Greenhouse-Geisser	1657.657	1.000	1657.657	182.323	.000
			Huynh-Feldt	1657.657	1.000	1657.657	182.323	.000
			Lower-bound	1657.657	1.000	1657.657	182.323	.000
	Error(Muscle Type)	Mean Velocity	Sphericity Assumed	487.526	11	44.321		
			Greenhouse-Geisser	487.526	11.000	44.321		
			Huynh-Feldt	487.526	11.000	44.321		
			Lower-bound	487.526	11.000	44.321		
		Peak Velocity	Sphericity Assumed	3749.749	11	340.886		
			Greenhouse-Geisser	3749.749	11.000	340.886		
			Huynh-Feldt	3749.749	11.000	340.886		
			Lower-bound	3749.749	11.000	340.886		
		Absolute Displacement	Sphericity Assumed	29.477	11	2.680		
			Greenhouse-Geisser	29.477	11.000	2.680		
			Huynh-Feldt	29.477	11.000	2.680		
			Lower-bound	29.477	11.000	2.680		
		Relative Displacement	Sphericity Assumed	100.010	11	9.092		
			Greenhouse-Geisser	100.010	11.000	9.092		
			Huynh-Feldt	100.010	11.000	9.092		
			Lower-bound	100.010	11.000	9.092		
'KFHF-tuck'	Muscle Type	Mean Velocity	Sphericity Assumed	29135.375	1	29135.375	727.086	.000
			Greenhouse-Geisser	29135.375	1.000	29135.375	727.086	.000
			Huynh-Feldt	29135.375	1.000	29135.375	727.086	.000
			Lower-bound	29135.375	1.000	29135.375	727.086	.000
		Peak	Sphericity Assumed	114596.030	1	114596.030	179.239	.000

		Velocity	Greenhouse-Geisser	114596.030	1.000	114596.030	179.239	.000
			Huynh-Feldt	114596.030	1.000	114596.030	179.239	.000
			Lower-bound	114596.030	1.000	114596.030	179.239	.000
		Absolute Displacement	Sphericity Assumed	28.202	1	28.202	19.544	.001
			Greenhouse-Geisser	28.202	1.000	28.202	19.544	.001
			Huynh-Feldt	28.202	1.000	28.202	19.544	.001
			Lower-bound	28.202	1.000	28.202	19.544	.001
		Relative Displacement	Sphericity Assumed	139.010	1	139.010	15.893	.003
			Greenhouse-Geisser	139.010	1.000	139.010	15.893	.003
			Huynh-Feldt	139.010	1.000	139.010	15.893	.003
			Lower-bound	139.010	1.000	139.010	15.893	.003
	Error(Muscle Type)	Mean Velocity	Sphericity Assumed	400.714	10	40.071		
			Greenhouse-Geisser	400.714	10.000	40.071		
			Huynh-Feldt	400.714	10.000	40.071		
			Lower-bound	400.714	10.000	40.071		
		Peak Velocity	Sphericity Assumed	6393.460	10	639.346		
			Greenhouse-Geisser	6393.460	10.000	639.346		
			Huynh-Feldt	6393.460	10.000	639.346		
			Lower-bound	6393.460	10.000	639.346		
		Absolute Displacement	Sphericity Assumed	14.430	10	1.443		
			Greenhouse-Geisser	14.430	10.000	1.443		
			Huynh-Feldt	14.430	10.000	1.443		
			Lower-bound	14.430	10.000	1.443		
		Relative Displacement	Sphericity Assumed	87.466	10	8.747		
			Greenhouse-Geisser	87.466	10.000	8.747		
			Huynh-Feldt	87.466	10.000	8.747		
			Lower-bound	87.466	10.000	8.747		
			Lower-bound	2796.126	10.000	279.613		

Appendix 8- ANOVA- Running Gait between Subjects

TABLE 25- Running gait ANOVA

ANOVA								
Speed	Subclass			Sum of Squares	df	Mean Square	F	Sig.
Running	'KEHE-late mid stance'	Muscle speed	Between Groups	573.743	1	573.743	11.616	.009
			Within Groups	395.142	8	49.393		
			Total	968.885	9			
		Muscle velocity	Between Groups	4086.269	1	4086.269	82.730	.000
			Within Groups	395.142	8	49.393		
			Total	4481.411	9			
		Muscle displacement (cm)	Between Groups	1.547	1	1.547	15.953	.004
			Within Groups	.776	8	.097		
			Total	2.323	9			
		Muscle displacement (% thigh)	Between Groups	9.006	1	9.006	11.916	.009
			Within Groups	6.047	8	.756		
			Total	15.053	9			
		Muscle maximum length	Between Groups	983.848	1	983.848	164.189	.000
			Within Groups	47.937	8	5.992		
			Total	1031.785	9			
	'KEHE-terminal swing'	Muscle speed	Between Groups	42.573	1	42.573	.637	.448
			Within Groups	534.331	8	66.791		
			Total	576.904	9			
		Muscle velocity	Between Groups	1680.934	1	1680.934	7.762	.024
			Within Groups	1732.471	8	216.559		
			Total	3413.406	9			
		Muscle displacement (cm)	Between Groups	.098	1	.098	.328	.582
			Within Groups	2.382	8	.298		
			Total	2.480	9			
		Muscle displacement (% thigh)	Between Groups	.390	1	.390	.333	.580
			Within Groups	9.374	8	1.172		
			Total	9.764	9			
		Muscle maximum length	Between Groups	1248.855	1	1248.855	223.171	.000
			Within Groups	44.768	8	5.596		
			Total	1293.622	9			
	'KEHF-mid swing'	Muscle speed	Between Groups	8236.071	1	8236.071	31.997	.000
			Within Groups	2059.179	8	257.397		
			Total	10295.250	9			
		Muscle velocity	Between Groups	8236.071	1	8236.071	31.997	.000
			Within Groups	2059.179	8	257.397		

			Total	10295.250	9			
		Muscle displacement (cm)	Between Groups	20.909	1	20.909	12.959	.007
			Within Groups	12.908	8	1.613		
			Total	33.817	9			
		Muscle displacement (% thigh)	Between Groups	118.593	1	118.593	9.073	.017
			Within Groups	104.570	8	13.071		
			Total	223.163	9			
		Muscle maximum length	Between Groups	1292.360	1	1292.360	377.244	.000
			Within Groups	27.406	8	3.426		
			Total	1319.767	9			
	'KFHE-early terminal stance'	Muscle speed	Between Groups	425.371	1	425.371	30.044	.005
			Within Groups	56.633	4	14.158		
			Total	482.004	5			
		Muscle velocity	Between Groups	425.371	1	425.371	30.044	.005
			Within Groups	56.633	4	14.158		
			Total	482.004	5			
		Muscle displacement (cm)	Between Groups	.341	1	.341	4.000	.116
			Within Groups	.341	4	.085		
			Total	.683	5			
		Muscle displacement (% thigh)	Between Groups	1.903	1	1.903	4.276	.107
			Within Groups	1.780	4	.445		
			Total	3.683	5			
		Muscle maximum length	Between Groups	512.216	1	512.216	174.261	.000
			Within Groups	11.757	4	2.939		
			Total	523.974	5			
	'KFHE-heel strike'	Muscle speed	Between Groups	1944.494	1	1944.494	6.051	.039
			Within Groups	2570.705	8	321.338		
			Total	4515.198	9			
		Muscle velocity	Between Groups	1944.494	1	1944.494	6.051	.039
			Within Groups	2570.705	8	321.338		
			Total	4515.198	9			
		Muscle displacement (cm)	Between Groups	1.070	1	1.070	4.008	.080
			Within Groups	2.136	8	.267		
			Total	3.207	9			
		Muscle displacement (% thigh)	Between Groups	6.304	1	6.304	4.035	.079
			Within Groups	12.499	8	1.562		
			Total	18.804	9			
		Muscle maximum length	Between Groups	1179.035	1	1179.035	207.518	.000
			Within Groups	45.453	8	5.682		
			Total	1224.488	9			
	'KFHE-early mid stance'	Muscle speed	Between Groups	627.030	1	627.030	7.937	.023
			Within Groups	632.040	8	79.005		

			Total	1259.070	9			
		Muscle velocity	Between Groups	627.030	1	627.030	7.937	.023
			Within Groups	632.040	8	79.005		
			Total	1259.070	9			
		Muscle displacement (cm)	Between Groups	.229	1	.229	2.075	.188
			Within Groups	.882	8	.110		
			Total	1.111	9			
		Muscle displacement (% thigh)	Between Groups	1.261	1	1.261	1.927	.202
			Within Groups	5.234	8	.654		
			Total	6.495	9			
		Muscle maximum length	Between Groups	1100.698	1	1100.698	195.314	.000
			Within Groups	45.084	8	5.636		
			Total	1145.783	9			
	'KFHE-toe off'	Muscle speed	Between Groups	180.752	1	180.752	16.546	.007
			Within Groups	65.546	6	10.924		
			Total	246.298	7			
		Muscle velocity	Between Groups	180.752	1	180.752	16.546	.007
			Within Groups	65.546	6	10.924		
			Total	246.298	7			
		Muscle displacement (cm)	Between Groups	.027	1	.027	3.921	.095
			Within Groups	.042	6	.007		
			Total	.069	7			
		Muscle displacement (% thigh)	Between Groups	.154	1	.154	3.745	.101
			Within Groups	.247	6	.041		
			Total	.401	7			
		Muscle maximum length	Between Groups	650.253	1	650.253	87.857	.000
			Within Groups	44.408	6	7.401		
			Total	694.660	7			
	'KFHF/late terminal stance'	Muscle speed	Between Groups	3.288	1	3.288	.087	.778
			Within Groups	227.901	6	37.983		
			Total	231.189	7			
		Muscle velocity	Between Groups	3.288	1	3.288	.087	.778
			Within Groups	227.901	6	37.983		
			Total	231.189	7			
		Muscle displacement (cm)	Between Groups	.002	1	.002	.080	.786
			Within Groups	.152	6	.025		
			Total	.154	7			
		Muscle displacement (% thigh)	Between Groups	.009	1	.009	.094	.769
			Within Groups	.600	6	.100		
			Total	.609	7			
		Muscle maximum length	Between Groups	911.873	1	911.873	183.710	.000
			Within Groups	29.782	6	4.964		

			Total	941.655	7			
	'KFHF-initial swing'	Muscle speed	Between Groups	38.206	1	38.206	.902	.370
			Within Groups	338.936	8	42.367		
			Total	377.141	9			
		Muscle velocity	Between Groups	49.080	1	49.080	1.056	.334
			Within Groups	371.822	8	46.478		
			Total	420.902	9			
		Muscle displacement (cm)	Between Groups	.083	1	.083	.290	.605
			Within Groups	2.301	8	.288		
			Total	2.385	9			
		Muscle displacement (% thigh)	Between Groups	.455	1	.455	.216	.655
			Within Groups	16.863	8	2.108		
			Total	17.318	9			
		Muscle maximum length	Between Groups	815.106	1	815.106	117.631	.000
			Within Groups	55.435	8	6.929		
			Total	870.541	9			
	'KFHF-foot flat'	Muscle speed	Between Groups	.182	1	.182	.003	.955
			Within Groups	430.946	8	53.868		
			Total	431.129	9			
		Muscle velocity	Between Groups	3814.597	1	3814.597	111.579	.000
			Within Groups	273.500	8	34.188		
			Total	4088.097	9			
		Muscle displacement (cm)	Between Groups	.720	1	.720	2.706	.139
			Within Groups	2.128	8	.266		
			Total	2.848	9			
		Muscle displacement (% thigh)	Between Groups	3.824	1	3.824	2.608	.145
			Within Groups	11.732	8	1.466		
			Total	15.556	9			
		Muscle maximum length	Between Groups	831.748	1	831.748	102.435	.000
			Within Groups	64.958	8	8.120		
			Total	896.706	9			
Walking	'KEHE-late mid stance'	Muscle speed	Between Groups	378.984	1	378.984	69.391	.000
			Within Groups	43.693	8	5.462		
			Total	422.677	9			
		Muscle velocity	Between Groups	696.625	1	696.625	127.550	.000
			Within Groups	43.693	8	5.462		
			Total	740.318	9			
		Muscle displacement (cm)	Between Groups	3.491	1	3.491	38.863	.000
			Within Groups	.719	8	.090		
			Total	4.210	9			
		Muscle displacement (%	Between Groups	18.832	1	18.832	38.714	.000
			Within Groups	3.891	8	.486		

		thigh)	Total	22.723	9			
		Muscle maximum length	Between Groups	996.206	1	996.206	113.469	.000
			Within Groups	70.236	8	8.780		
			Total	1066.442	9			
	'KEHE-terminal swing'	Muscle speed	Between Groups	3.963	1	3.963	.332	.581
			Within Groups	95.611	8	11.951		
			Total	99.574	9			
		Muscle velocity	Between Groups	78.162	1	78.162	2.003	.195
			Within Groups	312.125	8	39.016		
			Total	390.287	9			
		Muscle displacement (cm)	Between Groups	.004	1	.004	.136	.722
			Within Groups	.261	8	.033		
			Total	.266	9			
		Muscle displacement (% thigh)	Between Groups	.033	1	.033	.145	.713
			Within Groups	1.829	8	.229		
			Total	1.862	9			
		Muscle maximum length	Between Groups	1100.621	1	1100.621	123.545	.000
			Within Groups	71.269	8	8.909		
			Total	1171.890	9			
	'KEHF-mid swing'	Muscle speed	Between Groups	1224.976	1	1224.976	14.065	.006
			Within Groups	696.759	8	87.095		
			Total	1921.735	9			
		Muscle velocity	Between Groups	1224.976	1	1224.976	14.065	.006
			Within Groups	696.759	8	87.095		
			Total	1921.735	9			
		Muscle displacement (cm)	Between Groups	8.715	1	8.715	46.808	.000
			Within Groups	1.490	8	.186		
			Total	10.205	9			
		Muscle displacement (% thigh)	Between Groups	47.907	1	47.907	47.076	.000
			Within Groups	8.141	8	1.018		
			Total	56.049	9			
		Muscle maximum length	Between Groups	1108.467	1	1108.467	132.445	.000
			Within Groups	66.954	8	8.369		
			Total	1175.421	9			
	'KFHE-heel strike'	Muscle speed	Between Groups	49.739	1	49.739	1.822	.248
			Within Groups	109.192	4	27.298		
			Total	158.932	5			
		Muscle velocity	Between Groups	50.205	1	50.205	1.831	.247
			Within Groups	109.671	4	27.418		
			Total	159.875	5			
		Muscle displacement (cm)	Between Groups	.047	1	.047	2.209	.211
			Within Groups	.086	4	.021		

			Total	.133	5			
		Muscle displacement (% thigh)	Between Groups	.247	1	.247	2.484	.190
			Within Groups	.398	4	.099		
			Total	.645	5			
		Muscle maximum length	Between Groups	707.661	1	707.661	92.318	.001
			Within Groups	30.662	4	7.665		
			Total	738.323	5			
	'KFHE-early mid stance'	Muscle speed	Between Groups	337.414	1	337.414	20.054	.004
			Within Groups	100.953	6	16.825		
			Total	438.367	7			
		Muscle velocity	Between Groups	337.414	1	337.414	20.054	.004
			Within Groups	100.953	6	16.825		
			Total	438.367	7			
		Muscle displacement (cm)	Between Groups	.694	1	.694	5.638	.055
			Within Groups	.739	6	.123		
			Total	1.433	7			
		Muscle displacement (% thigh)	Between Groups	3.838	1	3.838	5.010	.067
			Within Groups	4.597	6	.766		
			Total	8.434	7			
		Muscle maximum length	Between Groups	872.343	1	872.343	79.611	.000
			Within Groups	65.745	6	10.958		
			Total	938.088	7			
	'KFHE-toe off'	Muscle speed	Between Groups	264.874	1	264.874	30.335	.001
			Within Groups	69.853	8	8.732		
			Total	334.726	9			
		Muscle velocity	Between Groups	265.023	1	265.023	30.312	.001
			Within Groups	69.944	8	8.743		
			Total	334.968	9			
		Muscle displacement (cm)	Between Groups	1.359	1	1.359	18.562	.003
			Within Groups	.586	8	.073		
			Total	1.944	9			
		Muscle displacement (% thigh)	Between Groups	7.198	1	7.198	20.107	.002
			Within Groups	2.864	8	.358		
			Total	10.061	9			
		Muscle maximum length	Between Groups	856.685	1	856.685	102.460	.000
			Within Groups	66.890	8	8.361		
			Total	923.575	9			
	'KFHF-early/mid swing'	Muscle speed	Between Groups	5.427	1	5.427	.304	.596
			Within Groups	142.645	8	17.831		
			Total	148.072	9			
		Muscle velocity	Between Groups	557.553	1	557.553	9.296	.016
			Within Groups	479.816	8	59.977		

			Total	1037.369	9			
		Muscle displacement (cm)	Between Groups	.075	1	.075	.070	.798
			Within Groups	8.548	8	1.068		
			Total	8.622	9			
		Muscle displacement (% thigh)	Between Groups	.774	1	.774	.180	.682
			Within Groups	34.310	8	4.289		
			Total	35.084	9			
		Muscle maximum length	Between Groups	840.870	1	840.870	69.946	.000
			Within Groups	96.174	8	12.022		
			Total	937.044	9			

Appendix 9- Human Subject Land Marking

The individual palpation procedure occurred as follows:

1) Right ASIS & left ASIS- These landmarks were palpated with the subject in a standing position, using the Iliac Crest as a reference point.

2) Right PSIS- The right "dimple of Venus" was visually located on each subject's back with the subject in a standing position. The right PSIS was taken to be just inferior and lateral to this indent and its exact location was confirmed with palpation.

3) Right GT- The location of the right GT was determined using cross validation of two palpation methods. First the hip joint was palpated as the subject abducted and adducted the thigh in a standing position. An estimation of the position of the right GT was achieved through this method alone. To increase land marking precision, the right GT was palpated as the hip was sequentially internally and externally rotated. This occurred with the subject in a standing position with the hip in anatomical position and the knee fully extended.

4) Right IT- For the pilot trials, the right IT was palpated from a side lying or standing position, with the hip in maximum flexion. For an additional calibration trial in a single subject, an additional test was added to increase the validity of the palpation. The subject was instructed to sit on the investigator's hand, and the boney point where the maximum amount of weight has placed was taken to be the right IT.

5) Right LFC – The palpation of this landmark involved multiple steps. First, the knee joint center line was found by having the subject stand upright with their knee flexed to 90 degrees. Next, the joint center location was visually estimated and then confirmed as a point above the head of the fibula (see palpation procedure for this landmark below). The investigators' hand was placed slightly superior to the joint center, and the knee was extended. From this extended position, the circular shape of the right LFC was palpated, and the centroid of this circle was visually estimated.

6) Right HF - the right HF was palpated by following the distal tendon of the right BF_L to the boney prominence, while the knee joint was flexed to 90 degrees. If needed, a forceful contraction of the BF_L was elicited through manual resistance placed by the investigator on the posterior aspect of the subject's ankle and foot.

7) Right LM- this boney marking was easily identified both visually and manually from anatomical position.

All markers except the one on the right GT, and the one on the right IT (in the pilot trails), were placed directly on the skin. The right GT marker was placed on the subjects' shorts due to the observed obstruction of the right GT markers when the subject's shorts were rolled up. The marker placed on the right IT was placed on the subjects' shorts, due to the impracticality of requiring the subject to be essentially nude to enable direct placement on the skin.

References

An, K., Takahashi, K., Harrigan, T. P. and Chao, E. (1984) Determination of muscle orientations and moment arms. *J Biomechanical Engineering* **106,** 280-282.

Arnold, A. S., Salinas, S., Asakawa, D. J. and Delp, S. (2000) Accuracy of Muscle Moment Arms Estimated from MRI-Based Musculoskeletal Modelsof the Lower Extremity. *Computer Aided Surgery* **5,** 108-119.

Aruin, A. S., Zatsiorski, V. M., Prilutsky, B. I. and Shakhnazarov, A. I. (1987) *the biomechanical method used for determining the arms of muscular force*. Human Kinetics Publishers, inc.: Champaign, Illinois.

Askling, C. M., Tengvar, M., Saartok, T. and Thorstensson, A. (2007) Acute first time hamstring strains during high speed running: a longitudinal study including clinical and magnetic resonance imaging findings. *American Journal of Sports Medicine* **35,** 197-206.

Auleley, G., Rousselin, B., Ayral, X., Eduard-Noel, R., Dougados, M. and Ravaud, P. (1998) Osteoarthitis of the hip: agreement between joint space width measurements on standing and supine conventional radiographs. *Annals of the rheumatic diseases* **57,** 519-523.

Bollens, E.C., De Proft, E., Clarys, J.P. (1987). The accuracy and muscle monitoring in soccer kicking, *Biomechanics X-A* (ed B.Johnsson), Human Kinetics: IL, pp.283-288.

Brand, R. A., Crowninshield, R. D., Wittstock, C. E., Pedersen, D. R., Clark, C. R. and Van Krieken, F. M. (1982) A model of lower extremity muscular anatomy. *J Biomechanics* **104,** 304-310.

Brockett, C. L., Morgan, D. L. and Proske, U. (2001) Human hamstring muscles adapt to eccentric exercise by chaning optimum length. *Med. Sci. Sports and Exerc.* **33,** 783-790.

Buford, W. L., Ivey, F. M., Malone, J. D., Patterson, R. M., Peare, G. L., Nguyen, D. K. and Stewart, A. A. (1997) Muscle Balance at the Knee: Moment Arms for the Normal Knee and the ACL-Minus Knee. *Ieee Transactions on Rehabilitation Engineering* **5,** 367-379.

Buford, W.L. (2001) Internal/external rotation moment arms of muscles at the knee: moment arms for the normal knee and the ACL-deficient knee. *The Knee* **8**, 293-303.

Chelbourn, G. S., France, A. R., Crill, M. T., Braddock, H. K. and Howell, J. N. (2001) In vivo measurement of fascicle length and pennation angle of the human biceps femoris muscle. *Cells, Tissues, Organs* **169,** 401-409.

Cleland, J. (1867) On the actions of muscles passing over more than one joint. *J of Anatomical Physiol.* **1,** 85-93.

Dagg, A. I. (1977) *Running, Walking and Jumping: The Science of Locomotion.* Wykeham: London.

Delp, S., Loan, J. P., Hoy, M. G., Zajac, F. E., Topp, E. L. and Rosen, J. M. (1990A) An Interactive Graphics-Based Model of the Lower Extremity to Study Orthopaedic Surgical Procedures. *IEEE Transactions on Biomedical Engineering.* **37,** 757-767.

Delp, S. (1990B) Surgery Simulation: A computer graphics system to analyze and design muscoskeletal reconstructions of the lower limb. PhD. Dissertation. Department of Mechanical Engineering, Stanford University.

DeSmet, A. A. and Best, T. M. (2000) MR imaging of the distribution and location of acute hamstring injuries in athletes. *American Journal of Roentgenology* **174,** 393-399.

Elftman, H. (1966) Biomechanics of Muscle: with particular application to studies of gait. *J. Bone Joint Surg. Am.* **48,** 363-377.

Enklaar, J. (1954) Isometric and paradoxical contractions of biarticular muscles in certain movements. *Ned Tijdschr Geneeskd.* (12):813-4.

Epstein, M. and Herzog, W. (1988) *Theoretical models of skeletal muscle: Biological and Mathematical Considerations*. John Wiley & Sons: England.

Fenn, W. O. (1931)Zur Nechanik des Radfahrens im Yergleich zu der des Laufens. Pflügers Archiv European Journal of Physiology **229** (1), 354-366.

Fenn, W. O. (1938) The mechanics of muscular contraction in man. *J of Applied Physics* **9,** 165-177.

Freeman, M. and Pinskerova, V. (2005) The movement of the normal tibio-femoral joint. *J. Biomechanics* **38,** 197-208.

Frigo, C. and Pedotti, A. (1978) Determination of muscle length during locomotion. *Biomechanics* **IV-A,** 355-360.

Garrett, W. E. (1996) Muscle strain injuries. *American Journal of Sports Medicine* **24,** S2 - S8.

Garrett, W. E., Califf, J. C. and Bassett, F. H. (1984) Histochemical correlates of hamstring injury. *American Journal of Sports Medicine* **12,** 98-103.

Garrett, W. E., Nikolaou, P. K., Ribbeck, B. M., Glisson, R. R. and Seaber, A. V. (1988) The effect of muscle architecture on the biomechanical failure properties of skeletal muscle under passive extension. *American Journal of Sports Medicine* **16,** 7-11.

Garrett, W. E., Rich, F. R., Nikolaou, P. K. and Vogler, J. B. (1989) Computer tomography of hamstring muscle strains. *Med. Sci. Sports and Exerc.* **21,** 506-514.

Garrett, W. E., Safran, M. R., Seaber, A. V., Glisson, R. R. and Ribbeck, B. M. (1987) Biomechanical comparison of stimulated and nonstimulated skeletal muscle pulled to failure. *American Journal of Sports Medicine* **15,** 448-454.

Gondin, W. R. and Sohmer, B. (1959) *Intermediate algebra and analytic geometry made simple*. Doubleday & Co, Inc.

Goslow, G. E. J., Reinking, R. M. and Stuart, D. G. (1973) The cat step cycle: hind limb joint angles and muscle lengths during unrestrained locomotion. *J Morphol.* **141,** 1-41.

Goswami, A. (1998) A new gait parameterization technique by means of cyclogram moments: Application to human slope walking. *Gait & Posture* **8,** 15-36.

Gray, H. (1918) Anatomy of the human body *Vol. 2007*. Ed. Bartleby.com.

Gregoire, L., Veeger, H. E., Huijing, P. A. and van Ingen Schenau, G. J. (1984) Role of mono and biarticular muscles in explosive movements. *Int. J. Sports. Med.* **5,** 301-305.

Green, D.P., Roberts, S.L. (2005) Kinesiology: Movement in the context of activity. Elsevier Mosby. USA.

Grieve, D. W., Pheasant, S. and Cavanagh, P. R. (1978) *Prediction of Gastrocnemius length from knee and ankle joint posture*.Biomechanics VI-A. University park press: Baltimore.

Gross, J.M, Fetto, J., Rosen, E. (2009) *Muscoskeletal Examination*. Blackwell publishing. UK.

Hall, S.(1999) Basic Biomechanics.WCB/McGraw-Hill. USA

Hawkings, D. and Hull, M. L. (1990) A method for determining lower extremity muscle-tendon lengths during flexion/extension movements. *J. Biomechanics* **23,** 487-494.

Heiderscheit, B. C., Hoerth, D. M., Chumanov, E. S., Swanson, S. C., Thelen, B. J. and Thelen, D. G. (2005) Identifying the time of occurrence of a hamstring strain injury during treadmill running: A case study. *Clinical Biomechanics* **20,** 1072-1078.

Herzog, W. and Read, J. L. (1993) Lines of action and moment arms of the major force-carrying structures crossing the human knee joint. *J. Anatomy* **182,** 213-230.

Hoy, M. G., Zajac, F. E. and Gordon, M. E. (1990) A musco-skeletal model of the human lower extremity: the effect of muscle, tendon, and moment arm on the moment angle relationship of musculotendon actuators at the hip, knee, and ankle. *J Biomechanics* **23,** 157-169.

Imran, A., Huss, A., Holstein, H. and O'Conner, J. J. (2000) The variation in the orientations and moment arms of the knee extensor and flexor muscles tendons with increasing muscle force: a mathematical analysis. *Proc. Inst. Mech. Engrs.* **214,** 277-286.

Kazai N, M Kumamoto N Yamashita H Maruyama & Y Tokuhara (1978). Role of two-joint muscle in joint movements. In E Asmussen & K Jorgensen (Eds.): *Biomechanics* VI-A. University Park Press, Baltimore, pp 413-418.

Koulouris, G. and Connell, D. (2003) Evaluation of the hamstring muscle complex following acute injury. *Skeletal Radiology* **32,** 582-589.

Kuo, A.D. (2001). The action of two-joint muscles: The legacy of W. P. Lombard, In *Classics in Movement Science*, ed. Latash, M. & Zatsiorski, V., Copyright 2001 Mark M. Latash & Vladimir Zatsiorski, Printed in the USA.

Knudson, D. Fundamentals of Biomechanics. Copyright 2003. Kluwer Academic/ Plenum Publishers, USA.

Leis, A., Trapani, V. (2000). Atlas of Electromyography . Oxford University Press. New York. USA.

Levangie, P. and Norkin, C. (2005) *Joint structure and function: a comprehensive analysis*. F.A. Davis company: Philadelphia.

Lieber, R. L. and Frieden, J. (1993) Muscle damage is not a function of muscle force but active muscle strain. *J. Appl. Physiol.* **74,** 520-526.

Loyd, D. G. and Buchanan, T. S. (1996) Strategies of muscular support of varus and valgus isometric loads at the human knee. *J. Biomechanics* **34,** 1257-1267.

Lombard, W.P. (1903) The action of two-joint muscles. *American Physical education,**8, 141-145***

Luttgens, K., Deutsch, H., Hamilton, N. (1992) Kinesiology: Scientific Basis of Human Motion. USA.

Lyons, K., Perry, J., Gronley, J., Barnes, L., Antonelli, D. Timing and Relative Intensity of Hip Extensor and Abductor Muscle Action during Level and Stait Ambulation: An EMG Study. *Physical Therapy*, **63**, 1597-1605

Macmillan, M.B. (1976) Kinesiological determinants of the path of the foot during the football kick, *Research Quarterly*, **47**, 33-40.

Mann,R.V. (1981) A kinetic analysis of sprinting. *Med. Sci. Sports Exerc*. **13**, 325-8.

Martinez-Villalpando, E.C., Herr, H (2009). Agonist-antagonist active knee prosthesis: A preliminary study in level-ground walking. *J. Rehab. Res. & Dev.*, **46**, 361-374. http://www.rehab.research.va.gov/jour/09/46/3/martinez-villalpando.html,

Moore, K. and Daley, A. (1999) *Clinically Oriented Anatomy*. Lippencott Williams & Wilkins.

Murray, W. M., Buchanan, T. S. and Delp, S. (2002) Scaling of peak moment arms of elbow muscles with upper extremity bone dimensions. *J Biomechanics* **35,** 19-26.

Nemeth, G. and Ohlsen, H. (1985) In vivo moment arm lengths for hip extensor muscles at different angles of hip flexion. *J. Biomechanics* **18,** 129-140.

Novacheck, T. F. (1998) The biomechanics of running. *Gait and Posture* **7,** 77-95.

Orchard, J. (2002) Biomechanics of muscle strain injury. *New Zealand Journal of Sports Medicine* **30,** 92-98.

Peters, S. A. and Rick, C. R. (1977) The actions of three hamstring muscles of the cat: a mechanical analysis. *J. Morphology* **152,** 315-28.

Perry, Jacquelin (1992). *Gait analysis: normal and pathological function,* Slack Corporation. NJ. USA,

Prior, B. M., Jayaraman, R. C., Reid, R. W., Cooper, T. G., Foley, J. M., Dudley, G. A. and Meyer, R. A. (2001) Biarticular and mono-articular muscle activation and injury in human quadriceps muscle. *European Journal of Applied Physiology* **85,** 185-190.

Raikova, R. A. (2000) Investigation of the Peculiarities of Two-joint Muscles using a 3 DOF Model of the Human Upper Limb in the Sagittal Plane: an Optimization Approach. *Computer Methods in Biomechanics and Biomedical Engineering*, **00,** 1-28.

Sallay, P. I., Friedman, R. L., Coogan, P. G. and Garrett, W. E. (1996) Hamstring muscle injuries among water skiers. Functional outcome and prevention. *American Journal of Sports Medicine* **24,** 130-136.

Sherwood, L. (2010). Human Physiology: From Cells to Systems(7th ed.), Brooks/Cool Centrgage Learning: USA.

Shields, M., Gorber, S., Tremblay, M. (2008) Methodological Issues in Anthropometry: Self-reported versus Measured Height and Weight. Component of Statistics Canada Catalogue no. 11-522-X. Statistics Canada's International Symposium Series: Proceedings

Simonsen, E., Thomsen, L., Klausen, K. (1985) Activity of mono and biarticular muscles during sprint running. Eur. J. Appl. Physiol. **54**, 524-532.

Smidt, G. L. (1973) Biomechanical analysis of knee flexion and extension. *J. Biomechanics* **6,** 79-92.

Sneath, R. S. (1955) The insertion of the biceps femoris. *J. Anatomy* **89,** 550-553.

Speer, K. P., Lohnes, J. and Garrett, W. E. (1993) Radiographic imaging of muscle strain injury. *American Journal of Sports Medicine* **21,** 89-95.

Spoor, C. W. and van Leeuwen, J. L. (1992) Knee muscle moment arms from MRI and from tendon travel. *J Biomechanics* **25,** 201-206.

Steindler, A. (1935) *Mechanics of normal and pathological locomotion in man*. Tindall and Cox. Printed in London..

Stredney, D. (1982) The representation of anatomical structures through computer animation for scientific, educational, and artistic applications, M.Sc. Thesis. Ohio State University.

Sykes, K. (1975) Technique and observation of angular gait patterns in running. *British Journal of Sports Medicine* **9**, 181-186.

Terry, G. C. and LaPrade, R. F. (1996) The biceps femoris muscle complex at the knee: Its anatomy and injury patterns associated with acute anterolateral-anteromedial rotator instability. *American Journal of Sports Medicine* **24,** 2-8.

Thelen, D. G., Chumanov, E. S., Best, T. M., Swanson, S. C. and Heiderscheit, B. C. (2005a) Simulation of biceps femoris musculo-tendon mechanics during the swing phase of sprinting. *Med. Sci. Sports and Exerc.* **37,** 1931-1938.

Thelen, D. G., Chumanov, E. S., Hoerth, D. M., Best, T. M., Swanson, S. C., Li, L., Young, M. and Heiderscheit, B. C. (2005b) Hamstring muscle kinematics during treadmill sprinting. *Med. Sci. Sports and Exerc.* **37,** 108-114.

Thelen, D. G., Chumanov, E. S., Sherry, M. A. and Heiderscheit, B. C. (2006) Neuromuscular models provide insights into the mechanisms and rehabilitation of hamstring strains. *Exercise and Sport Science Reviews* **34,** 135-141.

Tsaopoulos, D. E., Baltzopoulos, V. and Maganaris, C. N. (2006) Human patellar tendon moment arm length: Measurement considerations and clinical implications for joint loading assessment. *Clinical Biomechanics* **21,** 657-667.

Tubbs, R. S., Caycedo, F. J., Jerry Oakes, W. and Salter, E. G. (2006) Descriptive anatomy of the insertion of the biceps femoris muscle. *Clinical Anatomy* **19,** 517-512.

van Bolhuis, B. M., Gielen, C. C. A. M. and van Ingen Schenau, G. J. (1998) Activation patterns of mono- and bi-articular arm muscles as a function of force and movement direction of the wrist in humans. *J. Physiol.* **508,** 313-324.

van Ingen Schenau, G. J. (1994) Proposed actions of biarticular muscles and the design of hindlimbs of bi and quadrupeds. *Human Movement Sciences* **13,** 665-681.

Visser, J. J., Hoogkamer, J. E., Bobbert, M. F. and Huijing, P. A. (1990) Length and moment arm of human leg muscles as a function of knee and hip-joint angles. *Eur J Appl Physiol* **61,** 453-460.

Watkins, J. (2009) Structure and function of the muscoskeletal system. Human Kinetics publishing. USA.

White, S. C., Yack, H. J. and Winter, D. A. (1989) A three dimensional musco-skeletal model for gait analysis. Anatomical variable estimates. *J. Biomechanics* **22,** 885-893.

Wickiewicz, T. L., Roy, R., Powell, P. L. and Edgerton, V. R. (1983) Muscle architecture of the lower limb. *Clinical orthopaedics and Related Res.* **179,** 275-283.

Winstein, C.J., Garfinkel, A. (1989). Qualitative dynamics of disordered human locomotion: a preliminary investigation. *J Mot Behav*. **21**, 373-91.

Winter, D. A. and Scott, S. H. (1991) Technique for interpretation of electromyography for concentric and eccentric contractions in gait. *J Electromyography and Kinesiology* **1,** 263-269.

Woodley, S. P. and Mercer, S. R. (2004) Hamstring strains- Where do they occur? *New Zealand Journal of Physiotherapy* **32,** 22-28.

Zajac, F. E. (1989) Muscle and tendon: properties, models, scaling, and application to biomechanics and motor control. *Crit. Rev. in Biomed. Eng.* **7,** 359-411.